

Metal-organic Framework-based enzyme biocomposites

Weibin Liang,^{a,†,‡} Peter Wied,^{b,‡} Francesco Carraro,^b Christopher J. Sumby,^a Bernd Nidetzky,^c Chia-Kuang Tsung,^d Paolo Falcaro,^{b*} and Christian J. Doonan^{a,*}

a) Department of Chemistry and Centre for Advanced Nanomaterials, The University of Adelaide, Adelaide, SA 5005, Australia.

b) Institute of Physical and Theoretical Chemistry, Graz University of Technology, Stremayrgasse 9, 8010 Graz, Austria.

c) Institute of Biotechnology and Biochemical Engineering, Graz University of Technology, Petersgasse 12/1, 8010 Graz, Austria.

d) Department of Chemistry, Merkert Chemistry Center, Boston College, Chestnut Hill, Massachusetts 02467, United States

ABSTRACT: Due to their efficiency, selectivity, and environmental sustainability, there are significant opportunities for enzymes in chemical synthesis and biotechnology. However, as the three-dimensional active structure of enzymes is predominantly maintained by weaker non-covalent interactions, thermal, pH and chemical stressors can modify or eliminate activity. Metal-organic Frameworks (MOFs), which are extended porous network materials assembled by a bottom-up building block approach from metal-based nodes and organic linkers, can be used to afford protection to enzymes. The self-assembled structures of MOFs can be used to encase an enzyme in a process called encapsulation when the MOF is synthesized in the presence of the biomolecule. Alternatively, enzymes can be infiltrated into mesoporous MOF structures or surface bound via covalent or non-covalent processes. Integration of MOF materials and enzymes in this way affords protection and allows the enzyme to maintain activity in challenge conditions (e.g. denaturing agents, elevated temperature, non-native pH and organic solvents). In addition to forming simple enzyme/MOF biocomposites, other materials can be introduced to the composites to improve recovery or facilitate advanced applications in sensing and fuel cell technology. This review canvasses enzyme protection via encapsulation, pore infiltration and surface adsorption and summarizes strategies to form multi-component composites. Also, given that enzyme/MOF biocomposites straddle materials chemistry and enzymology, this review provides an assessment of the characterization methodologies used for MOF-immobilized enzymes and identifies some key parameters to facilitate development of the field.

CONTENTS

1. Introduction
 2. MOF-based enzyme biocomposite compositions and the concept of encapsulation
 3. MOF-based enzyme biocomposites formed via encapsulation
 - 3.1. Templating methods
 - 3.2. One-pot embedding (non-templated)
 - 3.3. Parameters influencing the chemistry of enzyme@MOF biocomposites
 - 3.3.1. Additives
 - 3.3.2. Enzyme surface chemistry
 - 3.3.3. MOF precursors and structures
 - 3.4. Alternative synthesis strategies
 4. Infiltration (post insertion of enzymes in pre-formed MOFs)
 - 4.1. Early results and the advantages of MOFs for infiltration
 - 4.2. Tuning the framework structure in infiltrated enzyme@MOF biocomposites
 - 4.3. Towards applications of infiltrated enzyme@MOFs
 5. Surface bound enzymes
 - 5.1. Immobilization via physical adsorption
 - 5.2. Immobilization via coordinate bonds
 - 5.3. Immobilization via covalent bonding
 - 5.4. Enzymatic activity upon surface-immobilization
 6. Multicomponent biocomposites
 7. Characterization of MOF immobilized enzymes
 - 7.1. Overview
 - 7.2. Key immobilization parameters
 - 7.3. One-pot enzyme MOF formation
 - 7.4. Highlights of MOF-immobilized enzyme performance
 - 7.4.1. Experimental determination of key immobilization parameters
 - 7.4.1.1. Determination of protein concentrations
 - 7.4.1.2. Activity determination
 - 7.4.2. Advanced characterization of immobilized enzymes
 - 7.4.2.1. Apparent enzyme kinetics
 - 7.4.2.2. Structural analysis and localization of enzymes immobilized into MOFs
 - 7.4.2.3. Enzyme-MOF materials in bio-catalysis: usage range, stability and catalyst recycling
 8. Outlook
- Associated Content
Author Information
Acknowledgements
Abbreviations
References

1. INTRODUCTION

Enzymes offer the potential to enhance the efficiency, selectivity and environmental sustainability of many commercial processes, especially in the areas of chemical synthesis and biotechnology.¹⁻³ However, a significant impediment to their wide-spread industrial application is that the activity of many enzymes is compromised, or extinguished, when exposed to non-aqueous media and/or elevated temperatures.^{4, 5} An enzyme's sensitivity to its environment is largely due to the thermodynamic instability of its tertiary structure in artificial conditions. Thermal stress and/or organic solvents can disrupt the specific and complex network of covalent and non-covalent interactions that engender the naturally folded state of an enzyme and, as a consequence, modify or eliminate its catalytic activity. A number of strategies have been explored to overcome the structural fragility of enzymes including, genetic engineering,⁶ chemical modification,^{7, 8} immobilization,^{5, 9} changes to the reaction medium and encapsulation.^{5, 9-11} While each of these approaches show promise for meeting real-world challenges, this review will focus on the burgeoning research area of employing Metal-organic Frameworks (MOFs) for the immobilization of enzymes.

MOFs are materials assembled by connecting organic links and metal-based nodes (metal ions or clusters) into extended networks.¹² These materials are well known for their high degree of crystallinity and remarkable surface areas and pore volumes. Owing to their modular construction and chemical mutability of their components (nodes and links) the structure topology, pore functionality and crystal morphology of MOFs can be precisely tailored. These design features have inspired researchers from a broad range of scientific and engineering disciplines to investigate the fundamental and applied properties of these unique materials. An area of MOF chemistry that is experiencing considerable growth is the synthesis, characterization, and application of enzyme/MOF biocomposites. The immobilization of enzymes via porous solids, such as mesoporous silica is a mature research field;^{11, 13, 14} however, MOFs represent a recent class of support material for enzymes with extensive scope for development. Furthermore, many of the traditional strategies that have been employed to stabilize enzymes, e.g. covalent grafting onto a particle or surface, and encapsulation via physical adsorption are readily compatible with MOF chemistry. For example, the pore dimension and chemical functionality of a framework can be optimized for the encapsulation of a specific enzyme to a level of precision that is not attainable for other porous materials such as zeolites (ultra-microporous to microporous) and mesoporous silicas (mesoporous). This is a clear advantage of MOFs as the design of such bespoke systems would, in principle, allow for the systematic investigation of protein-surface interactions and their relationship to the preservation and protection of enzymes. Another aspect of MOF chemistry relevant to protein encapsulation is that, for a number of examples, biocompatible synthesis conditions (room temperature, H₂O) have been developed. Thus, the MOF precursors can be assembled in the presence of an enzyme to yield enzyme@MOF biocomposites where the proteins are tightly encased within a single MOF crystal.

In general MOF-based enzyme biocomposites can be conveniently classed according to how they are composed.

Encapsulation, (termed, enzyme@MOF) - The MOF is synthesized in the presence of an enzyme. This gives rise to a biocomposite where the enzyme is encased within the MOF crystals.

Pore infiltration (termed, enzyme@MOF) - The enzyme is introduced within the pore network of a pre-synthesized MOF.

Surface bound (termed, enzyme-on-MOF) - The enzyme is anchored to the surface of a pre-synthesized MOF via covalent bonds or non-covalent interactions.

After providing an overview of the strategies to form enzyme/MOF biocomposites (section 2), composites formed via each specific approach will be discussed in turn. In addition to these various configurations, the synthetic versatility and chemical mutability of MOFs allows the ready formation of multicomponent biocomposites. Where enzymes can be combined with additional materials, e.g. ceramic or metal nanoparticles. These biocomposites can be formed by any of the methods outlined above but are distinguished herein as a class of *multicomponent* systems and are accorded their own section to highlight the opportunities present but also the distinct assembly requirements.

The above classifications illustrate that MOFs are a versatile platform material for the synthesis of enzyme-based biocomposites that show great promise for application to commercial challenges in biocatalysis. Nevertheless, to fully realize their potential, a multidisciplinary research approach will be required to properly evaluate their performance characteristics and benchmark these data to state-of-the-art systems. This is discussed in section 7.

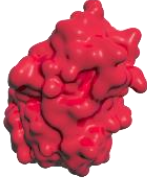
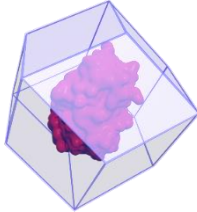
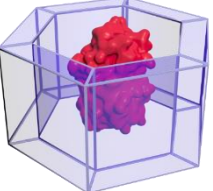
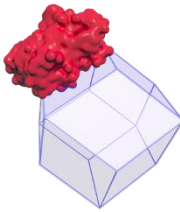
This review will canvass progress in the emerging area of enzyme/MOF biocomposites. Each class of material (*vide supra*) will be addressed separately, and important conceptual advances will be highlighted. Furthermore, we will discuss methods for characterizing MOF-based biocomposites and suggest good practice for the collection of reliable data.

2. MOF-BASED ENZYME BIOCUMPOSITE COMPOSITIONS AND THE CONCEPT OF ENCAPSULATION

Research focused on the immobilization of enzymes in/on solid supports is primarily aimed at preserving their biocatalytic activity and facilitating recyclability. The secondary structure of proteins (α -helices, β -sheets, and turns) is determined by hydrogen bonding between the amino acid sequences (primary structure). Salt and disulfide bridges give rise to the tertiary structure of the protein where hydrophobic interactions are maximized and the energetic requirements engendered by the interaction of the folded protein with the solvent are optimized. In general, the tertiary structure determines functionality and yields proteins that have a hydrophobic core and ionizable amino acids, which can establish hydrogen bonds, on the surface. In some cases, non-covalent interactions of multiple enzyme subunits can also occur and is termed the quaternary structure.¹⁵ The following section briefly introduces the various types of enzyme/MOF biocomposites and compares the immobilization methods.

In comparison to surface immobilized enzymes, which can either be physically adsorbed or grafted onto the surface (covalent or supramolecular attachment), infiltration and encapsulation methods offer enhanced shielding from harsh environments (e.g. elevated temperature, organic solvents, proteolytic agents).¹⁶ The preparation of biocomposites via infiltration is part of a two-step process where the enzyme is post-synthetically incorporated into the MOF pores (typically through large mesoporous channels) whereas, for biocomposites formed via the encapsulation approach, the enzyme is added during the synthesis of the MOF (we note that if a hollow enzyme/MOF composite is being prepared the enzyme is added prior to the synthesis of the MOF shell, see section 3). Thus, a significant distinction between enzyme/MOF biocomposites formed by encapsulation is that this synthetic strategy readily allows for the inclusion of enzymes that have larger dimensions than the pore diameter of the framework. This synthetic process leads to tight confinement of the enzyme within a mesoporous pocket within the framework^{14, 20} and offers a high level of protection from external environments (**Table 1**). An illustrative example of such protection is that enzymes encapsulated within a MOF matrix are insulated from contact with proteases, such as trypsin (TRY).¹⁶⁻¹⁹

Table 1. A general comparison of enzyme immobilization methods using MOFs.

	 Free enzyme	 Encapsulated enzyme	 Infiltrated Enzyme	 Surface bioconjugation
Main advantage(s)	Ready to use	Facile one-pot synthesis for a number of proteins	The synthesis of MOFs does not affect immobilization, chemically robust MOFs used	Synthesis does not affect immobilization, large number of MOFs
Main drawback(s)	Fragility/recyclability	Limited number of MOFs available, substrate/co-factor restrictions, interaction at the MOF/enzyme interface may be more complex than surface conjugation/infiltration	Different MOFs are needed for different sized proteins and there are a limited number of mesoporous MOFs	Leaching, protection of the protein
Stability to:				
Proteolytic agents	LOW	HIGH	Depends on the MOF pore size	LOW
Temperature	LOW	HIGH	HIGH	LOW/MEDIUM
Solvents	LOW	HIGH	HIGH	LOW/MEDIUM

For enzyme@MOF biocomposites the cavity size surrounding the enzyme is directly related to its capacity to protect the enzyme from environmental stressors (**Figure 1**). For example, encapsulation via single-step synthesis approach occurs via a heterogeneous nucleation mechanism where the enzymes serve as the nucleus for MOFs growth. Detailed analysis of small-angle X-ray scattering

(SAXS) data suggests that this process leads to the entrapment of enzymes within pockets of marginally larger volume than the radius of gyration (R_g) of the protein.^{14,20} The relative protective capacity of different cavity sizes on the activity of the enzyme (horseradish peroxidase, HRP) have been examined and a correlation was found between enzyme activity (preservation of the tertiary structure) and pore size of carriers (see **Figure 1a**).

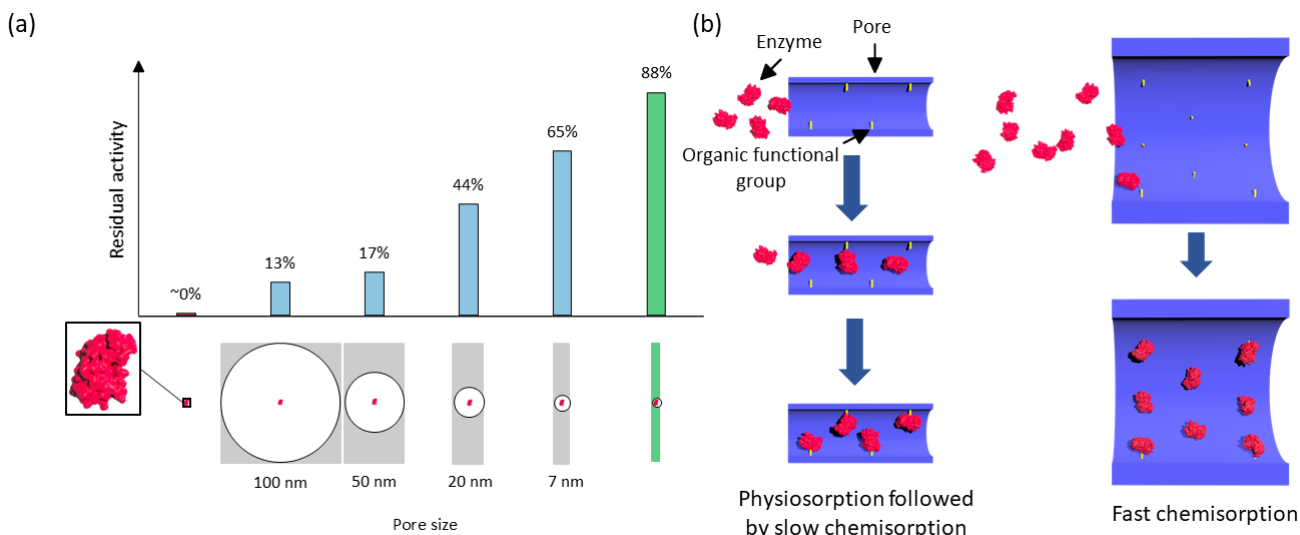


Figure 1. (a) Pore size vs residual activity after thermal treatment (e.g. boiling water, 1h) for encapsulation in materials with different pore size (see SI: 01a_small_pore.mp4) (obtained from data of Ref. 21) and (b) size of the pores for infiltration depending on the dominant adsorption process. (See SI: 01b_large_pore.mp4) Adapted from Ref. 22, copyright[2005] The Royal Society of Chemistry.

Infiltration of enzymes also leads to a biocomposite where the enzyme is often tightly housed within the MOF pore network. Typically, for successful diffusion of enzymes, the MOF pores should be larger than the protein. However, there are limited examples that show the size restriction imposed by a framework's pore apertures can be overcome by a process in which the protein partially unfolds to facilitate infiltration into the MOF and then refolds once inside.^{23,24} Nevertheless, encapsulation approaches offer a distinct advantage over infiltration as the MOF pore size is independent of the size of the protein. A caveat is that single-step encapsulation methods, that provide the highest level of protection, (*vide supra*) impose a restriction on the size of the substrate or cofactor that can access the enzyme. Additionally, there are a limited number of MOFs which can be utilized for one-pot encapsulation of enzymes, due to the general requirements of facile room temperature synthesis under biologically relevant conditions. For infiltration or surface attachment, the MOF synthesis and the infiltration/surface attachment steps are separated and thus biocompatible conditions do not limit the matrix preparation.

Like encapsulation strategies, enzyme infiltration in MOFs is still in its infancy. However, insight can be drawn from the more mature field of enzyme infiltration within the pores of silica-based mesoporous materials.^{25,26} In studies focused on such silica-based biocomposites the internal loading of biomolecules depends on the nature of the adsorption.²⁶ For example, if the adsorption is reversible (or adsorption is rapid and immobilization is slow), then the pore size only needs to exceed the size of the protein as diffusion proceeds until a high loading is achieved. Conversely, if permanent immobilization is rapid, a high loading can only be obtained by using a matrix with a pore diameter at least three times larger than the protein size (**Figure 1b**). For intermediate cases (i.e. the speed of adsorption and permanent immobilization are equivalent) a pore diameter of more than twice the biomolecular radius

would be required. Generally, examples of enzyme infiltration into MOFs occur where the adsorption is reversible and thus the pore size only marginally exceeds the size of the enzyme. Furthermore, to minimize pore blocking during infiltration, three-dimensional connectivity is an inherent advantage over one dimensional channels; this is also critical for substrate and cofactor access.

Compared to surface conjugated enzymes, encapsulated enzymes typically maintain better performance during recycling as the enzyme is imbedded within MOF particles. For surface adsorbed enzymes both washing procedures and reutilization of the biocomposite lead to randomly oriented enzymes on the surface and a progressive release of enzyme in solution.²⁷ This can be ameliorated by covalently linking enzymes to the MOF surface. However, post-modification linker exchange methods^{28,29} and room temperature Ostwald ripening mechanisms^{30,31} suggest that MOF structures are dynamic and thus the release of enzymes into solution may occur. An assessment of leaching should be carried out for each enzyme/MOF system to accurately determine catalytic activity of the biocomposites during cycling studies.^{11,32}

Another advantage of encapsulation over infiltration and surface conjugation strategies is the facile 'one-pot' synthesis of multi-enzyme biocomposites. By simply exposing the MOF precursors to a solution containing two (e.g. glucose oxidase (GOx) and HRP) or three (β -galactosidase (β -gal), GOx and HRP) enzymes in the desired weight ratio, Chen et al. prepared multi-enzymes@ZIF-8 (ZIF = zeolitic imidazolate framework) biocomposites.³³ When compared with a mixture of free enzymes in solution, the multi-enzyme@ZIF-8 confines the chemical reaction within the MOF matrix resulting in a 7.5-fold enhancement in the activity of the biocatalytic cascade reaction. Conversely, multi-enzyme biocomposites formed via infiltration can require intricate strategies for successful incorporation of both enzymes.³⁴ To prepare similar multi-enzyme biocomposites via infiltration protocols, MOFs possessing hierarchical structures (different pore sizes) need

to be specifically chosen, or orthogonal conjugation strategies need to be employed, respectively.

Though the encapsulation process offers excellent protective capacity and recyclability with respect to infiltration and surface conjugation strategies, there are several areas where these enzyme@MOF biocomposites are not as synthetically flexible or are outperformed by the other systems, these include:

- 1) Synthetic constraints required for the preparation of the biocomposite.^{35, 36}
- 2) The reduced catalytic conversion rates. The catalytic conversion rate of the encapsulated enzyme will be limited, with respect to the free enzyme, by mass transfer of reagents and products through the MOF network.^{37, 38, 39}
- 3) Hitherto, the encapsulation strategy is limited to a narrow range of MOFs.⁴⁰ Research in this area has predominantly focused on ZIF-based biocomposites as they can be synthesized under biocompatible conditions.^{16, 17, 33, 38, 41-46} Zn-based ZIFs degrade in acidic pHs^{47, 48} and in presence of phosphate ions^{40, 49, 50} and possess narrow pore apertures $< 3.4 \text{ \AA}$.⁵¹

3. MOF-BASED ENZYME BIOCOMPOSITES FORMED VIA ENCAPSULATION

Enzymes can be encapsulated within individual MOF particles or hollow, polycrystalline, MOF shells with the aim of protecting the biological cargo from external environments. The former type of biocomposites are typically synthesized via a single-step approach where the MOF precursors and selected enzyme are combined, under biocompatible conditions (e.g. water-based solution, room

temperature), to precipitate enzyme@MOF materials (**Figure 2a**). This approach physically confines the enzymes within adventitious mesopores that are formed in the MOF crystal. However, very recent work has shown that single enzyme@MOF crystals can be post-synthetically 'hollowed' to afford macroporous cavities which provide a less constrictive environment.⁵² Typically, to generate hollow MOF particles, templating methods are required where the enzymes are encapsulated within the template and then the MOF particles are grown on the template surface. A salient aspect of both encapsulation strategies is that they allow for the incorporation of enzymes within MOF particles where the enzyme has considerably larger dimensions than the pore diameter of the framework. The obvious benefit of such systems is that leaching of the enzyme is not possible without first decomposing the MOF. Furthermore, the MOF pores can enforce selective permeability^{19, 38, 53} and can thus regulate molecule transport to and from encapsulated enzymes (**Figure 2b**).

By careful choice of the reaction conditions, enzyme@MOF biocomposites can be obtained as particles ranging from tens of nanometres⁵⁴ to tens of micrometres¹⁸ and various morphologies, including single crystal particles (e.g. rhombic dodecahedron morphology for enzymes@ZIF-8) and hollow particles with polycrystalline shells (e.g. MIL-88, MIL = Materials Institute Lavoisier).¹⁸ In this section, we focus on the encapsulation and protection of enzymes within MOFs for biocatalysis; however, it is worth noting that encapsulation methods can be successfully applied to other biomacromolecules (e.g. insulin, hyaluronic acid (HA), heparin (HEP), deoxyribonucleic acid (DNA), and antibodies).⁵⁵⁻⁵⁸

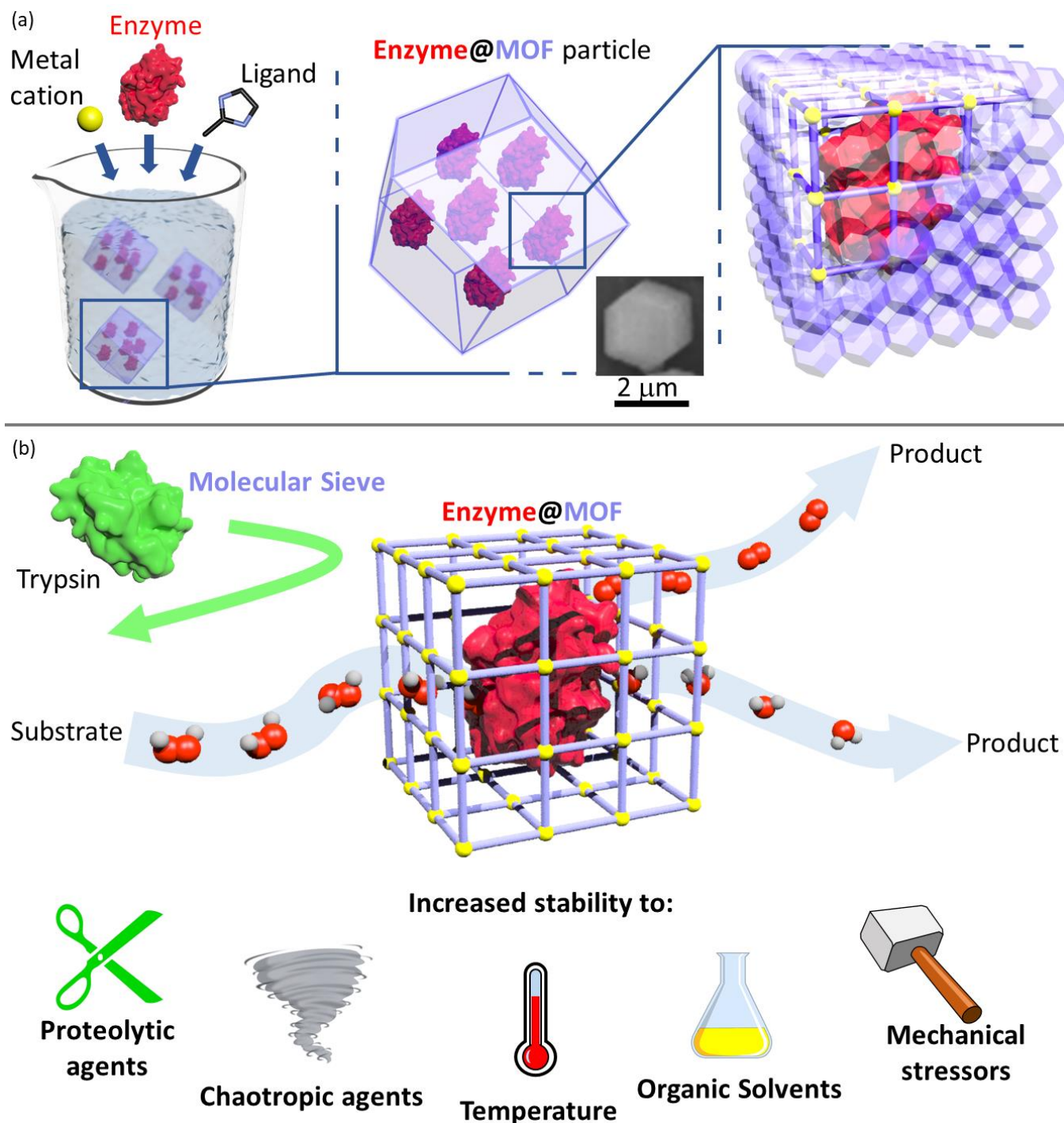


Figure 2. (a) A schematic showing the procedure for enzyme encapsulation in MOFs by the one-pot (non-templated) method and showing the nature of the resulting enzyme@MOF biocomposite. (b) A representation of the advantages of MOF encapsulation in terms of increased stability coupled with substrate access. (See SI: 02_overview_enzyme_mof.mp4).

3.1. Templating methods

The synthesis of hollow and core-shell MOF capsules has been achieved via template-free or template-based strategies.^{59, 60} With respect to the formation of MOF-based biocomposites, either soft- or hard-templating approaches are employed.¹⁰ The first example of soft templating was reported by Bradshaw and co-workers⁶¹ who encapsulated a variety of proteins (e.g. green fluorescent protein

(GFP), fluorescein-tagged enzymes *Candida Antarctica* lipase B (CalB), and β -gal) into agarose hydrogel droplets, which were stabilized by UiO-66 (Universitetet i Oslo) and magnetite nanoparticles (**Figure 3**). These particle-coated droplets served as a surface for the growth of a crystalline ZIF-8 shell. Each component of the biocomposite played a specific role: i) imbedding proteins in agarose gel preserved the structure of the proteins from alcohols (isopropanol and 2-butanol) that were used to grow a continuous

4 - 5 μm thick ZIF-8 shell; ii) the MOF coating acted as a molecular sieve for transesterification reactions (1-butanol and vinyl acetate to yield butyl acetate - 100% conversion in 12 h, and 3-(4-hydroxyphenyl) propan-1-ol and vinyl laurate to yield 3-(4-hydroxyphenyl)propyl dodecanoate - 7.5% conversion in 48 h); and, iii) the Fe_3O_4 nanoparticles, allowed for the 40 μm MOF-biocomposite particles to be magnetically separated and cycled six times. In another example, Kim and co-workers¹⁸ adopted the previously reported interfacial synthesis⁶² approach to prepare enzyme@MIL-88A systems (**Figure 4**). Reagents were separated into two immiscible solutions: fumaric acid (H_2fum) was dispersed in 1-octanol (organic phase) while Fe^{3+} and proteins (glycerol dehydrogenase (GDH), HRP, and acetylcholinesterase enzyme (AChE)) were dispersed in water (aqueous phase). By injecting droplets of the aqueous phase into the continuous organic phase, a MIL-88A shell formed at the droplet-solution interface to yield

GDH@MIL-88A, HRP@MIL-88A, and AChE@MIL-88A. The MOF coating protected the encapsulated proteins from exposure to protease; however cycling studies showed a rapid loss in activity that was attributed degradation of the capsule and subsequent release of enzymes into solution. Another templating system was reported by Li and co-workers⁶³ who encapsulated GOx in CaCO_3 and then coated the composite with polydopamine (PDA) and ZIF-8. The authors used ethylenediaminetetraacetic acid (EDTA) to selectively remove the internal CaCO_3 template and realize hollow PDA/ZIF particles. The aforementioned templating strategies confine enzymes within hollow MOF capsules¹⁸. Such architectures are likely to offer the best protective performance as a shield that prevents diffusion of large molecules that are harmful to enzymes (e.g. pepsin, TRY). However, the large cavities (relative to protein size) cannot prevent the protein unfolding (*vide infra*), thus offer limited protection to elevated temperature, chemical denaturants and organic solvents is limited.

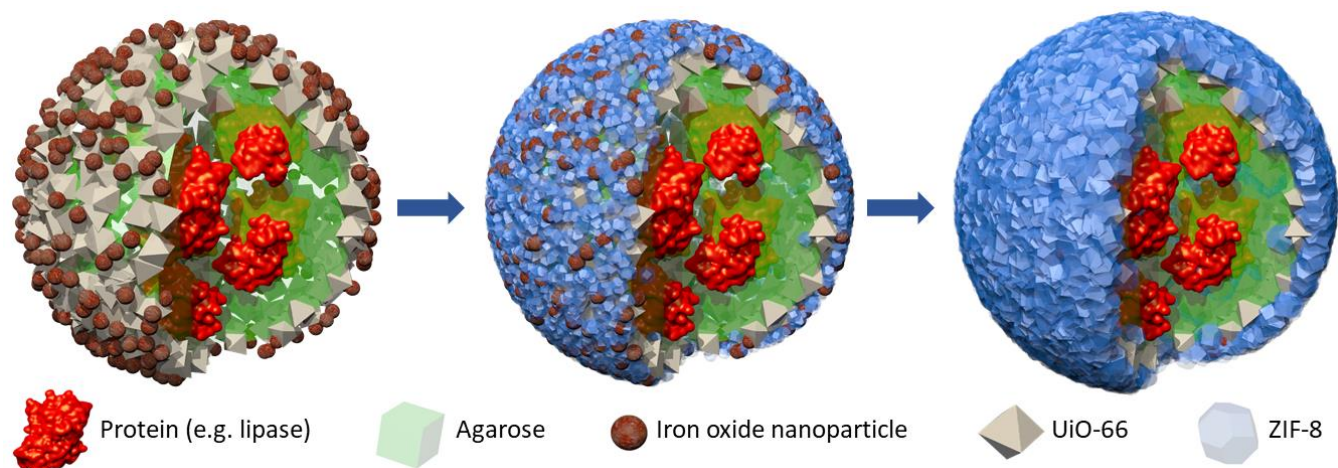


Figure 3. Soft templating approach where proteins are imbedded in agarose hydrogel droplets, stabilized by UiO-66 and MNPs, and a ZIF-8 coating is grown over this droplet. (See SI: 03_soft_templating.mp4).

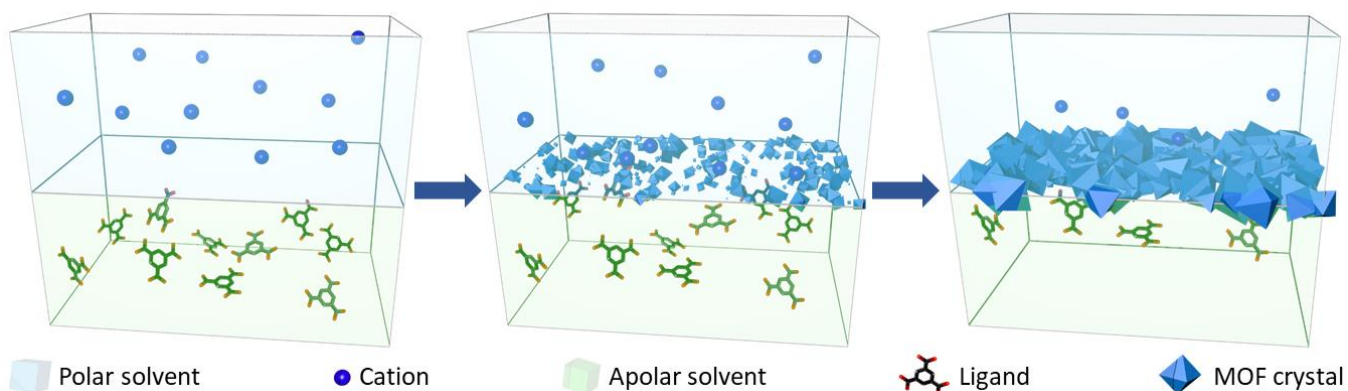


Figure 4. Interfacial synthesis of MOFs. Proteins (e.g. GDH, HRP, and AChE) can be introduced into the aqueous layer and are incorporated into the MOF crystals which form at the interface.⁶⁴(See SI: 04_interfacial_growth.mp4.) Figure adapted from concepts described in Ref. 64.

We have thus far discussed examples where enzymes are encased in protective MOF shells; however, MOFs can also be used as sacrificial templates (**Figure 5**). For example, Wang et al. imbedded penicillin G acylase (PGA) in a CaCO_3 /ZIF-8 composite which was then coated with TiO_2 . Subsequently, full removal of the CaCO_3 /ZIF-8 core could

be achieved by treating the biocomposite with EDTA.⁶⁵ After the dissolution of the MOF template, PGA encapsulated in TiO_2 retained activity, furthermore, the composite was reused eight times and showed higher activity than the same enzyme immobilized into silica-based monoliths. Alternatively, Chen and co-workers⁶⁶ encapsulated bovine serum albumin (BSA) and catalase (CAT) in ZIF-90 or ZPF-

2 (constructed from Zn^{2+} and 2-hydroxy-5-fluoropyrimidine; ZPF = zeolitic pyrimidine framework), which allowed a covalent-organic framework (COF) shell to be grown on the surface of the composites via condensation of 1,3,5-triformylbenzene (or 1,3,5-tris(*p*-formylphenyl)benzene) and 2,5-bis(ethoxy)terephthalohydrazide (COF-42-B or COF-43-B). The ZIFs were then

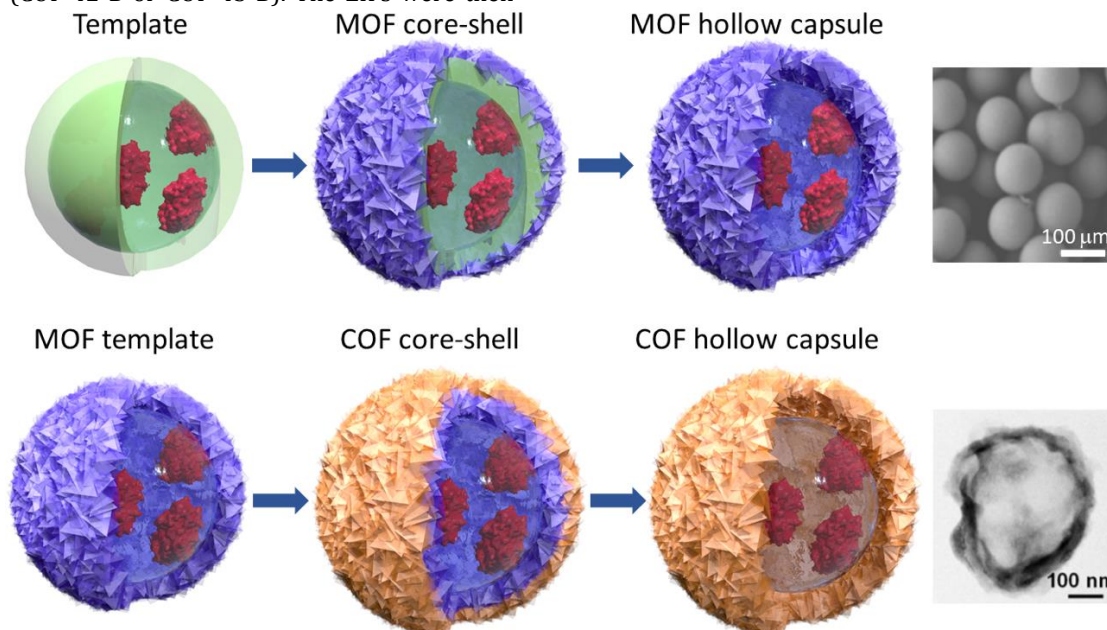


Figure 5. Encapsulation using the templating method: (a) a MOF shell is grown on a template (see SI: 05_encapsulation_by_templating.mp4) (SEM micrograph adapted from Ref. 67, Copyright [2015] American Chemical Society) or (b) protein@MOF is used as a template for the subsequent growth of a different porous shell (e.g. COF) (SEM micrograph adapted from Ref. 68, Copyright [2015] American Chemical Society).

3.2. One-pot embedding (non-templated)

MOF biocomposites can also be formed via a one-pot encapsulation method. There are two closely related synthetic approaches, the first employs additives (such as biocompatible polymers) and/or organic solvents to promote biocomposite formation while the second termed 'biomimetic mineralization' is where the biomacromolecule induces the growth of the MOF in water without additives.¹⁰ The first report of a protein@MOF biocomposite via the one-pot strategy was in 2014 by Ge, Liu and co-workers.¹⁷ The authors described the rapid precipitation of CytC@ZIF-8 from a solution of 2-methylimidazole (2-mIM), zinc nitrate hexahydrate, cytochrome C (CytC) and polyvinylpyrrolidone (PVP) in methanol. Transmission electron microscopy (TEM) analysis on CytC@ZIF-8 particles calcined at 325 °C (2h) showed the presence of 'pockets' within their sub-surface region that were of sufficient size to accommodate CytC. Notably, the activity of CytC@ZIF-8 showed a 10-fold enhancement compared to the same concentration of free enzyme in solution (**Figure 6a**). This process was termed *co-precipitation* and has been successfully extended to different bioactive molecules such as HRP and lipase to form HRP@ZIF-8 and lipase@ZIF-8 biocomposites.⁶⁹ In 2015, Shieh et al¹⁹ synthesized biocomposites via the '*de novo*' approach, by mixing CAT, PVP, 2-imidazolecarboxaldehyde (ICA) and zinc nitrate hexahydrate in water to yield the formation of CAT@ZIF-90. The authors showed that the resulting bio-

dissolved under acidic conditions (pH=5.5) to yield catalytically active and recyclable enzyme@COF composites. In summary, these examples highlight the versatility of MOF materials in the synthesis of biocomposites using template strategies as both the protective shell of hollow capsules or as hard templates.

composite allowed selective diffusion of H_2O_2 while protecting the enzyme from a protease (proteinase K). A noteworthy advance of this study was that water was used as solvent rather than methanol, which can have a deleterious effect on enzyme activity.⁷⁰ An alternative one-pot encapsulation strategy for the encapsulation of enzymes in MOFs was reported by Liang et al. who showed that ZIF-8-based biocomposites were spontaneously formed, in water, from the simple combination of a selected protein, 2-mIM and zinc acetate.^{16, 71} This method revealed that neither PVP nor alcohol is necessary for the encapsulation of proteins in ZIF-8 crystals. (see SI: biomimetic mineralization.mp4) The process was termed *biomimetic mineralization* due to its similarities to the natural heterogeneous seeding process of biomineralization where living organisms form minerals without the need for additional crystallization facilitators.^{16, 37, 39, 72, 73} The enzymatic activity of the biocomposite HRP@ZIF-8 obtained via biomimetic mineralization of HRP was examined and was largely retained after being exposed to proteolytic agents (e.g. TRY), an organic solvent (*N,N*-dimethylformamide (DMF)) and elevated temperature (up to 100 °C).¹⁶ Additionally, it was shown that proteins maintained their function after dissolving the ZIF-8 shell by lowering the solution pH to 6. Two different biocomposites were prepared, DQ-OVA@ZIF-8 (DQ-OVA = DQ-ovalbumin), which contained the fluorogenic protein DQ-OVA and TRY@ZIF-8. When combined in the same reaction vessel at pH 7 no fluores-

cence signal was detected; however, when the pH was reduced to 6 and the ZIF-8 coating dissolved, both DQ-OVA and TRY were released and TRY degraded DQ-OVA into fluorescent fragments (**Figure 6b**).

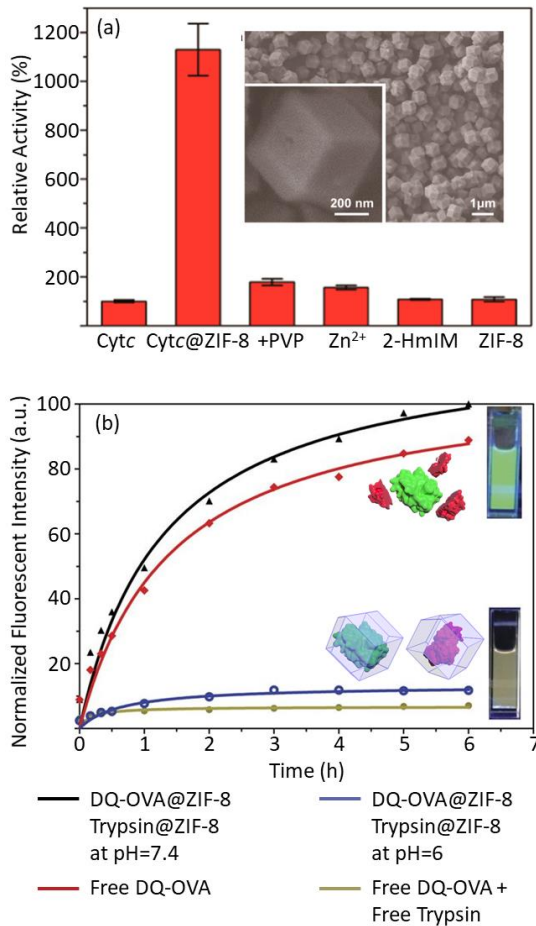


Figure 6. (a) SEM micrographs of calcined CytC@ZIF-8 and relative activity data for CytC@ZIF-8 composites compared to the activity of an equivalent quantity of free enzyme in solution. Figure adapted from Ref. 74, Copyright [2014] American Chemical Society (b) Data showing that enzymes encapsulated in ZIF-8 via biomimetic mineralization retain activity. In this experiment enzymes from two composites are combined and the enzyme release is triggered by lowering of the pH. Adapted with permission from Ref. 16 under the terms of the CC BY 4.0 license.

To confirm that the biomimetic mineralization describes a process where MOF formation is induced by the presence of a biomacromolecule, it is necessary to determine the MOF particle growth kinetics of water-based precursor solutions with and without the biomacromolecules (e.g. enhanced MOF nucleation time, particle growth, and yield).^{16, 39} In one study the co-precipitation and biomimetic mineralization processes were compared for the enzyme Jack bean urease. ZIF-8-based biocomposites were prepared with and without PVP during the synthesis and it was found that PVP can influence the particle size of the biocomposite, catalytic performance, and the level of protection to elevated temperature (**Figure 7**).⁴² Under the synthetic conditions employed for this study the two methods engender distinct spatial localization of the enzymes within the ZIF-8 crystal. Synthesis in the presence of PVP produced a composite that when calcined engendered ‘pockets’ of sufficient size to incorporate enzymes, located towards the surface region of the MOF particles.³⁹ These results were consistent with the prior report of Ge and co-workers.¹⁷ In contrast the PVP free synthesis yielded a biocomposite where the enzymes were homogeneously distributed throughout the ZIF-8 crystals. This difference in spatial location of the encapsulated enzymes within the MOF crystals may account for the slightly superior activity under elevated temperature for the biocomposites synthesized via the biomimetic mineralization method.

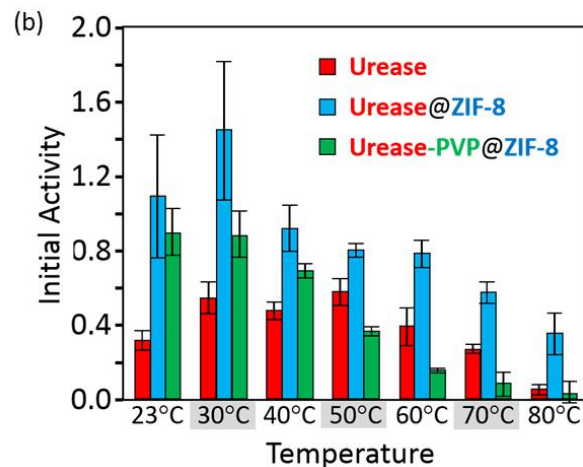
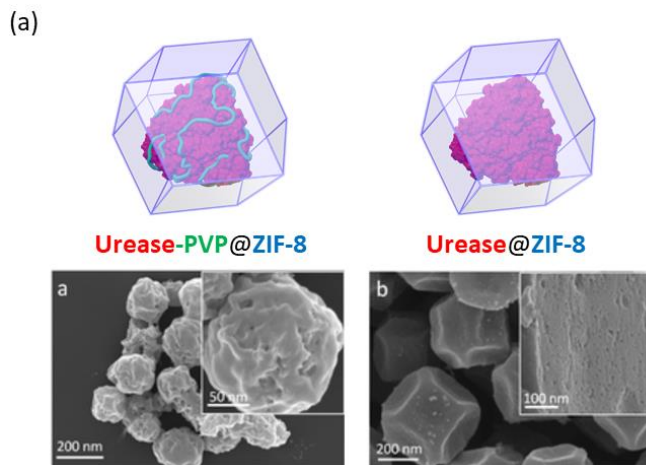


Figure 7. (a) Urease@ZIF-8 prepared with and without PVP as an additive and resulting SEM image (b) Initial activity at different reaction temperatures. Figures adapted from Ref. 75, copyright [2016] The Royal Society of Chemistry.

In addition to batch synthesis, one-pot enzyme encapsulation can be carried out via continuous flow methods. Indeed, Carraro et al. reported that continuous flow is a con-

venient method for synthesizing protein@ZIF-8 biocomposites with tunable particle size.⁷⁶ Previously, *in situ* SAXS experiments had confirmed that the crystalline biocomposites are formed from amorphous material⁷⁷ and

that crystallization can be triggered by ethanol exposure.⁷⁸ Under flow conditions, particle size control was achieved by modulating the residence time of the growing protein@ZIF-8 particles in a reactor prior to the introduction a flow of ethanol. The authors also showed continuous 5h production of 60 nm BSA@ZIF-8. In another study, Hu et al. controlled protein encapsulation by adjusting the residence time of the growing ZIF-8 particles prior to injecting the solution with enzymes.⁷⁹ By employing a microfluidic device the precursor and enzyme concentrations could be modified in the gradient mixing on-chip to introduce defects in the MOF structure (e.g. Zn coordination defects). The presence of defects facilitated the diffusion of reagents through the MOF; as a result, compared to non-defective enzyme@ZIF-8, the enzymatic activity was considerably increased.

The one-pot embedding strategy for the synthesis of MOF-based biocomposites has been achieved for a variety of enzymes and studies have highlighted the potential of enzyme@MOF systems for application to biotechnology and biomedicine.⁴⁶ However, the preparation of these materials is highly sensitive to the synthesis conditions. Literature reports^{80, 21, 75, 81-83} indicate that the synthetic method can play a significant role in: 1) the formation kinetics of biomacromolecule@MOF particles and their topology; 2) the bioactivity of the biocomposite; 3) the protection of the bioactive molecules; and, 4) the release of the encapsulated cargo. Thus, a fundamental understanding of how the synthetic parameters influence the properties of enzyme@MOF is crucial for their translation to real-world applications.

3.3. Parameters influencing the chemistry of enzyme@MOF biomcomposites

Several parameters are known to influence the formation, structure, activity and release of proteins encased within MOFs. In the following section the effect of chemical additives, enzyme surface charge and MOF precursor concentration will be canvassed.

3.3.1. Additives

Additives, such as PVP, act as a co-precipitant to a solution of MOF precursors and enzyme to facilitate composite formation.^{17, 19} PVP is a biocompatible and FDA (The Food and Drug Administration) approved polymer⁸⁴ that is used to stabilize enzymes in solution through electrostatic/hydrogen bonding interactions.^{4, 85} In the co-precipitation method PVP-functionalized enzymes are prepared by mixing PVP with enzymes in water (with or without the

MOF ligand) to form a PVP-modified enzyme.^{17, 19} However, we note although PVP is used in some enzyme extraction processes from plants to prevent the denaturation⁸⁶ it can also modify the native enzymatic activity.⁸⁷ Thus, in cases where PVP is employed as a co-precipitant the activity of the PVP-modified enzyme should be compared to the free enzyme as an experimental control. In addition, if the enzyme@MOF system is designed for biomedicine application, a low molecular weight PVP should be chosen to prevent its accumulation in body tissues.^{84, 88}

To understand the role of PVP in promoting MOF crystallization, it is instructive to look at studies where PVP is employed as a stabilizing and shape-directing agent in the synthesis of metallic nanoparticles (NPs).⁸⁹ It is well known that PVP has a high affinity for metallic NPs due to its

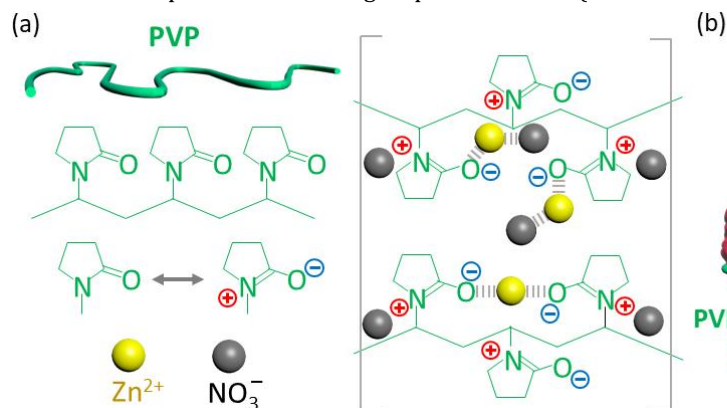


Figure 8),^{89, 90} moreover, PVP has been used for the preparation of inorganic NP@MOF composites.^{53, 91, 92} In MOF crystallization, PVP was found to play an active role due to its affinity, via the weak coordination sites of the pyrrolidone moieties, towards metal cations (e.g. ZIF-8, ZIF-90, ZIF-67, Fe^{III}-MOF-5, HKUST-1 (HKUST = The Hong Kong University of Science and Technology), and MOF-505).⁹³⁻⁹⁶ The capacity of PVP to increase the concentration of metal cations at its surface is critical to promoting the growth of ZIF-8. Indeed, Maddigan et al. showed the importance of the local concentration of Zn²⁺ to rapid crystallization of enzyme@ZIF-8 biocomposites in the absence of PVP.⁹⁷ Although PVP is the most common polymer employed for the preparation of biocomposites based on ZIFs (e.g. ZIF-8, ZIF-90)^{17, 19} and a few other MOFs (e.g. GOx@Fe-BTC (BTC = 1,3,5-benzenetricarboxylic acid)),⁹⁸ other biocompatible polymers and MOFs could be used to expand this research.

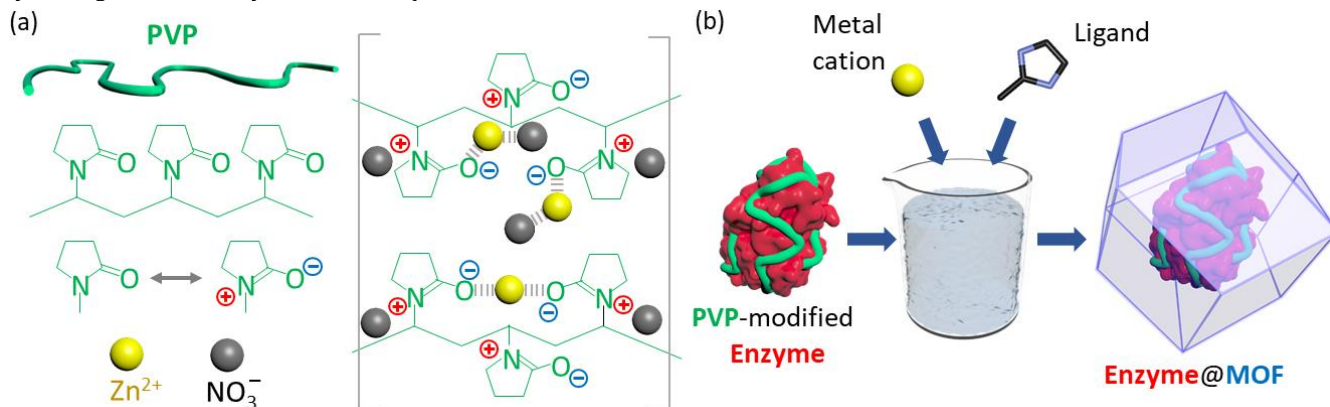


Figure 8. (a) The structure of PVP and a schematic showing their attraction of metal ions and (b) a schematic showing enzyme immobilization using PVP.

The addition of a base to the reaction mixture can also promote the formation of MOF-based biocomposites. Bases enhance the kinetics of crystallization by deprotonating the organic ligands and thus promoting their interaction with metal cations.⁹⁹ For example, Gascón and co-workers reported that laccase (LAC) and β -glucosidase can be encapsulated in three different MOFs (MIL-53-NH₂(Al), MIL-53(Al) and Mg-MOF-74) employing either triethylamine, ammonium hydroxide or sodium hydroxide, to deprotonate the MIL-53(Al) and MIL-53-NH₂(Al) linkers.¹⁰⁰ In another study by Liang et al.³⁹ CAT@MAF-7 and urease@MAF-7 biocomposites were prepared (MAF = metal azolate framework) using ammonia, which was required to deprotonate the 3-methyl-1,2,4-triazole (Hmtz) ligand. This strategy could be extended the encapsulation of enzymes within hitherto unexplored MOFs that otherwise do not spontaneously form on addition of proteins. However, we note that the base employed and its concentration should be compatible with the protein.

3.3.2. Enzyme Surface Chemistry

The distinct primary amino acid sequence and tertiary or quaternary structure of a protein determines which amino acids are surface exposed and thus its unique surface chemistry.¹⁰¹ The variance in surface chemistry can be significant, for example identical enzymes expressed by different organisms can show substantial variations in surface properties, via post-translational modifications.¹⁰²⁻¹⁰⁴ In the initial report of enzyme encapsulation via biomimetic mineralization, Liang et al. hypothesized that nucleation of ZIF-8 was induced by: 1) the accumulation of Zn²⁺ cations on the surface of proteins and 2) the adsorption of 2-mIM on the biomacromolecules due to its intrinsic hydrophobic/hydrophilic domains.¹⁶ A subsequent study by Maddigan et al.⁹⁷ showed that some proteins do not induce the rapid crystallization of ZIF-8 and are not encapsulated via biomimetically mineralization.⁹⁷ Proteins that possess a high number of surface acidic residues (e.g. glutamate, pKa 4.3) are negatively charged under biocomposite synthesis conditions ([2-mIM]= 160 mM, [Zn²⁺]= 40 mM) while, under analogous conditions, proteins that possess a high number of externally directed basic residues (e.g. arginine (Arg), pKa 12.5) are positively charged. It was uncovered that only proteins with negatively charged proteins favor the accumulation of Zn²⁺ and consequently the

spontaneous formation of ZIF-8 under these conditions (**Figure 9a**). Accordingly, the protein ionization potential can be used as a, straightforward, proxy to determine whether a protein induces MOF formation. The authors confirmed this hypothesis by modifying the protein surface chemistry to either induce (e.g. lower isoelectric point (pI) via succinylation), or inhibit (e.g. raise pI via amination reactions) MOF crystallization (**Figure 9b**). These experiments were supported by computational studies that showed negatively charged proteins significantly enhance the concentrations of Zn²⁺ at its surface whilst the accumulation of 2-mIM to the protein surface via hydrophobic interactions plays a marginal role in triggering the self-assembly of the MOF.

Alternative methods for increasing metal cation concentration at the protein surface have been inspired by nature. For example, metallothioneins (MTs) are cysteine-rich polypeptides that can bind a large number of metal cations, including Zn²⁺, Cd²⁺, and Cu²⁺.¹⁰⁵ In these polypeptides, metal ions are mostly coordinated through cysteine (Cys) thiolates¹⁰⁶ (**Figure 9c**) and, in fewer cases, through histidine (His)-residues.¹⁰⁵ Chen et al. used this concept to develop an amino acid-boosted one-pot embedding strategy.⁴¹ The formation of Zn- and Cu-based MOFs (e.g. ZIF-8, HKUST-1) was induced by exposing the protein to PVP and Cys. PVP acts as a coating agent that facilitates embedding Cys on the surface of the protein. In the case of ZIF-8, Cys accumulates Zn²⁺ ions via mercaptide bond formation,¹⁰⁷ thereby triggering the nucleation of the MOF around the protein/PVP/Cys clusters (**Figure 9d**). Using this approach, the authors encapsulated myoglobin (Mb), a protein that does not spontaneously induce the crystallization of ZIF-8 due to its surface charge (typical isoelectric point = 7.6)⁹⁷ under 4:1 ligand:metal ratios. In addition to inducing MOF formation, proteins and certain amino acids can act as templates, playing a critical role in determining the resulting MOF topology.¹⁰⁸ For example, Wang et al. examined 20 natural amino acids on their effect on ZIF-8 topology and showed that His could redirect the topology from diamondoid (dia) to sodalite (sod). Furthermore, they observed that His can act as a co-templating agent during MOF synthesis, increasing the protein encapsulation efficiency (e.g. by 31% for BSA for ZIF-8).¹⁰⁸

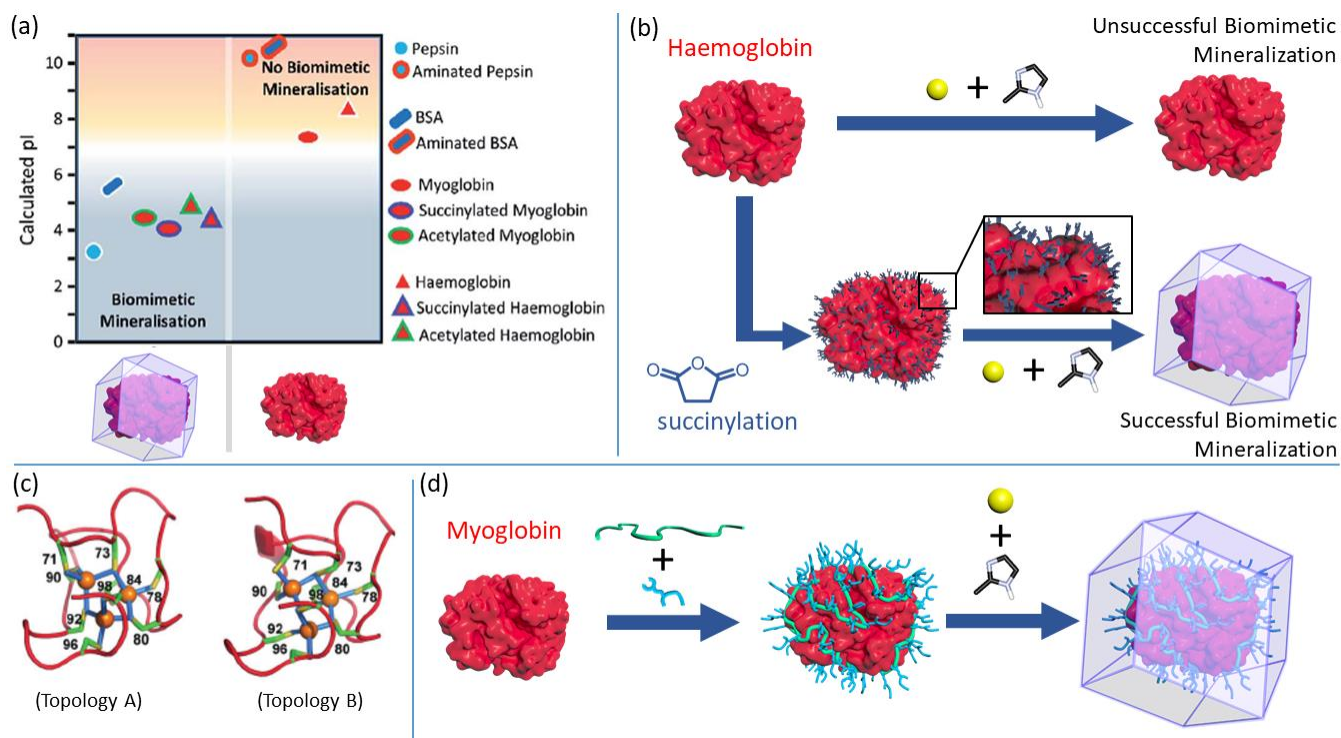


Figure 9. (a) Data showing how the calculated ionization potential can be used as a proxy to determine whether a protein induces MOF formation. (b) A schematic showing how modifying the protein surface chemistry by succinylation lowers the pI of a protein and induces MOF crystallization for proteins that would not normally be encapsulated. Panels (a) and (b) Adapted with permission from Ref. 109, under the terms of the CC BY 3.0 license. (c) The structure of the metallothioneins (MTs) showing the cysteine residues. Adapted with permission from Ref. 110, © 2017 Wiley - VCH Verlag GmbH & Co. KGaA, Weinheim. (d) Use of MTs in triggering the nucleation of MOFs around the protein/PVP/Cys clusters (PVP = green tape; MT = pale blue connector) where it would normally not form, e.g. for myoglobin. Adapted with permission from Ref. 111, © 2019 Wiley - VCH Verlag GmbH & Co. KGaA, Weinheim.

3.3.3. MOF precursors and structures

The majority of enzymes@MOF biocomposites employ ZIF-8 as a matrix. Typically, ZIF-8 possesses a sod topology with permanent microporosity.⁹¹ However, by changing the total precursor concentration or the Zn^{2+} :2-mIM:enzyme ratios ZIF-based biocomposites can be synthesized with different topologies including ZIF-L (dia) or katsenite (kat), ZIF- CO_3 -1 (ZIF-C, composed of Zn^{2+} , 2-mIM and CO_3^{2-}), unknown phases (U12, U13, ZIF-8X) or yield amorphous materials.^{37, 47, 57, 112, 113} The different phases possess distinct physical properties (e.g. porosity) and chemical stability (e.g. different dissolution kinetics in acidic environment). It is not yet understood how the different ZIF phases affect the protective capacity and the activity of an encapsulated enzyme; however, it is likely that controlling the crystalline phase of the ZIF matrix will prove to be a useful tool for modifying the chemistry of enzyme@ZIF biocomposites. For example, Wu et al. demonstrated that the enzyme (e.g. GOx) encapsulated in amorphous ZIF was up to 20 times more active when compared to the enzyme encapsulated in crystalline ZIF-8.³⁷ The improved performance was attributed to the presence of coordination defects that produced mesopores in the amorphous MOF particles and facilitated reagent diffusion.

Another important consideration for MOF-based biocomposites is the hydrophobicity/-philicity of the framework. In general, proteins tend to have a high affinity for hydrophobic surfaces.¹¹⁴ However, hydrophobic interactions can engender conformational changes that denature the protein and lead to loss of enzymatic activity.¹⁰¹ The effect of framework hydrophobicity on the activity of enzymes was examined by Liang et al. who synthesized three ZIF materials that possess the same topology but different hydrophobicity/-philicity: ZIF-8, ZIF-90 and MAF-7.³⁹ ZIF-90 (composed of Zn^{2+} and ICA) and MAF-7 (composed of Zn^{2+} and mtz) are hydrophilic ZIFs^{115, 116} and were shown to preserve the structure and activity of encapsulated enzymes, urease and CAT, even at elevated temperature ($T = 70^\circ\text{C}$) (Figure 10).³⁹ In contrast, for the hydrophobic material, ZIF-8, encapsulated and surface adsorbed enzymes were found to be largely inactive. Fourier transform infrared spectroscopy (FTIR) was used to examine the biocomposites and it was revealed that for CAT@ZIF-8 the secondary structure of the protein was perturbed, thus providing an explanation for the loss of enzymatic activity. These studies highlighted the importance of understanding the chemistry at MOF/biointerface to maximize the activity of both enzyme@MOF and enzyme-on-MOF systems.

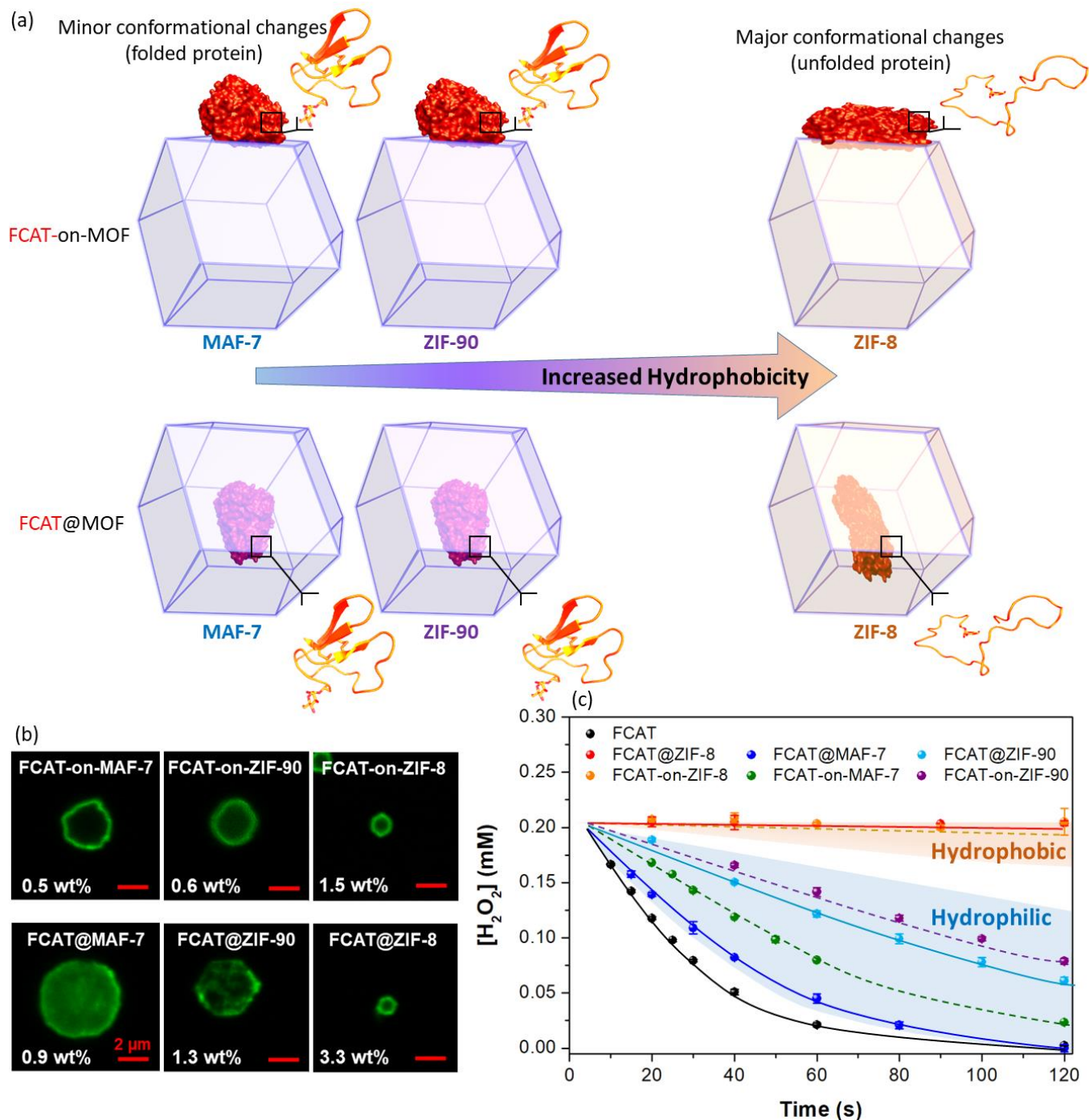


Figure 10. (a) Effects of MOFs with varying degree of hydrophobicity on CAT -on- or @ MAF-7, ZIF-90 and ZIF-8. (b) Confocal Laser Scanning Microscopy (CLSM) of CAT -on-/@ MAF-7, ZIF-90 and ZIF-8 showing differences in localization, particularly amongst the encapsulated samples. (c) Activity data for CAT -on-/@ MAF-7, ZIF-90 and ZIF-8 compared with the free enzyme. (See SI: 10_hydrophobic_effects_of_mofs.mp4) Figure adapted from Ref. 80, Copyright [2019] American Chemical Society.

3.4. Alternative synthesis strategies

The most widely employed synthetic procedures for enzyme@MOFs are via solution-based processes. As a consequence, the MOF synthesis conditions (temperature, solvent) need to be compatible with the stability of the enzyme. This typically limits solution-based approaches to mild conditions, i.e. room temperature, and water as the solvent.⁴⁷ Thus there are no examples of enzyme encapsulation via solution-based synthesis for MOFs, such as the UiO family, that require comparatively harsher conditions to form i.e. high temperature and organic solvents.¹¹⁷ Recently, mechanochemical synthesis has been reported as a potential alternative to solution-based processes for the direct encapsulation of enzymes in MOFs.¹¹⁸ Mechano-

chemical processes (e.g. ball milling) are industrially scalable, solvent-free methods that have been employed for the synthesis of several different MOFs.^{119, 120} Wei et al. explored the ball milling synthesis of several MOFs (e.g. ZIF-8, UiO-66-NH₂, Zn-MOF-74) in presence of lyophilized enzymes.¹¹⁸ In a ball milling synthesis of enzyme@MOFs, dried MOF precursors are added into a zirconia grinding jar containing lyophilized enzymes. The mixture is then ground to promote the MOF formation and to obtain the final biocomposite. This approach succeeded with the preparation of biocomposites that could not be achieved via solution synthesis. Although limited attention has been devoted to ball milling process for the preparation of composites,^{121, 122} it emerged as an attractive strategy that may facilitate the expansion of enzyme encapsulation to, as yet, unexplored MOFs.

Table 2. Examples of encapsulation of enzymes into MOFs by the one-pot (non-templated) approaches showing the MOF used, the enzyme, the method variation and the main application.

MOF	Enzyme	Immobilization method	Application	Ref.
ZIF-8	cytochrome C	One-pot/Co-precipitation (PVP)	Biosensor	17
ZIF-90	catalase	One-pot/De novo (PVP)	Biocatalysis	19
	horseradish peroxidase			
ZIF-8	Urease	One-pot/Biomimetic mineralization	Biocatalysis	16
	Pyrrroquinoline quinone-dependent glucose dehydrogenase			
ZIF-8	β -galactosidase	One-pot/Biomimetic mineralization	Biocatalysis, biobanking	123
ZIF-90	catalase	One-pot/De novo (PVP)	Biobanking, biocatalysis	124
MIL-53-NH ₂ (Al), MIL-53 (Al), Mg-MOF-74	β -glucosidase, laccase	One-pot* (base to deprotonate)	Biocatalysis, biobanking	100
ZIF-8	lipase, catalase, horseradish peroxidase	One-pot/Biomimetic mineralization	Growth mechanism investigation	97
ZIF-8	β -galactosidase	One-pot/Biomimetic mineralization	Biocatalysis, biobanking, biodelivery	72
ZIF-8	β -galactosidase, horseradish peroxidase, glucose oxidase	One-pot/Biomimetic mineralization	Biocatalysis	33
ZIF-8	lipase	One-pot*	Biocatalysis	44
ZIF-8, ZIF-90, MAF-7	catalase, horseradish peroxidase, urease	One-pot/Biomimetic mineralization, co-precipitation, (base to deprotonate MAF-7)	Biocatalysis, biobanking	39
ZIF-90	superoxide dismutase	One-pot*	Biocatalysis, biodelivery	125
ZIF-67	NHase1229	One-pot/Biomimetic mineralization	Biocatalysis	73
am-ZIF-8, ZIF-8	glucose oxidase, <i>Candida antarctica</i> lipase B, catalase	One-pot*	Biocatalysis, biodelivery	37
ZIF-8, UiO-66-NH ₂ , Zn-MOF-74	β -glucosidase, invertase, β -galactosidase	One-pot/Mechanochemical	Biocatalysis, biobanking	118
ZIF-8, HKUST-1	horseradish peroxidase, urease, glucose oxidase	One-pot/AAOPE (PVP / cysteine)	Biocatalysis, biobanking, biosensor	41

AAOPE = acid-boosted one pot embedding *=information related to kinetic of formation/mechanism of crystallization is missing in the original paper.

4. INFILTRATION (POST INSERTION OF ENZYMES IN PRE-FORMED MOFS)

Infiltration of enzymes into preformed porous materials requires a number of design criteria to be met.^{11, 126-128} These necessarily include selecting materials with sufficiently large pores, to both accommodate the biomolecule and to provide subsequent substrate access/product egress. The relative size needed for the pores with respect to the enzyme depends of the nature of adsorption; if adsorption is reversible, then smaller pore diameters can be tolerated.¹²⁹⁻¹³¹ Furthermore, the material must be capable of forming stabilizing interactions that limit enzyme leaching and favor the retention of the native conformation; this can be engendered by appropriate organic functional groups that interact with and stabilize the active enzyme. In more advanced concepts, a hierarchy of connected pores are useful to differentiate the enzyme(s) into the large(r) pores with the smaller, microporous, channels ideally providing unhindered cofactor, substrate and product access and egress; such composites might confer access to multi-enzyme biocatalysis or hybrid catalysts, some of which are discussed in a latter section of the review (section 6). Finally, the integrity of the framework must be sustained under the conditions of targeted enzyme use, which is often a departure from the typical biological conditions under which enzymes show optimal activity; this is often not a challenging requirement as the material synthesis and enzyme infiltration are separate steps.

Briefly considering these requirements and the types of solid-state porous materials available, a number of general observations can be made. Despite their stability, zeolites typically possess limiting pore apertures and pores which are too small to accommodate enzymes.¹³² Other materials, such as metallophosphates¹³³ again have pores that are too small to allow infiltration of enzymes. Silica-based materials¹³⁴ or layered materials such as clays¹³⁵ and metal oxides,¹³⁶ can possess pores of sufficient size but these are often irregularly arranged and broadly distributed in size. However, by using surfactants, mesoporous silica materials can be prepared with regular arrangements of uniform channels.¹³⁷ The dimensions of these channels, range from 20 - 200 Å, are dictated by the choice of surfactant, auxiliary chemicals and reaction conditions, furnishing materials ideally suited to enzyme infiltration, protection and biocatalysis.^{126, 127} However, while these materials possess pore sizes suited to encapsulation, a lack of specific interactions between the support and biomolecule can lead to enzyme leaching and hence loss of activity.^{126, 127} More intimate association of porous material and enzyme can be achieved through post-synthetic modification of pore walls with organic groups (before or after enzyme loading)^{126, 127} or via periodic mesoporous organosilicas (PMOs) and functionalized PMOs,^{138, 139} which can provide specific interactions with the immobilized enzymes.^{11, 140} This has been used to prevent leaching but in turn can diminish loading capacity and hinder substrate access.^{11, 126}

Due to the opportunities presented by enzyme immobilization, mesoporous MOFs¹⁴¹ have recently also emerged

as host materials into which biomolecules can be infiltrated.¹⁴² The particular advantages of MOFs for enzyme infiltration is that they are a chemically mutable family of materials, possessing designable pore sizes and complex, hierarchical pore networks, additionally, they are crystalline and hence provide precise pore size control; and finally, they provide a pore chemical environment that can be designed to complement the infiltrated enzyme's size and surface chemistry. The following section outlines studies which demonstrate the potential of mesoporous MOFs to protect enzymes and to deploy them for biocatalysis and delivery applications of enzymes into cells (Table 3). Some of the first examples outline the key advantages of using MOFs over other mesoporous materials for enzyme protection, including intimate, chemically-matched binding that can minimize leaching. Very large pore MOFs and, in particular, those with hierarchical porosity are used to facilitate both enzyme infiltration and/or cofactor/substrate access. Also, these hierarchical supports can facilitate more complex enzyme processes, including tandem reactions involving multiple enzymes or other catalytic processes. Finally, given the accessibility of different approaches for MOF synthesis, microporous MOFs can be converted to mesoporous supports (for example via defect engineering) for enzymes or nanoparticulate formulations of MOFs which can be prepared for cellular delivery of enzymes.

4.1. Early results and the advantages of MOFs for infiltration

The first example of infiltration of an enzyme into a MOF was reported by Pisklak et al.¹⁴³ Using a pillared CuMOF, $[\text{Cu}_2(\text{bpdc})_2(\text{DABCO})]_n$ (where bpdc = 4,4'-biphenyldicarboxylic acid and DABCO = 1,4-diazabicyclo[2.2.2]octane), immobilization of microperoxidase-11 (MP-11) was achieved. The enzyme was infiltrated into the CuMOF in DMF, presumably due to a lack of aqueous stability for this MOF. Based on 77K N₂ adsorption isotherms, the MOF is microporous and possesses an approximately 1.8 nm channel which requires an end-on entry of MP-11 (approximate dimensions of 3.3 x 1.7 x 1.1 nm). Despite these restrictions 30 μmol g⁻¹ of MP-11 was introduced into the CuMOF with minimal leaching in fresh DMF over a 72 hour period at room temperature. The MP-11@CuMOF composite was still able to oxidize methylene blue but the pore size and loading would suggest this is predominantly due to surface-/subsurface-based enzyme.

Given its relatively small dimensions, MP-11 was also the first enzyme targeted for infiltration into a mesoporous MOF.¹²⁸ Ming, Ma and co-workers used the terbium-based mesoporous MOF ([Tb(TATB)(H₂O)]), referred to as Tb-mesoMOF (**Figure 11**), where TATB = 4,4',4''-s-triazine-2,4,6-triyl-tribenzoic acid (**Figure 12**) to immobilize MP-11 and demonstrated that MP-11@mesoMOF composites exhibited superior catalytic performance compared to a mesoporous silica (Mobil Composition of Matter No.41 (MCM-41)) composite. Tb-mesoMOF was selected as it contains cavities of 3.9 and 4.7 nm in diameter, with measured mesopore apertures of approximately 3.0 and 4.1 nm, in addition to a small portion of micropores (0.9 nm), thereby allowing entry and accommodation of MP-11 as well as substrate access. Loading was detected by a color

change of the material (dark red) and adsorption studies demonstrated a $19.1 \mu\text{mol g}^{-1}$ loading after 50 hours; this compares with a $3.4 \mu\text{mol g}^{-1}$ loading for MCM-41. The enzyme location in Tb-mesoMOF was examined by 77 K N_2 adsorption isotherms which revealed the pore size distribution of the composite is predominately around 0.9 nm, showing the enzyme occupies the larger cavities of the MOF but smaller channels remain to facilitate substrate access. Part of the motivation for using MP-11 is that the free enzyme aggregates within minutes, but by encapsulation within both Tb-mesoMOF and MCM-41, its activity was retained. While, as anticipated, the free enzyme has a higher initial rate ($8.93 \times 10^{-4} \text{ mM s}^{-1}$ up to two minutes in HEPES buffer), it loses activity within several minutes whereas MP-11@Tb-mesoMOF has a lower initial rate ($7.58 \times 10^{-5} \text{ mM s}^{-1}$), but this is maintained over 30 minutes. Moreover, MP-11@Tb-mesoMOF is slightly more active than MP-11@MCM-41 ($3.57 \times 10^{-5} \text{ mM s}^{-1}$) but, more importantly, can be reused multiple times without a precipitous drop in activity (enzyme is detected in the supernatant of MP-11@MCM-41).

This better retention of loaded enzyme can likely be attributed to the provision of a hydrophobic surface: as noted in section 2, proteins tend to have a high affinity for hydrophobic surfaces.¹¹⁴ To probe this, Raman spectroscopic studies were used to rationalize the lack of leaching for MP-11@Tb-mesoMOF composites.¹²⁸ Through these studies, MP-11 molecules were shown to interact with the Tb-mesoMOF through π -interactions involving the heme of MP-11 and the aromatic rings in the organic ligand of the MOF. In contrast, similar studies on MP-11@MCM-41 showed Raman signals consistent with de-aggregation of MP-11 but a lack of interactions between MP-11 and the MCM-41 surface, which are consistent with the observed leaching. Similar π -stacking interactions were also noted for adsorption of vitamins B12 and B2 into the mesoporous MOF, Tb-mesoMOF.¹⁴⁴ These observations are consistent with the relatively long time needed to achieve maximum loading of MP-11 in Tb-mesoMOFs (materials with strong protein-surface interactions need much larger pore diameters for efficient infiltration).^{25, 26}

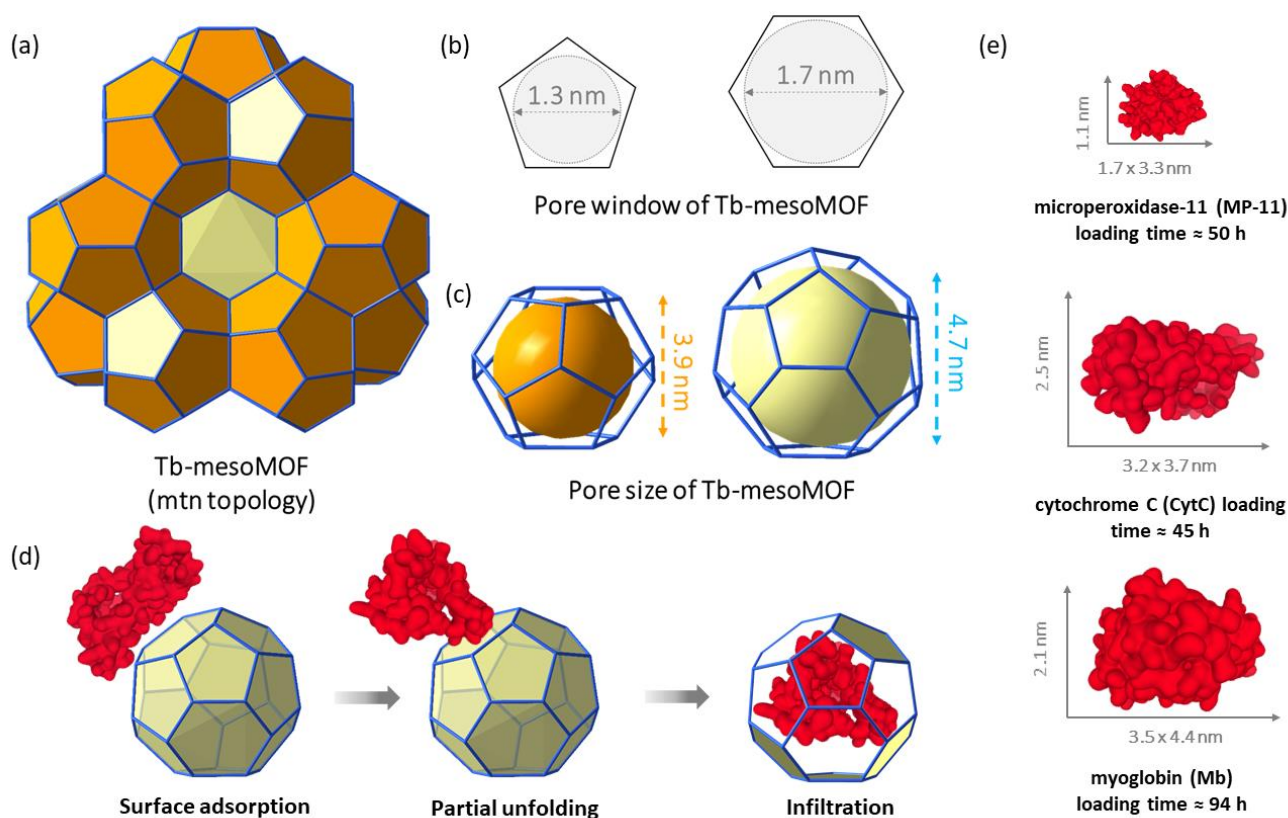


Figure 11. (a) The structure of Tb-mesoMOF showing the mnt topology and the constituent (b) pore openings and (c) pore diameters. (d) Enzymes with dimensions considerably larger than the pore windows need to undergo partial unfolding to access the larger pore cavity, as shown for CytC, whereas (e) enzymes, like MP-11 and Mb, with dimensions smaller than or comparable in size can gain access without an unfolding step. In the latter case this occurs over timescales commensurate with their relative size (i.e. slower for Mb vs. MP-11).

Given the initial success with MP-11, the group of Ma turned its attention to additional enzyme infiltration targets.¹⁴⁵ Mb is a small oxygen-binding protein with molecular dimensions of about $2.1 \times 3.5 \times 4.4 \text{ nm}$ that is capable of peroxidative activity attributable to the heme group. As with MP-11, Mb could be infiltrated into Tb-mesoMOF and

the mesoporous silica SBA-15 (Santa Barbara Amorphous-15) composite, Mb@SBA-15, was also prepared with a loading of $7.0 \mu\text{mol g}^{-1}$. Given the larger size of Mb, total uptake by Tb-mesoMOF ($9.1 \mu\text{mol g}^{-1}$) was reduced compared to MP-11 and loading time was longer (saturated loading of Mb in Tb-mesoMOF was reached after $\sim 94 \text{ h}$ compared with 50 h for MP-11 in Tb-mesoMOF).

Substrate access also appeared to be problematic. This was confirmed by testing the peroxidation of two compounds, 2,2'-azinobis(3-ethylbenzthiazoline)-6-sulfonate (ABTS) and 1,2,3-trihydroxybenzene (THB, pyrogallol); ABTS has molecular dimensions of $10.1 \times 17.3 \text{ \AA}$, whereas THB has dimensions of $5.7 \times 5.8 \text{ \AA}$ (and its colored dimer product $5.8 \times 7.5 \text{ \AA}$). Given the Mb loading blocks all but the 9 \AA pores of Tb-mesoMOF, the Mb@Tb-mesoMOF composite is inactive for ABTS peroxidation but still able to convert THB. Moreover, Mb@Tb-mesoMOF composites are less active for THB peroxidation than Mb@SBA-15, which possesses 8.5 nm channels for enzyme encapsulation and substrate access. It is worth noting at this point that enzymes@ZIF-8 composites, accessed via the encapsulation method, would provide hindered diffusion for these substrates due to the limiting pore diameter of ZIF-8. Composite reusability was also assessed and, due to the disparate pore sizes and pore surface chemistry, Mb@Tb-mesoMOF showed slow but consistent activity (no measurable leaching over the sixteen cycles), whereas Mb@SBA-15 leaches rapidly. The combined results showed not only that larger proteins can be infiltrated but the enzyme-loaded MOF can act to screen substrate access to encapsulated enzymes.

It has also been observed that proteins can access the interior of a MOF despite possessing larger molecular dimensions than the pore sizes of the MOF. Chen et al.^{24, 128} first demonstrated this by infiltrating the haem protein CytC (molecular dimensions $\sim 2.5 \text{ nm} \times 3.2 \text{ nm} \times 3.7 \text{ nm}$) into Tb-mesoMOF. Depending on how the pore sizes of the MOF are calculated, the pore opening through which the enzyme can enter the interior of a MOF are either comparable to the enzyme (pore size apertures measured by 77 K N_2 adsorption)¹⁴⁶ or smaller than the enzyme (calculated from the MOF structure and considering the van der Waal's diameter).¹⁴⁶ Regardless, mechanistic studies conducted using steady-state fluorescence spectroscopy suggest that the CytC molecules must undergo a partial unfolding step to allow them to access the interior of the MOF through the relatively small nanopores. Once inside, the protein regains its native conformation with the encapsulated protein displaying the expected spectroscopic signatures due to the haem unit.

Similar observations were also made for the infiltration of a protease into the structure of MIL-101-NH₂(Al) (mesoporous cavities of 3.6 and 2.9 nm diameters connected by pentagonal and hexagonal windows of 1.6 and 1.2 nm).²³ In the latter case an aspartic proteinase was incubated in a 1:10 mixture of TRIS buffer (0.1 M , $\text{pH } 7.4$) and hexane at mild temperatures to facilitate partial unfolding of the enzyme and entry into the mesoporous MOF (loading 0.05 g g^{-1}). These steps were confirmed by fluorescence spectroscopy, and supported by molecular dynamics simulations, to rationalize the infiltration steps. Due to the encapsulation the enzyme@MOF biocatalyst displays excellent the proteolytic activity for glycyl-L-tyrosine hydrolysis, better than that of the free enzyme. Moreover, its operating range can be extended to extreme conditions of pH and

temperature where the free enzyme becomes denatured. Finally, due to the small pore apertures, the protease@MIL-101-NH₂(Al) composite shows excellent recyclability and is even able to be used with other enzymes that normally would be degraded by the protease activity. This concept of partial unfolding could, depending on the enzymes used, be a mechanism by which loading rates are improved, and ultimately provide improved stability of enzyme@MOF biocomposites as leaching requires denaturation of the encapsulated enzymes.

These initial experiments, plus others which are outlined below, have provided the grounding for enzyme stabilization via infiltration into mesoporous MOFs. However, a series of fundamental studies remain to be tackled that will further improve our understanding of the basic infiltration and enzyme stabilization process. Nearly all mesoporous MOFs used have large aromatic linkers and there has been relatively little utilization of functional group chemistry to manipulate the interactions of the MOF pore surface with enzymes, such as increased hydrophilicity (which shows notable benefits for encapsulated enzymes) or hydrogen bond acceptors or donors to stabilize or destabilize enzymes. Also, some of the characterization tools outlined above,¹⁴⁷ such as resonance Raman or related infrared studies, are important experiments to be employed more widely as they can both probe the structure of an included enzyme but also look into the nature of the adsorption process in modified MOF structures to furnish a fundamental understanding of enzyme-MOF interactions.

4.2. Tuning the framework structure in infiltrated enzyme@MOF biocomposites

While enzymes can clearly be infiltrated into mesoporous MOFs with pore apertures smaller than the dimensions of the MOF, a distinct advantage of MOF chemistry over other mesoporous hosts is that these framework materials can be easily isoreticulated to form structures with expanded pores. Yaghi and co-workers employed this approach by systematically expanding the MOF-74 structure to an isoreticular series (IRMOF-74-I to XI, IRMOF = isoreticular metal-organic framework, see **Figure 12** for the ligand structures) with pore apertures ranging from 1.4 to 9.8 nm .¹⁴⁸ This represented a replacement of the original linker, which is based on a single phenylene ring (I), to two, three, four, five, six, seven, nine, and eleven phenylene rings (II to XI, respectively). Importantly, the pore apertures of IRMOF-74-VII and IRMOF-74-IX are large enough for biomolecule infiltration, even when the interior of the pores are oligoethylene glycol-functionalized. Mb (dimensions of 2.1 by 3.5 by 4.4 nm) could be infiltrated into IRMOF-74-VII-oeg (where oeg = triethylene glycol mono-methyl ether), and GFP (barrel structure with diameter of 3.4 nm and length of 4.5 nm) in IRMOF-74-IX. These studies also illustrated the importance of controlling pore surface chemistry which can be readily achieved for MOFs; Mb was only substantially taken up by hydrophilic IRMOF-74-VII-oeg whereas a hydrophobic variant of IRMOF-74-VII with hexyl side chains adsorbed only a negligible amount of enzyme.

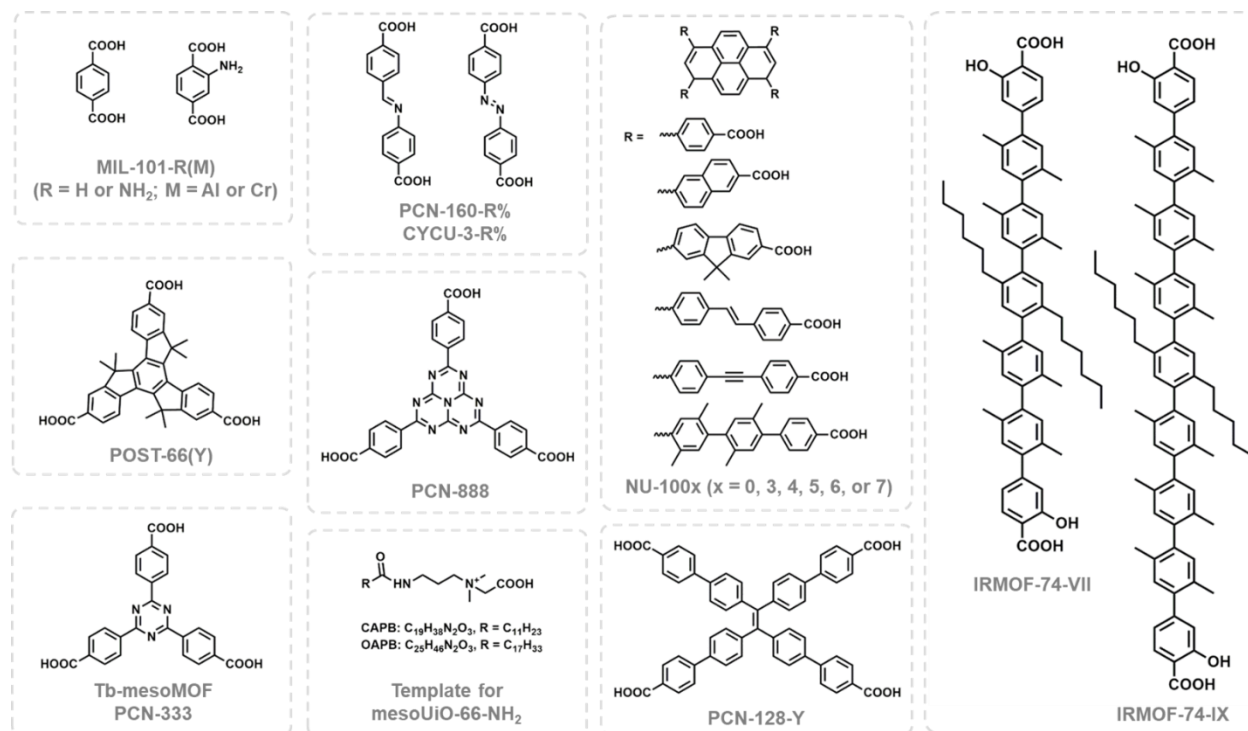


Figure 12. The main organic ligands used for the synthesis of the mesoporous MOFs discussed in this review along with the structures of the templating agents used for synthesis of mesoUiO-66-NH₂.

Once it had been shown that enzymes could be infiltrated into mesoporous MOFs, focus shifted to considering the arrangement of enzymes within the MOF pores and furthermore, how hierarchical pore structures¹⁴⁹ or structuralized MOF composites could be used to accommodate biomolecules.¹⁵⁰ Zhou et al. examined how enzyme loading in multi-pore PCN-333(Al) (PCN = porous coordination network) affected performance, specifically whether single-enzyme encapsulation (SEE) or multiple-enzyme encapsulation (MEE) was occurring within the mesoporous cages.¹⁴⁸ PCN-333(M) and PCN-332(M) (M = Al, Fe, V, Sc, In) are a series of materials that are isoreticular with MIL-100 and built by sharing the vertices of supertetrahedra possessing a 9 (PCN-332) or 11 Å (PCN-333) cavity. This results in two types of mesoporous cages; specifically for PCN-333 there is a smaller dodecahedral cage (4.2 nm diameter) with a pentagonal 2.6 nm pore aperture, and a larger hexacaidecahedral (hexagonal-truncated trapezoidal) cage (5.5 nm diameter) accessed by the same pentagonal windows, but also hexagonal apertures with a diameter of 3.0 nm. By choosing a series of enzymes, HRP, CytC and MP-11, representing a size continuum from large to small, Zhou et al. were able to show how these enzymes accessed different sites in the PCN-333(Al) framework, namely occupying the large pore only (HRP), the larger pores (CytC) and all pores (MP-11). Essentially single enzyme per pore encapsulation was achievable for the larger enzymes (HRP and CytC), whereas multiple MP-11 molecules are loaded into each mesoporous cage. Enzyme infiltration was quite rapid, even for large HRP biomolecules (40 mins for saturated loading whereas CytC and MP-11 required 30 and 10 mins respectively), and the experimental maximum loadings approached those expected based on mesopore sizes and accessibility. Catalytic activity was assessed for all three enzymes (pH 6 acid-sodium

citrate buffer at room temperature) with all immobilized enzymes showed lower k_{cat} values (diffusion limited) but more favorable K_m values (higher substrate affinity); as a consequence, the immobilized enzymes show comparable specific activity to their free counterparts. Immobilized CytC displays better specific activity than the free enzyme, possibly due to a combination of single enzyme loading and good substrate access. Leaching was again improved with respect to the corresponding SBA-15 composites and the CytC@PCN-333(Al) biocomposite showed improved specific activity with respect to the free enzyme in pure water.

Farha and co-workers developed this concept from a different perspective.¹⁵¹ The researchers infiltrated the esterase enzyme isolated from *Fusarium solani* pisi cutinase (PDB: 1CEX), into three different but structurally related Zr-based MOFs, NU-1000 (NU = Northwestern University), PCN-600 and CYCU-3 (CYCU = Chung Yuan Christian University) and assessed loading, and accessibility of the enzyme. NU-1000 possesses connected 3 nm hexagonal and 0.8 nm triangular channels which not only allows higher loading but presumably good substrate diffusion and access due to the connected channels (**Figure 13**). PCN-600 by comparison has only the hexagonal channels so high enzyme loading is possible but the lack of triangular channels limits substrate access. CYCU-3 was also examined as it has hexagonal and triangular channels like NU-1000 but these are not interconnected. The accessibility of active enzymes in each MOF biocomposite was quantified by determining the enzyme loading and then using a fluorescent dye reagent to titrate activity. Due to these distinct MOF architectures, 93% of the cutinase was available in NU-1000 while only 6% was available in PCN-600. Though it was anticipated that CYCU-3 biocomposites

would display similar problems to PCN-600 for enzyme activity studies, CYCU-3 turned out to not be stable under the conditions necessary for activity in this work. Given that NU-1000 gave the best performance as a support, the enzymatic activity of cutinase@NU-1000 biocomposites were compared to the free enzyme. The cutinase@NU-1000 composite retained activity upon exposure to chaotropic reagents like urea and in organic solvents such as THF, both conditions that caused loss of activity for the free enzyme. Cycling experiments, showed some loss of

activity over multiple runs (60% of the original activity after 5 cycles) presumably due to the relatively unhindered diffusion in the large hexagonal channels. A similar study was conducted for lipase by Sun et al.¹⁵² using the hierarchically porous COF, COF-ETTA-EDDA, rather than a MOF, indicating that there is considerable scope to further tune the performance of the biocomposites prepared by infiltration through the judicious selection multipore framework materials. Moreover, there is a clear opportunity to extend this research to mesoporous COFs,¹⁵³⁻¹⁵⁶ alongside MOFs.

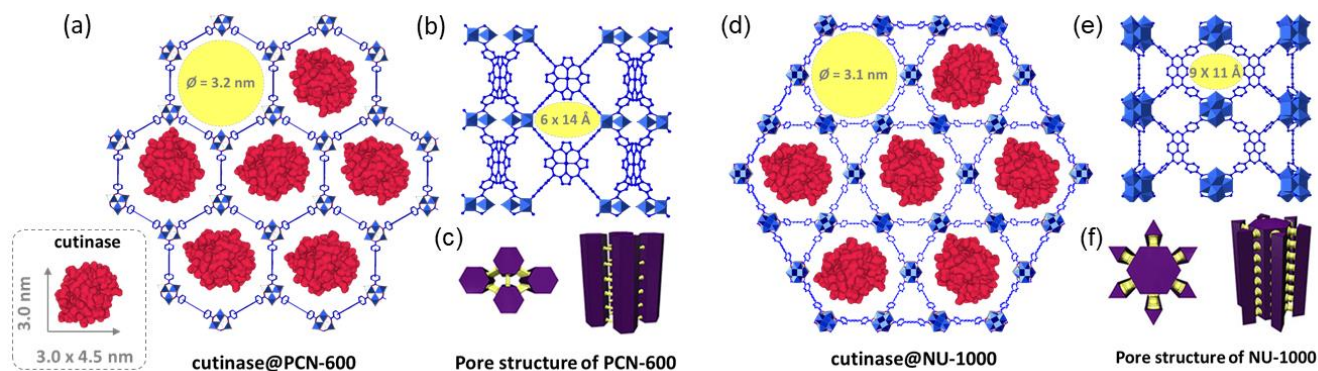


Figure 13. Loading of esterase *Fusarium solani* pisi cutinase (PDB: 1CEX) into PCN-600 (a-c) and NU-1000 (d-e) showing the benefit of a connected hierarchically structure for substrate and product diffusion. In both cases the enzymes are located in the large pores but NU-1000 has additional triangular pores (seen in d) that provide access for substrate and product ingress and egress via windows between the two types of pores (e). PCN-600, in comparison, lacks the triangular pores such that substrates and product have to enter and exit via the enzyme filled channels. Adapted with permission from Ref. 151, copyright [2016] Elsevier.

Hierarchically porous MOFs include materials that possess a conventional microporous MOF structure that is accessed via meso- and macro-porous channels. One way these can be prepared is by post-synthetic conversions of microporous materials into a mesoporous structure. This approach to preparing materials for enzyme infiltration was first investigated by Kim et al.¹⁵⁷ The precursor microporous material POST-66(Y) was synthesized by a solvothermal reaction yttrium nitrate with a truxene tricarboxylic acid linker. While POST-66(Y) was thermally stable and chemically stable in non-aqueous solvents, immersion of POST-66(Y) in water for 24 hours led to a conversion to a material with two distinct mesopores (with a diameters of 3.8 and 13.9 nm). Infiltration of biomolecules into in POST-66(Y)-wt-24h was demonstrated, including vitamin B12, CytC, Mb, and HRP. The catalytic activity of HRP embedded within POST-66(Y)-wt-24h (HRP@POST-66(Y)-wt-24h) for the co-oxidation of 4-aminoantipyrine (4-AAP) and phenol to N-antipyryl-p-benzoquinoneimine (APBQ) using hydrogen peroxide was monitored by Ultraviolet-visible (UV-vis) spectroscopy. HRP@POST-66(Y)-wt-24h was a recyclable catalyst for the oxidation and POST66(Y)-wt-24h was further able to protect HRP in organic solvents.

A related post-synthetic approach to form hierarchically porous MOF supports was employed by Zhou et al.¹⁵⁸ to convert a preformed mesoporous MOF into a more defect-rich form and thereby improve the diffusion of reagents and products of enzymatically-catalyzed reactions. Herein a parent MOF is formed from azobenzene dicarboxylate

(AZDC, **Figure 12**) linker, which can be partially substituted by an imine-based linker 4-carboxybenzylidene-4-aminobenzoate (CBAB) possessing the same structure metrics. The CBAB linker is hydrolytically unstable and its decomposition favors release of the linker components and node removal under mild conditions. Using CYCU-3, the mesoporous MOF previously used by Farha and colleagues for enzyme encapsulation, the group treated as-synthesized CYCU-3 with CBAB to replace 22% of the AZDC linkers before the labile CBAB linkers subsequently removed by treating with 0.2 mM HCl in DMF to create a defective MOF (CYCU-3D, **Figure 14a**) that presumably, lacks the ordered pore structure of the parent MOF. CytC was loaded into CYCU-3 and CYCU-3D, giving maximum loadings of 23.3 mmol g⁻¹ for CYCU-3 and 14.5 mmol g⁻¹ for CYCU-3D. An oxidation reaction performed on a small substrate (o-phenylene diamine) showed that CytC in both materials was active; however, only the defect-rich CytC@CYCU-3D composite showed appreciable activity for ABTS oxidation. This was attributed to hindered diffusion by ABTS in the CytC-loaded hexagonal channels of CYCU-3 that is somewhat relieved by formation of the defect-rich CYCU-3D support although it is worth noting that the enzyme loading is different in the two biocomposites.

Templates can also be used to generate hierarchically porous MOFs for enzyme infiltration. Using a template approach, mesoporous UiO-66-X (X = NH₂ or (OH)₂ to designate substituents on the 1,4-benzenedicarboxylate (bdc) linker) samples with hierarchical porosity have also been

prepared and the mesopores shown to be available to encapsulate CytC.¹⁵⁹ The UiO-66-type mesoMOFs (mesoUiO-66-X) were synthesized in aqueous solution by using the amphoteric surfactants cocamidopropyl betaine (CAPB) or oleyl amidopropyl betaine (OAPB) as the template (**Figure 12**). These templates form rod-like micelles which allow the growth of microporous UiO-66-X around the micelles and ultimately formation of hexagonal mesoporous superstructures. CytC infiltration experiments showed that, as expected, the mesopores adsorbed the enzyme but the micropores were retained. Using a similar templating approach, macro-microporous ZIF-8 structures suitable for enzyme encapsulation could be prepared.¹⁶⁰ The title material in that work, single-crystal ordered macropore zeolitic imidazolate framework-8 (SOM-ZIF-8), was prepared by assembling monodisperse polystyrene spheres (PSs) into highly ordered 3D PS monoliths, which once infiltrated with the ZIF-8 precursors can be converted into a single-crystalline MOF with 3D ordering of macro-micropores. Subsequent removal of the PSs gives the SOM-ZIF-8 (**Figure 14b**). Due to the ordering of the PS template, the macropores in SOM-ZIF-8 are accessible from the crystal surface whereas other ZIF-8 samples, such as crystalline ZIF-8 (C-ZIF-8), polycrystal hollow ZIF-8 (PHZIF-8), and macroporous ZIF-8 (M-ZIF-8) synthesized using disordered PSs as the template, either do not have macropores (C-ZIF-8) or do not have macropores unimpeded by the microporous matrix (PHZIF-8 and M-ZIF-8). The ramifications of this are that diffusion of GFP from the outside to the interior of individual SOM-ZIF-8 crystals was much faster than for M-ZIF-8 and C-ZIF-8.

Hierarchically porous MOF materials can also be prepared template-free, as is the case for a HKUST-1-derived material (aka Cu-BTC). Using a template-free strategy, nanosized microporous Cu-BTC particles are packed to form a mesoporous composite (**Figure 14c**),¹⁶¹ which in turn can be infiltrated by the enzyme.¹⁶² In this example, a lipase-surfactant enzyme complex was prepared which allowed the enzyme to be loaded in organic solvent, presumably to avoid stability issues with the Cu-BTC composite. The catalytic activity of the lipase enzyme (*Bacillus subtilis* lipase, BSL2) and the enzyme composite (BSL2@Cu-BTC) was then assessed for an esterification reaction between lauric acid and benzyl alcohol. BSL2@Cu-BTC composites showed high enzymatic activity compared to the free enzyme under the conditions used (isooctane, 30°C) and excellent reusability during the esterification reaction (90.7% of its initial enzymatic activity and 99.6% of its initial conversion after 10 cycles).

Given the burgeoning area of MOF structuralization there are further opportunities here for enzyme@MOF chemistry.¹⁶³⁻¹⁶⁵ Structuralized MOFs could form the basis of more complete reaction vessels, part of microfluidic devices or provide components for lab on a chip systems,¹⁶⁶⁻¹⁶⁸ which integrate enzyme@MOF reaction chemistry. The ability to form these via infiltration will allow fabrication via the approaches already established, without regard to enzyme stability or cost, and allow the late-stage incorporation the enzymes. Also, given the emerging area of core-shell MOF chemistry,^{169,170} there are opportunities to form enzyme@mesoporous MOF coated in a microporous MOF to ensure no leaching and provide substrate selectivity.

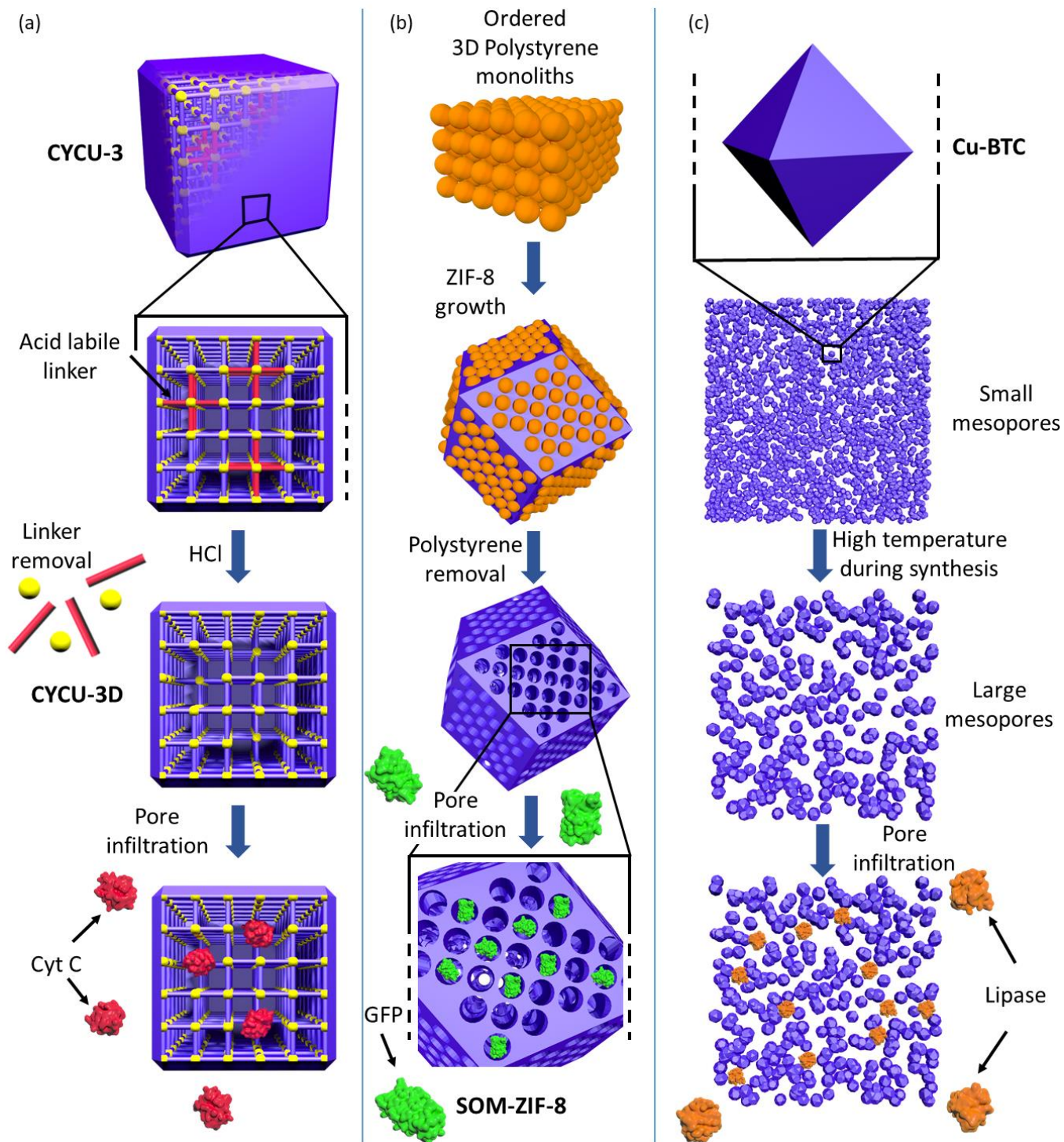


Figure 14. (a) Schematic representations showing the use of acid labile linkers to induce mesopores in CYCU-3.¹⁷¹ (b) Formation of SOM-ZIF-8 by initial ordering of polystyrene beads, MOF growth and subsequent polystyrene removal.¹⁶⁰ (c) Formation of a hierarchically porous HKUST-derived structure by aggregation of nanosized microporous Cu-BTC particles.^{172, 173} relevant enzymes and also toward increasing the complexity of the enzyme@MOF composites (i.e. tandem enzymes; nanoparticle enzyme composites, see section 6). An example of this was the infiltration of organophosphorus acid anhydrolase (OPAA), a prolidase which hydrolyses P-F, P-O, P-S, and P-CN bonds, into the hexagonal channels of the Zr-based MOF PCN-128y.¹⁷⁴ PCN-128y has hexagonal channels precisely sized to accommodate OPAA

4.3. Towards applications of infiltrated enzyme@MOFs

While not exclusively, many of the examples of enzymes infiltrated into MOFs are chosen as they are commercially available and have reliable, accessible assays. As an understanding of the MOF features needed for successful immobilization developed, focus has shifted to more application

allowing for a 12 wt% loading of the enzyme to be distributed throughout the crystals shown by energy dispersive X-ray line scans for Zr (MOF) and S (OPAA). PCN-128y also possesses triangular channels, like NU-1000, which are too small for enzyme loading but facilitate substrate access to the hexagonal channels through diamond-shaped windows. OPAA@PCN-128y was shown to hydrolyze the nerve agent simulant diisopropyl fluorophosphate (DFP) and the nerve agent O-pinacolyl methyl fluorophosphate (Soman) in assays. While initial rates for DFP hydrolysis were lower than the free enzyme, the OPAA@PCN-128y composite showed better thermal stability and, moreover, greater reusability. OPAA@PCN-128y hydrolyzes Soman, reaching 90% conversion in 60 mins, suggesting such composites might be useful for nerve agent decontamination.

The effect of MOF particle size on gas adsorption and catalysis are well established.¹⁷⁵⁻¹⁷⁷ With this in mind, Farha et al.¹⁷⁸ utilized one of their optimized NU-100X materials (NU-1003) to develop better enzyme carriers for nerve agent hydrolysis using OPAA. Like PCN-128y, NU-1003 possesses an ideal combination of large hexagonal channels for enzyme infiltration but also larger windows connecting the triangular and hexagonal channels. This combination of pore characteristics was expected to facilitate diffusion of substrates. Using a reported method^{179, 180} to control the crystal growth of Zr-based MOFs, hexagonal cylinder-shaped NU-1003 crystals were obtained with lengths ranging from 300 to 10000 nm (denoted here as NU-1003-size, where size = 300, 1000, 2000, 7000, and 10000 nm). OPAA@NU-1003 biocomposites were formed and assessed for their ability to hydrolyze DFP and Soman. Nanosized OPAA@NU-1003-300-nm showed comparable performance to free OPAA for the hydrolysis of DFP, and furthermore, for the hydrolysis of Soman, it significantly outperformed micro-sized NU-1003 composites and even exceeded that of the free OPAA enzyme. While there has been considerable investigation into particle size control for enzyme@MOF composites formed via encapsulation (*vide supra*), surprisingly, the same cannot be said for enzyme biocomposites formed by infiltration. This is more a

focus for *in vivo* biomedical applications of MOF composites as these need to be appropriately sized to avoid toxicity and premature clearance.¹⁸¹⁻¹⁸³ MOF synthesis, through judicious choice of reaction conditions, synthesis methods and the use of modulators,¹⁸⁴ allows remarkable control over particle size. Thus given that the MOF particles can be pre-synthesized this suggests that control over MOF particle size can be easily accomplished to optimize enzyme performance characteristics; for example larger particles for enzyme stability and small particles for improved activity, even perhaps to the extent of 10s-100s of enzyme molecules per particle.

Infiltration approaches have also been used to construct multi-enzyme biocomposites. Using PCN-888, which possesses three types of pore cavity, Zhou and co-workers¹⁸⁵ demonstrated the formation a model tandem enzyme system comprising GOx and HRP (**Figure 15**). The hierarchical porosity of PCN-888 is well tailored to multiple enzyme inclusion with a large cavity (6.2 nm) able to accommodate one molecule of GOx, an intermediate cavity (5.0 nm) suitable for a single HRP enzyme, and a small cavity (2.0 nm) which can accommodate neither of the enzymes but provides a pathway for substrate diffusion. Given the relative pore sizes, a stepwise infiltration strategy incorporating GOx before HRP is necessary to precisely control the distribution of GOx and HRP exclusively in the largest and medium cages, respectively. This method provided a GOx/HRP@PCN-888 composite with a GOx loading of 1.0 g g⁻¹ and HRP uptake of 2.0 g g⁻¹. A reversal of the order of addition leads to HRP occupying all pore cavities and preventing infiltration of GOx (GOx is only surface bound under this approach). In the tandem enzyme biocomposites, GOx catalyzes the reaction between glucose and molecular oxygen to form gluconolactone and hydrogen peroxide. The hydrogen peroxide that is formed is used by HRP for oxidation of ABTS. Given the intimate association of the enzymes in adjacent pores the GOx/HRP@PCN-888 composite outperforms a mixture of both GOx and HRP, and furthermore significantly outperforms the GOx coated HRP@PCN-888 composite.

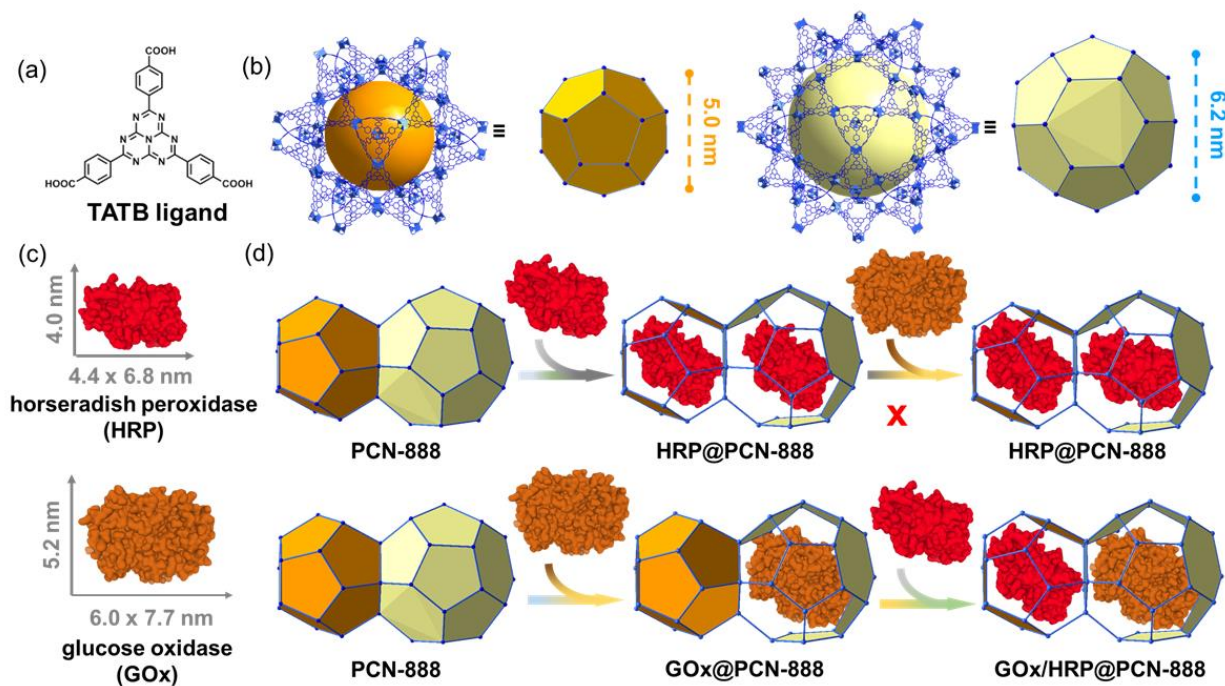


Figure 15. (a) The TATB ligand used to form PCN-888 and (b) representations showing the salient pore features of the mesoporous MOF. Formation of the GOx/HRP@PCN-888 composite requires consideration of the size match between the MOF mesopores and (c) the enzymes. As a consequence, (d) effective GOx/HRP@PCN-888 composites can only be generated if the larger GOx enzyme is introduced first as this circumvents complete pore saturation by HRP. Adapted with permission from Ref. 34 under the terms of the CC BY 3.0 license.

Many enzymes require cofactors to function. Farha and co-workers¹⁴¹ addressed this challenge using the hierarchical porosity of the NU-100x ($x = 3 - 7$) series of frameworks and PCN-128 to identify a material capable of accommodating an enzyme but also of facilitating effective substrate and cofactor access to the enzyme active site. A genuine cell-free system is only achievable with the NU-100x ($x = 5-7$) as this has sufficiently large windows connecting the hexagonal channels (which accommodate enzyme) with the triangular channels which provide cofactor/substrate access (i.e. to enable exchange of NADH/NAD⁺, NAD = nicotinamide adenine dinucleotide). The cell-free system with LDH@NU100x (LDH = lactate dehydrogenase; $X = 5-7$ only) converts L-lactate to pyruvate using an NADH cofactor which is supplied by diaphorase (adsorbed on surface).

Introduction of enzymes or biomolecules into cells, or delivery into the body requires the preparation of nanoparticle forms of biomolecule@MOF composites. This provides a route to avoid decomposition of the enzyme within the cell, yet confer cellular uptake. As an example of this, Zhou and co-workers¹⁸⁶ prepared nanoparticles of the Al-based MOF PCN-333 and infiltrated the enzymes superoxide dismutase (SODx) and CAT (a fluorescent tag was also appended to localize the biocomposites within cells). SODx/CAT@PCN-333 biocomposite formation protects both enzymes against TRY digestion and mildly acidic pHs (pH = 5). Both enzymes impart antioxidative properties on the cell and while the free enzymes are mildly effective over short periods, the SODx/CAT@PCN-333 composite protects human cells from toxic reactive oxygen species

(ROs) for up to a week and maintains cell viability. In a follow-up contribution an enzyme@MOF nanocomposite was used to activate a prodrug.¹⁸⁷ Tyrosinase (TYR) is able to oxidize paracetamol to its quinone derivative which in turn can generate ROs and react with glutathione (GSH), thereby removing this antioxidant. These combined effects lead to cancer cell death. Again, using PCN-333 nanocrystals, TYR is able to be infiltrated into the 5.5 nm hexacaidecahedral cage (shown by pore size distributions calculated on 77 K N₂ isotherms on TYR@PCN-333) giving a loading of 0.80 g g⁻¹. *In vitro* results indicated that TYR@PCN-333 nanoparticles are enzymatically active and thus experiments were conducted with an ovarian adenocarcinoma cell that is resistant to multiple treatments. Fluorescently tagged TYR@PCN-333 nanoparticles confirmed that cellular uptake occurred and the neither the prodrug (paracetamol) nor the TYR@PCN-333 nanoparticles showed appreciable cytotoxicity. However, when TYR@PCN-333 nanoparticles and the prodrug were co-administered, a significant decrease in cell viability was observed; this behavior could even be observed if the cells were pretreated with TYR@PCN-333 nanoparticles and cultured over several days before administration of the prodrug. Given the successful *in vitro* results, *in vivo* experiments were performed on a HeLa subcutaneous xenograft model and showed a 2.5 times reduction in tumor volume.¹⁸⁸

As noted above, the advantages of nanoparticle MOFs for catalysis are established. Gkaniatsou et al.¹⁸⁹ prepared nanoparticles of the ultra-stable MOF, MIL-101(Cr) by a microwave assisted hydrothermal synthesis method and

showed a further advantage of MOFs biocomposites for biocatalysis – the ability to preconcentrate substrates selectively. The small microperoxidase-8 (MP-8) enzyme was able to be infiltrated into the mesopores of the MIL-101(Cr) nanoparticles, albeit likely needing to undergo partial denaturation to pass through the restrictive cage windows as seen before for other MOFs.^{23,128} The resulting MP-8@MIL-101(Cr) composite retained enzyme activity and showed resistance to weakly acidic conditions that deactivate the free enzyme. The MIL-101(Cr) support can also preconcentrate negatively charged dye molecules, such as methyl orange, providing markedly greater reaction rates for the oxidation of methyl orange by MP-

8@MIL-101(Cr) with respect to free enzyme (positively charged dyes are repelled from the composite and oxidised at a much lower rate). These results show the encapsulating MOF can function synergistically with the enzyme to provide selectivity and/or catalytic rate enhancement. Moreover, given the growing body of work showing how MOF particles can be post-synthetically modified at the surface to improve stability and dispersion,¹⁹⁰ and within their pore network to enhance adsorption of small molecules (i.e. substrates),¹⁹¹ these approaches present a considerable opportunity to tune the biocatalytic functionality of infiltrated enzyme@MOF biocomposites.

Table 3. Examples of infiltration of enzymes into MOFs showing the MOF used, its pore dimensions, the infiltrated enzyme, and the main application.

MOF	MOF pore size	Enzyme	Application	Ref.
Tb-mesoMOF	0.9, 3.0, and 4.1 nm	microperoxidase-11 (MP-11, 1.1 x 1.7 x 3.3 nm) myoglobin (Mb 2.1 x 3.5 x 4.4 nm) cytochrome C (CytC) (2.5 x 3.2 x 3.7 nm)	Biocatalysis/Proof-of-concept	24, 128, 145, 192
IRMOF-74-VII-oeg	4.9 nm for IRMOF-74-VII-oeg ^a	myoglobin (Mb, 2.1 x 3.5 x 4.4 nm)	Proof-of-concept	148
IRMOF-74-IX	6.1 nm for IRMOF-74-IX ^a	green fluorescent protein (GFP, 3.4 x 3.4 x 4.5 nm)		
PCN-333(Al)	1.1, 4.2, and 5.5 nm	horseradish peroxidase (HRP, 4.0 x 4.4 x 6.8 nm) cytochrome C (CytC, 2.5 x 3.2 x 3.7 nm) microperoxidase-11 (MP-11, 1.1 x 1.7 x 3.3 nm)	Biocatalysis	193, 194
POST-66(Y)	3-20 nm ^b	horseradish peroxidase (HRP, 4.0 x 4.4 x 6.8 nm) cytochrome C (CytC, 2.5 x 3.2 x 3.7 nm) myoglobin (Mb, 2.1 x 3.5 x 4.4 nm)	Biocatalysis	157
NU-1003	3.8 and 4.5 nm	organophosphorus acid anhydrolase (OPAA, 4.4 x 4.4 x 7.8 nm)	Biocatalysis	178
Hierarchically porous Cu-BTC	34 nm	<i>Bacillus subtilis</i> lipase (BSL2, 3.5 x 3.6 x 4.2 nm)	Biocatalysis	162
NU-1000	3.1 nm	cutinase (4.5 x 3.0 x 3.0 nm)	Biocatalysis	151
PCN-600	~3.0 nm	cutinase (4.5 x 3.0 x 3.0 nm)	Biocatalysis	151
PCN-888	2, 5, and 6.2 nm	glucose oxidase (GOx, 5.2 x 6.0 x 7.7 nm)	Biocatalysis	185
PCN-128Y	4.4 nm	horseradish peroxidase (HRP, 4.0 x 4.4 x 6.8 nm) organophosphorus acid anhydrolase (OPAA, 4.4 x 4.4 x 7.8 nm)	Biocatalysis	174
PCN-160-R%	2-50 nm ^b	cytochrome C (CytC, 2.5 x 3.2 x 3.7 nm)	Biocatalysis	158
CYCU-3-R%				
PCN-333(Al)	1.1, 4.2, and 5.5 nm	superoxide dismutase (SOD, 2.8 x 3.5 x 4.2 nm) catalase (CAT, 4.4 x 4.9 x 5.6 nm)	Biocatalysis	186
MIL-101(Cr)	2.9 and 3.4 nm	microperoxidase - 8 (MP-8, 1.1 x 1.7 x 3.3 nm)	Biocatalysis	189
SOM-ZIF-8	191-466 nm ^c	green fluorescent protein (3.4 x 3.4 x 4.5 nm)	Proof-of-concept	160
mesoUiO-66-NH ₂	2.6-3.2 nm ^c	cytochrome C (CytC, 2.5 x 3.2 x 3.7 nm)	Biocatalysis	159

NU-100x	3.3-6.7 nm	lactate dehydrogenase (LDH, 4.4 x 4.4 x 5.6 nm)	Biocatalysis	141
(x = 3, 4, 5, 6, 7)				
NU-1000	3.3 nm	insulin (1.3 x 1.3 x 3.4 nm)	Biomolecule delivery	55, 195
PCN-333	1.1, 4.2, and 5.5 nm	tyrosinase (TYR, 5.5 x 5.5 x 5.6 nm)	Cancer therapy	187
NU-1006	6.2 nm	formate dehydrogenase (FDH, 4 x 6 x 11 nm)	Biocatalysis	196
MIL-101-NH ₂ (Al)	2.9 and 3.4 nm	<i>Aspergillus saitoi</i> proteinase ($\varnothing = 2.85$ nm) ^d	Biocatalysis	23

^a Pore diameter is referring to the shortest dimension of the pore aperture calculated from refined crystal structures.

^b The mesoporosity in the MOFs is attributed to ligand liberation during hydrolysis.

^c The mesoporosity in the MOF is generated by template removal.

^d The size of the enzyme was determined from dynamic light scattering (DLS) measurement.

5. SURFACE BOUND ENZYMES

Methods used to anchor enzymes to the external surface of MOF particles (aka enzyme-on-MOF composites) can be grouped into two general classes based on the fundamental nature of immobilization: 1) physical adsorption, and 2) covalent attachment. We note that the interface between biomolecules and MOFs is complex and in practice will involve a combination of different binding forces. For

example, in a study investigating surface adsorption of GDH and methylene green on a series of ZIFs,¹⁹⁷ Mao and co-workers showed that donor-acceptor and hydrogen-bonding interactions were present in addition to physical adsorption *via* hydrophobic effects. Thus, to simplify the discussion, we will categorize the nature of adsorption based upon the primary strategy for biocomposite synthesis.

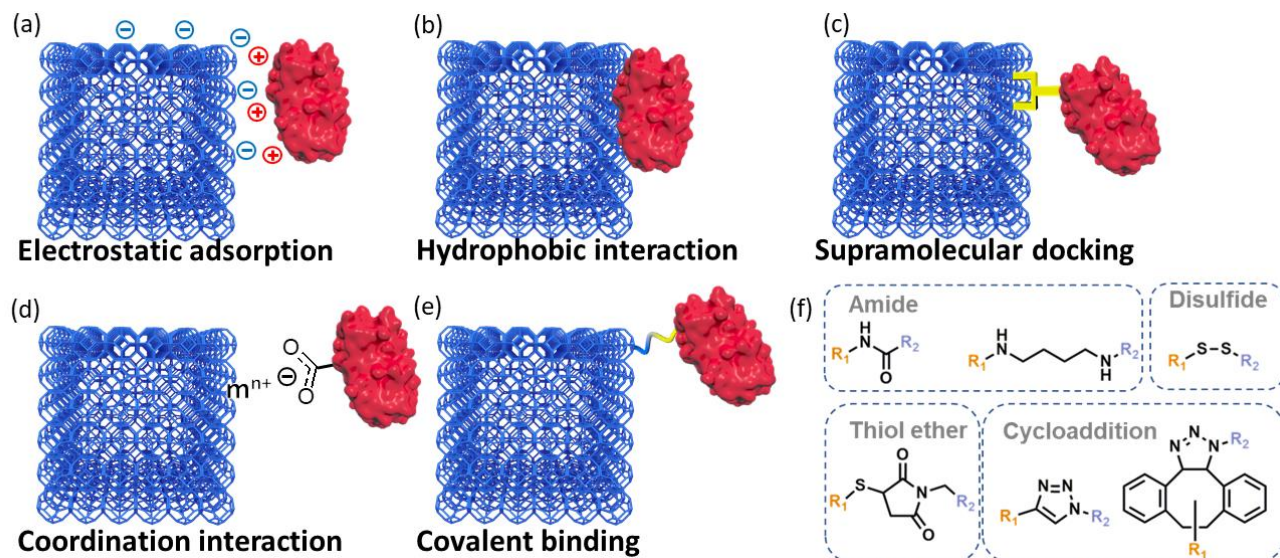


Figure 16. Schematic illustration of the synthesis strategies used to form enzyme-on-MOF biocomposites.

5.1. Immobilization via physical adsorption

Physical immobilization of biomolecules is the most straightforward approach to the synthesis of biomolecule-on-MOF composites. Surface functionalization *via* adsorption primarily relies on noncovalent van der Waals forces, hydrophobic interactions, π - π interactions and electrostatics (**Figure 16**).⁵ For example, the charged surface-exposed amino acids of a protein molecule facilitate an electrostatic interaction to the MOF support. At pH 7, aspartic acid (Asp) and glutamic acid (Glu) are negatively charged; while lysine (Lys), Arg, and His are positively charged. These individual, charged, amino acids moieties will interact with functional groups on the MOF surface (for example $-\text{COO}^-$) leading to attraction or repulsion of protein regions, or the whole protein. Electrostatic interactions between the biomolecule and support can be modulated by controlling the pH of the reaction solution.¹⁹⁸ In theory, the maximum loading of biomolecules on a surface is achieved when the pH of the solution is below the isoelectric point of the biomolecule and above that of the support material, or vice versa. For example, in pH 7 buffer solution, cutinase showed high affinity for the NU-1000 support. In order to explain this phenomenon, Farha and co-authors carried out zeta-potential measurements to determine the isoelectric point for NU-1000 (4.3) and cutinase (7.8). Thus, under physiological conditions, cutinase and NU-1000 are positively and negatively charged, respectively. The presence of columbic forces is a compelling explanation for significant interaction between the protein and the MOF substrate.¹⁵¹

When loading proteins onto a support material, the effect on their tertiary structure needs to be considered. Contact with a charged surface commonly leads to a change in protein conformation due to the formation of a hydrogen and/or salt ion gradient between the bulk solvent and the biomolecule/support interface.¹⁹⁹ Due to this partitioning effect, the pH and the ionic strength at the biointerface differ from those in the bulk solution. This environment gives rise to changes in the protonation state of amino acids, the strength of electrostatic interactions, and the nature of salt bridges: all phenomena that modulate protein folding. Thus, an ongoing challenge is that weak biomolecule/support interactions can allow leaching of the biomolecule from the support surface;¹⁵ however, strong interactions can result in a distortion of the protein structure and loss of or diminished activity. In order to obtain strong electrostatic interactions, while maintaining the native conformation, the net charge of the protein can be engineered to control its binding affinities to a support surface.^{200, 201} One example reported by Kumar and co-workers²⁰² cationized negatively charged GOx and methemoglobin (Hb) by modifying their surface aspartate and glutamate side chains with tetraethylenepentamine (TEPA). The cationized proteins retained their secondary structure and activity to a significant extent and showed a 250-fold increase in affinity for the negatively charged support $\alpha\text{-Zr}(\text{HPO}_4)_2 \cdot 2\text{H}_2\text{O}$. This strategy has been employed to facilitate the growth of ZIF-8-based enzyme@MOF composites;⁹⁷ however, its application to enzyme-on-MOF systems is untested. Nevertheless, modifying the surface charge of proteins may prove to be a promising approach towards stable and

high-performance enzyme-on-MOF composites. For example, Huang, Lin and co-authors immobilized trypsin onto various MOFs by tagging the enzyme with Fluorescein isothiocyanate (FITC) or 4-chloro-7-nitrobenzofurazan (NBD).²⁰³⁻²⁰⁵ The FITC or NBD facilitates a strong host-guest interaction arising from a close match between the molecular dimensions of the charged dye-molecule and pore window of the MOF. Another approach may be to tailor the surface charge of the MOF crystal. The presence of exposed metals (or metal clusters) and/or uncoordinated organic linkers at the framework surface render MOF particle either positively or negatively charged.²⁰⁶⁻²¹⁰ Furthermore, post-synthetic modification strategies allow for the surface-charge of MOF particles to be switched either *via* ligand installation, ligand exchange, ligand modification or post-synthetic metalation.^{211, 212} Surprisingly, although many examples of enzyme-on-MOF composites have been reported (Table 4), a systematic study on how the surface charge (charge and charge density) of a MOF particle affect the bioactivity of the surface-absorbed biomolecules is missing in the literature. We anticipate that this would be an important and fundamental research direction in MOF-based biocomposites.

Hydrophobic interactions between proteins and surfaces have been widely studied.^{199, 213, 214} It is accepted knowledge that, during the adsorption process, a protein's core hydrophobic residues can be transiently exposed to the surface. This engenders attractive surface-protein forces and results in varied degrees of unfolding that can modify the protein's native activity.¹⁴ It is worth noting that hydrophobic supports are generally unsuitable for surface immobilization of proteins, although there are exceptions. For example, the activity of lipase has been shown to increase when immobilized on a hydrophobic support,¹³ whereas direct anchoring onto hydrophilic surface leads to structural deformation.²¹⁵ Given that enzyme-on-MOF composites are a developing field, limited consideration has been given to the importance of the MOF-enzyme interfacial chemistry. A step in this direction was recently reported by Liang et al. who showed that catalase adsorbed on hydrophilic MAF-7 or ZIF-90 retains a significant degree of enzymatic activity. Whereas, the enzymatic activity was essentially deactivated when the enzyme was immobilized on the isorecticular but comparatively hydrophobic material, ZIF-8.³⁹ In another example, Du and co-workers increased the hydrophobicity of UiO-66 by coating the crystals with a layer of polydimethylsiloxane (PDMS) using chemical vapor deposition

(CVD). The PDMS-on-UiO-66 particles were then used as support for immobilization of *Aspergillus niger* lipase (ANL). The data showed that ANL adsorbed on the hydrophobic surface of PDMS-on-UiO-66 was more active and robust than when immobilized on UiO-66.²¹⁶ Based on these examples, it is clear that optimizing hydro-phobic/-philic interactions between enzymes and MOFs is crucial for the development of enzyme-on-MOF composites. Given that the field continues to grow, further fundamental studies in this area are necessary.

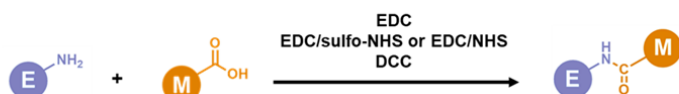
5.2. Immobilization via coordinate bonds

The coordinatively unsaturated metal sites present on the external surface of MOF crystals can serve as sites for coordinate bonds between MOFs and amino acid residues, such as the carboxylate moieties of glutamate and aspartate. Indeed, the coordinative potential of amino acids is exemplified by their use as the organic building blocks of MOFs.²¹⁷⁻²²⁰ For example, Asp has been utilized as the sole ligand to construct a zirconium-based MOF (MIP-202(Zr), MIP = Materials from Institute of porous materials of Paris).²²¹ Although there is no direct evidence in literature for this coordination mode at the enzyme-MOF interface, the aforementioned studies suggest it is highly probable that these occur amongst non-covalent interactions. In addition to carboxylate groups, the imidazole and guanidino units of His and Arg, respectively, are Lewis bases that can coordinate to unsaturated metal sites on the surface of MOF supports. Indeed, a recent report showed that His-tagged synthetic peptides and recombinant or chemically H6-modified proteins strongly interact with the surfaces of MIL-88A(Fe), HKUST-1(Cu), and Zr-fum(Zr) nanoparticles.²²² This work also determined that the binding strength of the biomolecule to the MOF surface depends on the number of oligohistidine residues in the biomolecule.²²²

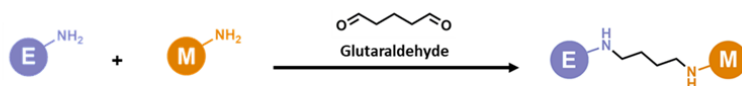
5.3. Immobilization via covalent bonding

Typically, physical interactions alone are not strong enough to prevent immobilized enzymes desorbing from solid-supports. To enhance protein binding to the support surface, for applications such as biocatalysis where recyclability is desired, immobilization *via* covalent chemical bonding has been employed (**Figure 17** and **Table 4**).^{223, 224} Jung et al. used this strategy to prepare the first example of biomolecule-on-MOF composite through covalent-binding.²²⁵ This concept has been adopted by other groups to create numerous biomolecule-on-MOF composites in recent years (**Table 4**).^{197, 226, 227}

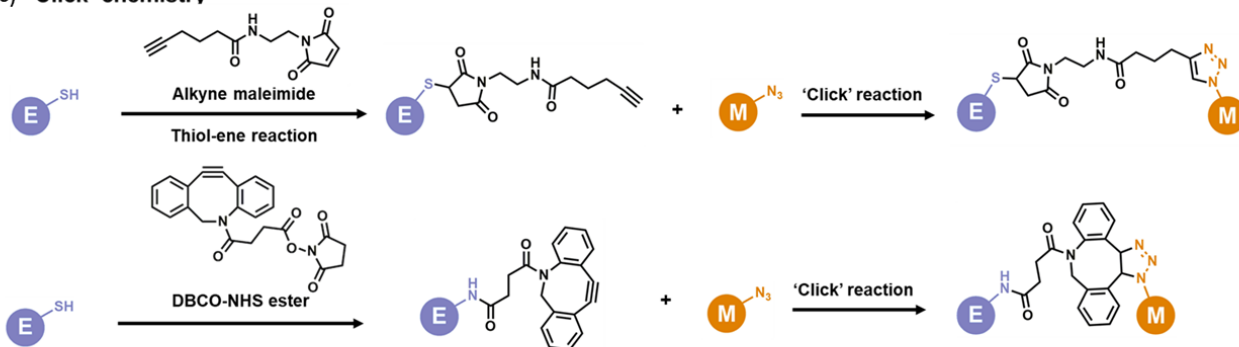
(a) Carbodiimide coupling



(b) Glutaraldehyde coupling



(c) 'Click' chemistry



(d) Thio-disulfide exchange reaction

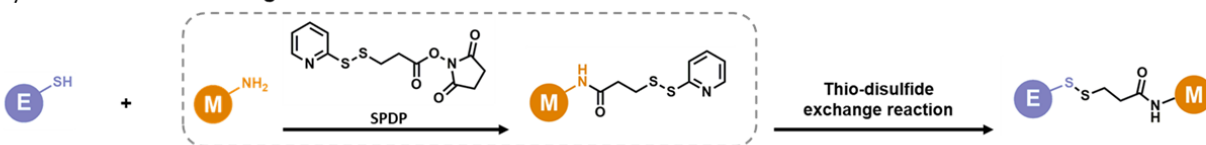


Figure 17. Reaction schemes showing the strategies to covalently anchor protein/enzyme on MOF surface. EDC = 1-ethyl-3-(3-dimethylaminopropyl)carbodiimide-hydrochloride (EDC·HCl); sulfo-NHS = N-Hydroxysulfosuccinimide sodium salt; NHS = N-hydroxysuccinimide; DBCO-NHS ester = Dibenzocyclooctyne-N-hydroxysuccinimidyl ester; SPDP = N-Succinimidyl 3-(2-pyridylthio)propionate. E represents enzymes and M represents MOF.

Owing to the near ubiquity of carboxylic acid-based functional groups the surface of MOFs, carbodiimide conjugation was a logical starting point for the preparation of enzyme-on-MOF composites (**Figure 18**). Carbodiimide conjugation is carried out by first activating the carboxyl functionality on the surface of the MOF particle by using 1-ethyl-3-(3-dimethylaminopropyl)carbodiimide-hydrochloride (EDC·HCl). In this case the exposed carboxyl moiety on the MOF surface can result from the non-coordinated carboxylate ligand, in the as-synthesized material, or introduced onto the MOF particle via post-synthetic modification. Upon reaction with EDC, an active o-acylisourea intermediate is formed which is easily displaced by nucleophilic attack from a primary amino groups on a protein surface in the reaction mixture (**Figure 18**). Thereafter, the primary amine forms an amide bond with the original carboxyl group and an EDC-derived by-product is released. However, the o-acylisourea intermediate is unstable in aqueous solutions where it can undergo hydrolysis, prior to forming the amine, and release of the isourea by-product. As a consequence, EDC is often supplied in a large molar excess of the amine-containing biomolecules to assure

the success of the carbodiimide coupling. N-hydroxysuccinimide (NHS) or its water soluble analog (sulfo-NHS) is often included in EDC-coupling protocols to improve efficiency. In this reaction, EDC activates the carboxylic acid and couples NHS (or sulfo-NHS) to form an NHS ester which is considerably more stable than the o-acylisourea intermediate. The NHS esters then irreversibly react with primary amine to form the amide linkage and the NHS is released to the medium.²²⁸ This strategy facilitates efficient conjugation between carboxylic acids and primary amines at neutral pH. Dicyclohexyl carbodiimide (DCC) is another crosslinking agent used to link carboxylic acids and primary amines. However, DCC is not soluble in water and thus it is primarily used in manufacturing and organic synthesis applications rather than in protein research.²²⁸ The carbodiimide conjugation method is widely used to covalently immobilize biomolecule on MOF supports and was first utilized by Park and co-workers to covalently link an enhanced green fluorescent protein (EGFP) or CalB on bulk MOF materials to form protein-on-MOF composites.²²⁵ Selected examples of this strategy are listed in **Table 4**.

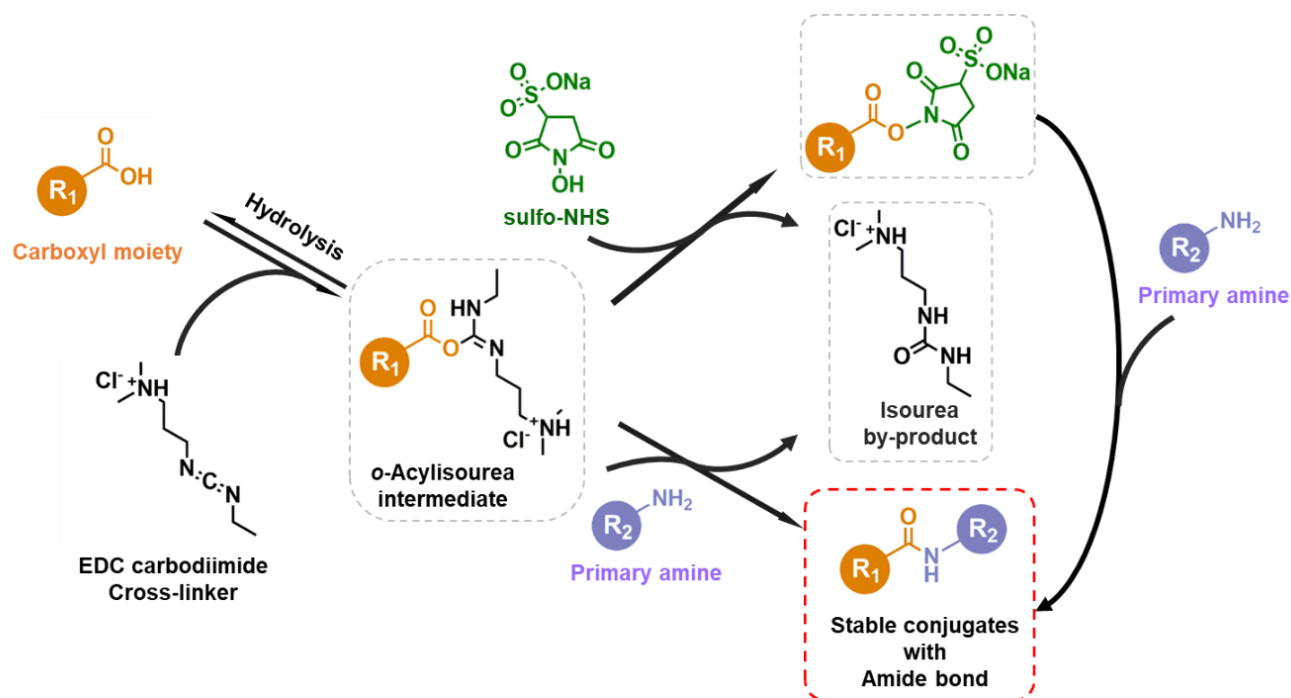


Figure 18. Schematic illustration of EDC and EDC/sulfo-NHS cross coupling reaction (EDC = 1-ethyl-3-(3-dimethylaminopropyl)carbodiimide-hydrochloride (EDC·HCl); sulfo-NHS = N-Hydroxysulfosuccinimide sodium salt). The addition of sulfo-NHS (can be substituted by N-hydroxysuccinimide (NHS)) can greatly increase the overall reaction efficiency.

Biomolecule-on-MOF biocomposites have also been synthesized using glutaraldehyde as cross-linking agent.²²⁹ The amine anchoring point on the MOF surface can arise from the as-synthesized material (*e.g.* IRMOF-3) or be introduced *via* post-synthesis ligand modification. In the case of the proteins the accessible amine functionality originates from surface-exposed lysine residues. Typically, the crosslinking is achieved by first adsorbing the protein onto the MOF surface followed by the introduction of glutaraldehyde which covalently links the exposed amines on the MOF and protein surfaces. Several examples of protein-on-MOF composites have been reported in literature employing this strategy. For example, in 2013, Falcaro and co-workers used glutaraldehyde to immobilize β -glucosidase onto patterned films of MIL-53-NH₂(Al).²³⁰ Similarly, Lou and co-workers covalently grafted soybean epoxide hydrolase (SEH) onto UiO-66-NH₂ crystals.²³¹

'Click' chemistry could in principle also be applied to prepare protein-on-MOF biocomposites by linking dibenzylcyclooctyne (DBCO) or alkyne moieties on the biomolecules with the azide functionality on MOF surface. DBCO can be chemically grafted on the protein surface by reacting cysteine residues with DBCO-PEG_n-maleimide or lysine residues with a DBCO-NHS ester moiety, and alkyne groups can be introduced by reacting cysteine residues with alkyne maleimide. With respect to the MOF surface, azide functionality can be realized *via* the organic building block or post-synthesis modification. Hitherto, click chemistry has been successfully utilized to prepare nucleotide- and PEG-functionalized MOF particles.^{230, 232-235} However, we posit that this strategy can be successfully applied to prepare protein-on-MOF biocomposites in the future.

Besides lysine functionality, biomolecules can also be covalently anchored on MOF surfaces *via* surface exposed

cysteine residues.²²⁸ The thiol group of cysteine is more nucleophilic than the primary amine in lysine, especially at biologically relevant pHs (*i.e.* below 9), where the amine is protonated. As a result, cysteine often reacts faster than lysine, giving rise to selective modification of cysteine over lysine residues. The caveat is that free thiols are relatively rare in proteins as they are often present in the oxidized disulfide form. Therefore, it is often required to expose proteins to reducing agents, such as dithiothreitol, as a pre-treatment to free the thiol groups.²³⁶ Thereafter, the free thiol group can be modified selectively and stoichiometrically by maleimides to form stable carbon-sulfur bond.²³⁷ Alternatively, forming disulfide bonds under oxidative conditions can be employed as a strategy to covalently link proteins to surfaces. This was exemplified by the immobilization of ovalbumin (OVA) on MIL-101-NH₂(Fe).²³⁸ Here, the surface-exposed amino functionality of as-synthesized MIL-101-NH₂(Fe) was chemically modified using N-succinimidyl 3-(2-pyridyldithio)-propionate (SPDP) to graft a disulfide bond onto the MOF surface. The MOF particle was then covalently functionalized with OVA *via* thio-disulfide exchange process.

In all, covalent linkage of proteins onto MOFs surfaces has proved to be a powerful tool to form a variety of new protein-on-MOF biocomposites. The covalent conjugation reactions described in this section encompass the majority of examples; however, the scope for this chemistry is broad and as this field develops we anticipate that new approaches will be reported.

5.4. Enzymatic activity upon surface-immobilization

When a protein is immobilized on a solid support, the structure, orientation, and conformational mobility of the protein can be modified and this typically leads to a

change in its native functionality. The structural perturbation experienced by an adsorbed protein is related to the: 1) composition of amino acids on the protein surface; 2) physical/chemical properties of the support; 3) particle size and topography of the support; and 4) the nature of interaction between protein and support. In proteins, hydrophobic residues can be present at the surface.¹⁵ Indeed, proteins that possess solvent accessible hydrophobic groups have been shown to adsorb tightly to hydrophobic surfaces,^{199, 214} which leads to dehydration at the interface and structural change.^{239, 240} Such interactions may stabilize a non-active structure or even cause the enzyme to spread across the hydrophobic surface, which can also diminish enzyme activity. This mechanism of adsorption-driven enzyme deactivation is commonly reported in the literature and therefore needs to be avoided for the formation of functioning enzyme-on-MOF composites.

A promising approach to optimize the biomolecule/MOF biointerface is to graft (either via physical adsorption or chemical modification) hydrophilic polymers (e.g. poly(ethylene glycol) (PEG), polyethylenimine (PEI), aldehyde dextran, dextran sulfate) or small molecules (such as carbohydrates) either on the protein or the MOF support.²⁴¹⁻²⁴⁴ The hydrophilic shell formed by the polymer/small molecule acts to shield each individual protein in non-aqueous media.^{245, 246} Furthermore, the surface modification that results for a hydrophilic MOF surface may provide a more suitable interface for retention of the active conformation of an adsorbed protein. For example, a recent report from Wuttke and coworkers showed that coating the surface of Zr-fum nanoparticles with seven different types of polymer improved protein binding and facilitates retention of the active structure. Fluorescence correlation spectroscopy (FCS) and fluorescence cross-correlation spectroscopy (FCCS) illustrated that the binding affinity of albumin (Alb) and immunoglobulin (IgG) on polymer-on-MOF composites was coating dependent.²⁴⁷ The highly mutable chemistry of MOFs and straight-forward post-synthesis modification strategies point towards this being promising concept to be further developed to optimize the binding affinity and bioactivity of immobilized enzymes.

For some enzymes, local or global dynamics are necessary for their function; obviously, this can be perturbed by immobilization. Artificially modifying protein dynamics may hinder the initial substrate recognition or prevent the protein from accessing active conformations. However, there are some cases where non-native conditions can stabilize active forms. An example is that many lipases possess an α -helix fragment, termed the 'lid', which provides access to the catalytically active cleft in the presence of a hydrophobic phase. This lid-movement has been known as interfacial activation. When in contact with hydrophobic support, the lid-open form of lipases can be stabilized resulting in higher specific activity.²⁴⁸⁻²⁵⁰

Another consideration for protein-on-MOF biocomposites is that metal ions are well known to act as enzyme inhibitors.^{251, 252} A recent study published by Zhou and co-workers showed that a 2D Cu-MOF ($[\text{Cu}(\text{bpy})_2(\text{OTf})_2]$, bpy = 4,4'-dipyridyl) inhibits the active site of α -chymotrypsin (ChT), through competitive binding rather than disrupting

the active conformation of the protein.²⁵³ The competitive inhibition resulted from the electrostatic interaction between the Cu^{2+} center of the MOF metal node with the surface exposed His-57 residues on ChT, and irreversible coordination interactions. The authors proposed that, in pH 7.4 buffer, the triflate ligand on the strong Lewis-acidic Cu^{2+} center in Cu-MOF nanosheets is likely to be displaced by the nucleophilic nitrogen of HEPES ($\text{pK}_a = 7.5$). As the pK_a of His-57 (7.0 to 12) in ChT is larger than that of HEPES, the nitrogen of His-57 might easily replace the nitrogen of HEPES and coordinate to the Cu^{2+} center of the 2-D Cu-MOF. This irreversible coordinative interaction between the copper metal site and ChT His-57 residue was elucidated by UV-vis measurements. Such strong interactions fully inhibit the bioactivity of ChT; in comparison, another 2D MOF material $[\text{Zn}_2(\text{bim})_4]$ (bim = benzimidazole), shows no significant inhibition effect.

The orientation of an enzyme with respect to the support surface is another important parameter that determines its activity. Orienting the biomolecule active site towards the bulk solution after immobilization is expected to have several advantages: 1) improved guest diffusion; 2) minimize the interfacial effects on the active site, such as local pH or salt gradient; 3) limit active site deformation. However, if the active site is oriented towards the surface of the support, access of the substrate molecule can be restricted. As previously mentioned, the presence of highly charged regions in some enzymes, such as lysozyme, can influence its orientation when in contact with a charged surface.²⁵⁴ By using computational models, Talasaz et al. predict the influence of the charge of the support on the orientation of enzymes on biological and non-biological surfaces.²⁵⁵ Additionally, Mroginski and co-workers analyzed the ionic strength dependence of the initial surface adsorption of sulfite oxidase onto mixed amino- and hydroxyl-terminated self-assembled monolayers (SAMs).²⁵⁶ Such simulations have provided insight into the surface-protein adsorption; however, it is challenging to couple these to experimental evaluation of enzyme orientation on solid supports. By applying a combination of sum frequency generation (SFG) and ATR-FTIR (attenuated total reflection-Fourier transform infrared spectroscopy) vibrational spectroscopy techniques, Marsh and co-authors have studied protein orientation when in contact with a support.²¹³ Nevertheless, this technique may be difficult to apply into the biomolecule-on-MOF biocomposites, due to the high absorption background of the MOF materials. In a recent study, by using site-directed spin labeling (SDSL) coupled electron paramagnetic resonance (EPR) technique, Yang and co-workers studied the steric driven orientation of lysozyme immobilized on ZIF-8 surface. In combination with computational modeling, the authors revealed the tendency of different regions of lysozyme to be exposed to the solvent once immobilized and predicted the preferential orientation of lysozyme on ZIF-8 surface.²⁷ These studies are non-routine and, due to the diverse and complex interfacial chemistry, it is difficult to extrapolate general information about the orientation of enzymes on MOF surfaces. Because the orientation of biomolecule on MOF support would greatly affect the diffusion of solvent/guest to its functional core and thus its overall biofunctionality, we anticipate there will be more

concerted effort to understand and thus allow control of the orientation of enzymes on the surface of MOF crystals. The size of the support can also affect the activity of an adsorbed enzyme. In general, if the curvature of the support surface allows for an optimal geometric congruence between a support and an enzyme, it can favor multipoint interactions and higher stabilization.¹⁴ While there has been no systematic study related to the size-effect of protein-on-MOF composites, some general principles can be gar-

nered from studies of enzymes adsorbed on inorganic nanoparticles. For example, lysozyme adsorbed onto hydrophilic silica nanoparticles (SNPs) retained more of its native secondary structure and enzymatic activity on smaller SNPs (with high degrees of surface curvature) than on larger ones.²⁵⁷ However, it is worth noting that, recently, monodispersed MOF nanoparticles have been realized via synthesis using modulators or epitaxial growth strategies.²⁵⁸⁻²⁶⁰ Thus, effect of MOF crystal size on the activity of surface adsorbed enzymes is possible and should be pursued.

Table 4. Summary of the preparation methods and applications of protein-on-MOF composites.

MOF	Enzyme	Immobilization method	Application	Ref.
[Cu ₂ (bpdC) ₂ (DABCO)] _n	Microperoxidase-11(MP-11)	Physical adsorption	Biocatalysis	143
HKUST-1	Bacillus subtilis lipase (BSL2)	Physical adsorption	Biocatalysis	162
			(esterification reaction)	
HKUST-1	Trypsin	Physical adsorption ^a	Biocatalysis	261
	Cytochrome <i>c</i>			
	α -chymotrypsin			
UiO-66(Zr)	porcine pancreatic lipase (PPL)	Physical adsorption	Biocatalysis	205
UiO-66-NH ₂ (Zr)			(warfarin synthesis)	
MIL-53(Al)				
Carbonized MIL-53(Al)				
ZIF-7	glucose dehydrogenase (GDH)	Physical adsorption ^b	Electrochemical biosensor	262
ZIF-8				
ZIF-67				
ZIF-68				
ZIF-70				
MIL-101-NH ₂ (Al)	Hemin	Physical adsorption	Biosensor	263
MIL-160(Al)	Carbonic anhydrase (CA)	Physical adsorption ^c	Biocatalysis (CO ₂ capture)	43
ZIF-8				
Co-FeMOF	glucose oxidase	Physical adsorption	Biocatalysis	264
ZIF-L	Carbonic anhydrase (CA)	Physical adsorption	Biocatalysis (CO ₂ capture)	265
MIL-100(Fe)	laccase	Physical adsorption	Biocatalysis	266
MIL-100(Fe)	glucose oxidase (GOx)	Physical adsorption ^d	Biosensor	267

MIL-100(Al)				
MIL-100(Cr)				
MIL-127(Fe)				
Zr-MOF	laccase	Physical adsorption	Biocatalysis	268
Cu-MOF	tyrosinase	Physical adsorption ^e	Biosensor	269, 270
MIL-100(Fe)	Laccase	Physical adsorption ^f	Biocatalysis	271
	BSA		(oxygen reduction reaction)	
MIL-53(Al)	β -glucosidase	Physical adsorption	Biocatalysis	100
MIL-53-NH ₂ (Al)	Laccase			
MOF-74(Mg)				
Cu(bpy) ₂ (OTf) ₂	α -Chymotrypsin	Physical adsorption ^g	Enzyme inhibitor	253
Zn ₂ (bim) ₄				
MIL-101(Fe)	polyphosphate kinase 2 (ArPPK2)	Physical adsorption ^g	Biocatalysis	272
MIL-101-NH ₂ (Fe)				
PCN-222(Fe)	glucose oxidase	Physical adsorption	Biocatalysis	273
UiO-66-COOH	methioninase	Physical adsorption	Biological application (anticancer agent)	274
Zr-fum	Albumin (Alb)	Physical adsorption ^h	Biological application (proof-of-concept)	247
	Immunoglobulin G (IgG)			
UiO-66	Aspergillus niger lipase (ANL)	Physical adsorption ⁱ	Biocatalysis	216
ZIF-8	cellulase	Physical adsorption	Biocatalysis	275
UiO-66-NH ₂				
MIL-100(Fe)				
PCN-250				

UiO-66-NH ₂	Pectinase	Physical adsorption ^l	Biocatalysis	276
MOF-545(Fe)	glucose oxidase (GOx)	Physical adsorption	Biocatalysis	277
UiO-66-NH ₂	Candida Antarctica lipase B (CalB)	Physical adsorption ^k	Biocatalysis	278
	glucose oxidase (GOD)			
	green fluorescent protein (GFP)			
CYCU-4	FITC-trypsin	Physical adsorption ^l	Biocatalysis	203, 204
MIL-101(Cr)	NBD-trypsin		(protein digestion)	
MIL-100(Cr)				
UiO-66(Zr)				
ZIF-8	Trypsin	Covalent conjugation	Biocatalysis	279
		(EDC/NHS) ^m	(protein digestion)	
IRMOF-3	enhanced green fluorescent protein	Covalent conjugation	Biocatalysis	225
(Et ₂ NH ₂)(In(pda) ₂)	Candida antarctica lipase B (CalB)	(EDC or DCC)		
Zn(bpydc)(H ₂ O)				
MIL-125-NH ₂	Hemoglobin	Covalent conjugation	Biological application	280
		(EDC/sulfo-NHS) ⁿ	(oxygen carrier)	
MIL-53-NH ₂ (Al)	glucose oxidase (GOx)	Covalent conjugation	Biocatalysis	281
MIL-53-NH ₂ (Cr)		(EDC/NHS) ^o		
ZnGlu	Aspergillus niger lipase (ANL)	Covalent conjugation	Biocatalysis	282
		(EDC/NHS) ^o		
UiO-66-NH ₂	Candida Antarctica lipase B (CalB)	Covalent conjugation	Biocatalysis	283
		(DIC) ^p		
MIL-101(Cr)	Trypsin	Covalent conjugation	Biocatalysis	284
		(DCC)	(Protein digestion)	

MIL-88B(Cr)				
MIL-88B-NH ₂ (Cr)				
UiO-66-NH ₂	Soybean epoxide hydrolase	Covalent conjugation (glutaraldehyde)	Biocatalysis	231
MIL-53-NH ₂ (Al)	β-D-Glucosidase	Covalent conjugation (glutaraldehyde)	Biocatalysis	230
MIL-101-NH ₂ (Fe)	ovalbumin	Covalent conjugation	Biological application	238
	cytosine–phosphate–guanine (CpG) oligonucleotide	(disulfide-thio exchange reaction) ^f	(drug delivery)	

^aHKUST-1 was formed on polydopamine functionalized Fe₃O₄ particle to form magnetic particle;

^bBesides physical hydrophobic and electrostatic interactions, chemical interaction between GDH and ZIF-70 was also evidenced;

^cAs evidenced by FTIR, CD and computational studies, the structure deformation of CA on hydrophobic ZIF-8 is more pronounced than that on hydrophilic MIL-160(Al);

^dAfter surface adsorption, the GOx/MOF composites was coated by a protection layer formed by glutaraldehyde and BSA;

^eTyrosinase was surface-adsorbed on MOF surface together with chitosan;

^fAfter surface-adsorbed onto MOF, the protein is cross-linked using glutaraldehyde;

^gThe MOF and protein interact coordinatively through the histidine-metal binding;

^hPrior to protein surface-immobilization, the Zr-fum was first coated with different type of polymers (BPEI, PAMAM, Pglu, PAA, PEG, Tween, or Pglu-Psar). The protein binding affinity to the polymer/MOF particle is found to be dependent on the type of the polymer coating;

ⁱUiO-66 particle was surface functionalized with PDMS by CVD treatment to tune its hydrophobicity prior to enzyme immobilization;

^jUiO-66-NH₂ was surface functionalized with PMAA covalently prior to enzyme immobilization;

^kUiO-66-NH₂ was surface-modified using lauric acid coordinatively to tune its hydrophobicity prior to enzyme immobilization;

^lFITC or NBD was used to functionalized trypsin and as probe to trapped-molecule in MOF pore to facilitate enzyme immobilization;

^mZIF-8 surface was coordinatively functionalized with N-(3-aminopropyl)-imidazole. Thereafter trypsin was covalently immobilized via EDC/NHS chemistry;

ⁿMIL-125 was surface-functionalized with succinic anhydride to increase the carboxyl population on MOF surface prior to enzyme immobilization;

^oThe amino residues on MOF surface were functionalized with glutaric anhydride to increase the carboxyl population prior to enzyme immobilization;

^pThe amino residues on MOF surface were functionalized with fatty acid (C12-C22) to tune its hydrophobicity prior to enzyme immobilization; DIC = diisopropylcarbodiimide.

^rMOF was surface modified with N-succinimidyl 3-(2-pyridyldithio)propionate (SPDP) prior to the disulfide-thio exchange conjugation reaction.

6. MULTICOMPONENT BIOCOMPOSITES

A variety of different synthetic strategies have been employed to synthesize MOF-based composite materials.²⁸⁵⁻²⁸⁷ Through careful design, MOF composites have shown exceptional performance characteristics in areas including gas uptake, molecular sensing, metal sequestration and catalysis.²⁸⁷ However, limited attention has been devoted to integrating MOF-based composite materials with biomacromolecules. Nevertheless, a number of pioneering reports have explored the synthesis, characterization and potential applications of these novel materials. In this section, we classify multicomponent MOF-biocomposites as materials that integrate at least 3 distinct components. For example, a biomacromolecule, encapsulated within a MOF (components 1 and 2) deposited on a support (component 3) or a biomacromolecule and second component (such as a coordination complex or functional nanoparticle) associated via a MOF matrix. An important synthetic consideration to optimize the performance of this class of composite is whether a one-pot or multi-step protocol is employed. For example, the biomacromolecule is typically the most fragile component as it typically loses activity when exposed to solvothermal MOF synthesis conditions (elevated temperature^{2, 16, 288} and organic solvents^{2, 16, 289, 290}). Thus, chemistries that afford them protection out the outset of the composite synthesis or otherwise allow late-state introduction of the enzyme are critical. In this section we will canvass strategies employed to integrate enzyme@MOFs with other materials (e.g. magnetic nanoparticles²⁹¹, silica nanoparticles²⁹², polymer capsules²⁹³) for the preparation of multicomponent biocomposites.

Recently, enzyme@MOFs have been combined with micro and nanoparticles to form multi-component systems.^{63, 291-297} In such materials the desired application

of the multicomponent biocomposite determines the type of nanoparticle selected. Organic and inorganic materials have been integrated with enzyme@MOF systems to modify electron conduction,^{63, 294} biocompatibility,²⁹⁸ stability to harsh conditions (e.g. high temperature²⁹², organic solvents²⁹⁵) molecular diffusion²⁹³ and fluorescence²⁹⁶ properties of the original MOF biocomposite. Selected examples are reported in **Table 5**.

Enzyme@MOF biocomposites are intrinsically poor electron conductors, thus to employ these materials in electrochemical sensing devices or biofuel cells, strategies to enhance conductivity are necessary. This has been achieved by synthesizing multicomponent systems composed of enzymes@MOFs and conductive nanomaterials such as graphene nanosheets⁶³ and carbon nanotubes.²⁹⁴ For example, Li et al.²⁹⁴ sonicated a sample of laccase that had been encapsulated in ZIF-8, LAC@ZIF-8, in presence of carboxylated multiwalled carbon nanotubes (c-MWCNTs) to afford the MOF-based electrode c-MWCNTs/LAC@ZIF-8. In this study, LAC was used for the oxidation of bisphenol A (a toxic monomer widely used in the synthesis of commercial polymers²⁹⁹) to 1,4 benzoquinone. The carbon nanotubes were used to improve the electrical conductivity, and ZIF-8 was employed as a porous matrix to permit the diffusion of bisphenol A and 1,4 benzoquinone through the electrode (**Figure 19**), however, given the size of these molecules, diffusion is anticipated to be slow or facilitated through crystal defects.³⁰⁰ This composite was used for the successful fabrication of an enzymatic biofuel cell and, as a result, clearly demonstrates that an extrinsic property (electrical conductivity) can be imparted to an insulating enzyme@MOF system.

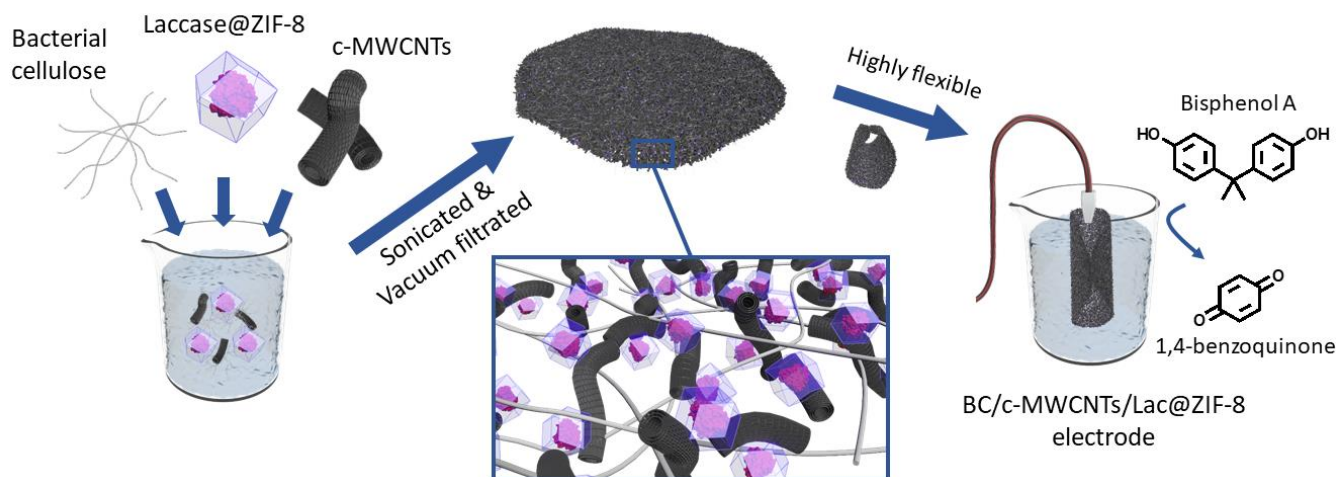


Figure 19. Preparation of enzymatic biofuel cell consisting of Laccase@ZIF-8, bacterial cellulose and carboxylated-multi walled carbon nano tubes (c-MWNTs).²⁹⁴

Another important technological challenge is to enhance the cyclability of biocatalysts and biosensors.³⁰¹ In general this can be addressed by immobilizing enzymes on a solid support that allows for an easy separation and reuse of the bioactive species on demand.³⁰¹ To facilitate separation, or dynamic localization of MOF-based biocomposites, magnetic nanoparticles or fibers can be incorporated. These materials termed Magnetic Framework Composites (MFCs)²⁸⁹ have been applied to

areas including sensing,³⁰² catalysis,³⁰³ environmental remediation³⁰⁴ and drug delivery.^{305, 306} Typically, the magnetically responsive inorganic component acts as a heterogeneous nucleation seed for the crystallization of MOFs.³⁰⁴ Thus, magnetic NPs, enzyme and MOF precursors solutions can be mixed in different sequences to synthesize magnetic biocomposites.^{291, 307-311} The final MOF biocomposite can be easily collected and, thus, with respect to the free enzyme, the recyclability of the

biocatalyst improved (**Figure 20**).^{61, 307, 311} In addition, magnetic fields can also be employed to precisely control the position of the MOF-based materials opening up

the potential to integrate these biocomposites into microfluidic systems and lab-on-a-chip devices^{312, 313}.

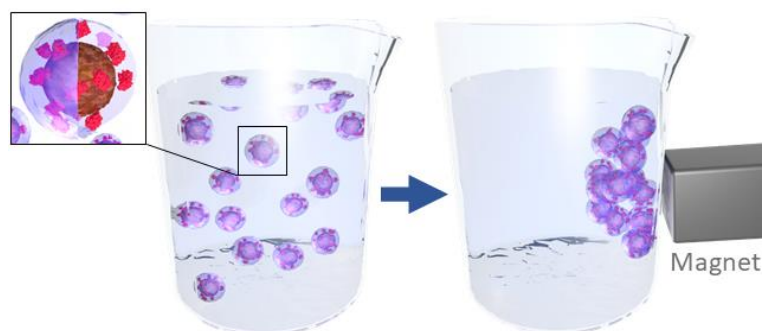


Figure 20. A schematic representation of MFCs comprising a magnetically responsive component (core) and an enzyme@MOF shell. These can be collected or positioned by use of an external magnetic field. (See SI: 20_MFC_dynamic_positioning.mp4).

MFCs commonly use iron oxide particles as the magnetically responsive component. Indeed, when compared to other materials, Fe_2O_3 and Fe_3O_4 nanoparticles offer several advantages: 1) they are commercially available and easy to be synthesized; 2) their surface functionality can be tailored; 3) they are biocompatible and can be dispersed in biocompatible media.^{287, 314} These properties render iron oxide-based MFCs attractive targets for enzyme immobilization and encapsulation (see **Table 5**). The most straightforward approach to synthesize such multicomponent biocomposites is to expose preformed MFCs to a solution containing free enzymes (**Figure 21a**). In this case, the affinity of biomolecules for the MOF surface results in enzyme-decorated MFC particles (enzymes-on-MFCs).^{10, 307, 308, 315} For example, Zhai et

al.³¹⁶ used ZIF-90-coated Fe_3O_4 particles as solid supports for the covalent immobilization of TRY. The resulting biocomposite ((TRY-on-(Fe_3O_4 @ZIF-90)) was tested for its capacity to digest proteins (**Figure 21a**). This approach provides the clear advantage that the MOF matrix does not limit diffusion as the TRY is immobilized on the crystal surface. However, this configuration offers limited protection for trypsin to the reaction environment. Given the two-step synthesis: 1) preparation of the magnetic NP@MOF and 2) immobilization of the enzymes on the surface of magnetic NP@MOF, a variety of MOFs could be employed as there is no requirement to maintain biocompatible conditions. Nevertheless, the MOF support must be water stable to allow for repeated use.

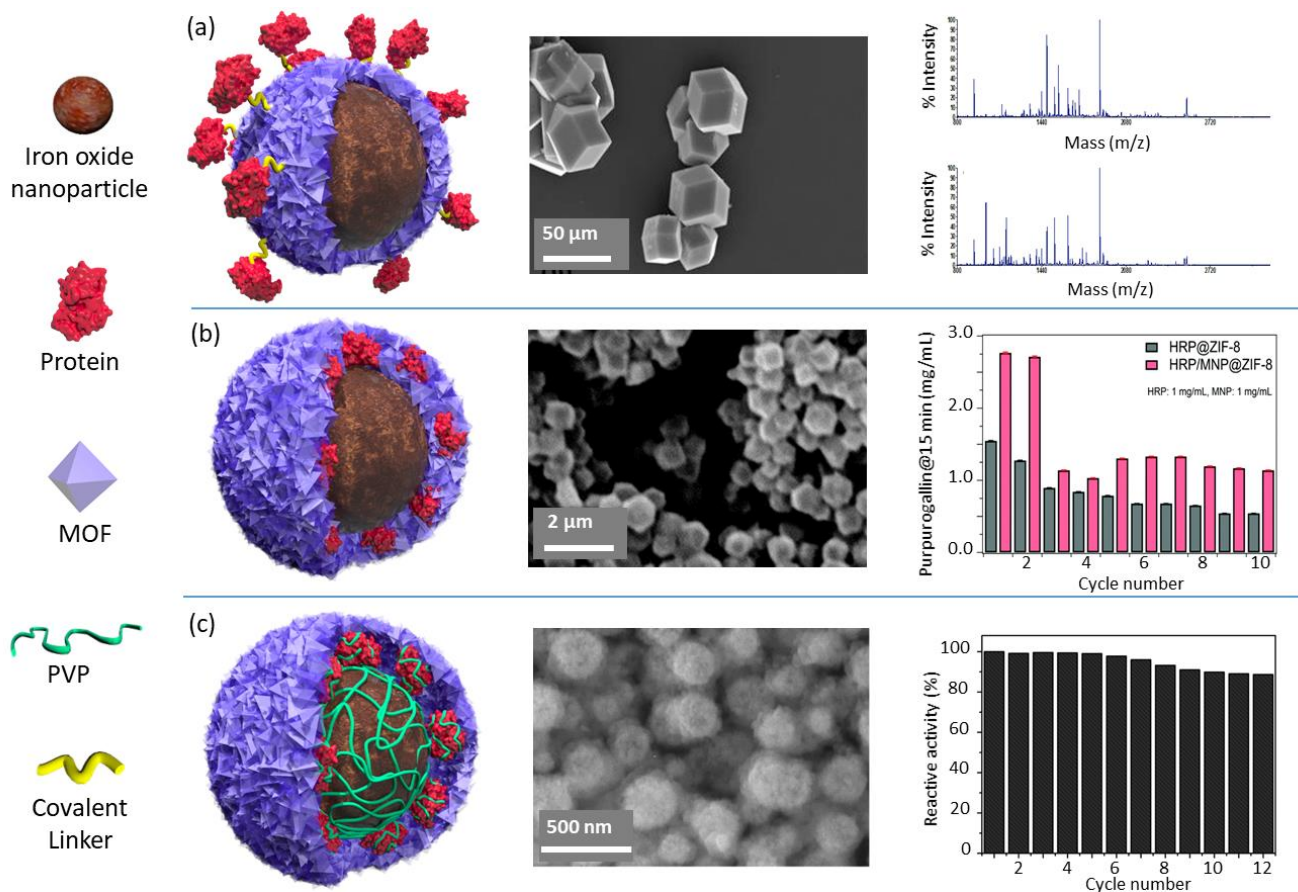


Figure 21. Schematic representations, scanning electron microscopy images and activity data for selected multicomponent composites: (a) (TRY-on-Fe₃O₄)@ZIF-90; (b) HRP/Fe₃O₄@ZIF-8; and (c) (GOx-on-Fe₃O₄)@ZIF-8. (a) Adapted with permission from Ref. 317, copyright [2017] Elsevier. (b) Adapted with permission from Ref. 318 under the terms of the CC BY 3.0 license. (c) Adapted with permission from Ref. 309, copyright [2020] The Royal Society of Chemistry.

An alternative strategy to synthesize MFCs is via the simultaneous addition of enzymes and magnetic NPs to the MOF precursor solution (**Figure 21b**). Using this one-pot approach, the formation of homogenous MOF-biocomposites have been reported.^{291, 311} Ricco et al.²⁹¹ prepared HRP/Fe₃O₄@ZIF-8 by adding a model enzyme (HRP) and iron oxide nanoparticles in an aqueous solution of 2-mIM and Zn²⁺. The formation of the magnetic MOF biocomposites was studied *in situ* with both small and wide angle scattering methods. These data indicated that the presence of both protein and the magnetic nanoparticles in solution affords a faster nucleation and growth for ZIF-8 compared to the separate preparation of HRP@ZIF-8 and Fe₃O₄@ZIF-8 (**Figure 21b**). Additionally, the authors measured an encapsulation efficiency of ca. 90% and demonstrated that the composite could be cycled. The authors also established that the enzymatic activity is influenced by the relative amount of nanoparticles and MOF precursors. For the same concentration of enzyme and MOF precursors, the catalytic activity was improved when a higher concentration of magnetic NPs was used to synthesize the magnetic biocomposite. The improved activity was attributed to a larger number of magnetic nanoparticles within the MOF crystal inducing more defects and thus improving the diffusion of reagents and products within the porous framework.^{291, 319} Co-crystallization agents can also be used to afford the formation of MOF-based composites (**Figure 21c**). For example, the use of PVP as a crystallization agent for ZIF-8 was suggested by Lu et al.⁹² and

used for the preparation of a number of inorganic composites (NPs@ZIF-8). PVP has also been added to solutions containing enzymes for the one-pot preparation of CytC@ZIF-8¹⁷ and CAT@ZIF-90.¹⁹ Synthetic approaches to magnetically active multicomponent bio-composites have also employed PVP. For example, Hou et al.³⁰⁹ synthesized (GOx-on-Fe₃O₄)@ZIF-8 by adding an ethanolic solution of citric acid-functionalized Fe₃O₄ nanoparticles and Zn(NO₃)₂ to a different ethanolic solution of PVP, 2-mIM and GOx. The authors suggested that in this *de novo* synthesis, PVP enhanced the stabilization of the enzyme and promoted the uniform crystallization of ZIF-8 on the surface of the citric acid-functionalized Fe₃O₄ nanoparticles. The magnetic biocomposite was used as colorimetric sensor for the detection of glucose (**Figure 21c**). Notably, in this work, both the MOF and the enzyme are catalytically active components. Indeed, the authors showed that ZIF-8 possesses peroxidase-like activity which was exploited to perform a catalytic cascade in combination with the encapsulated GOx. Although PVP is the most used co-precipitating agent, other polymers are currently under investigation, for example cellulose use has been reported by Cao et al.³¹⁰ Although using neutral polymers to protect enzymes or seed MOF growth is a promising strategy for the synthesis of multicomponent biocomposites the mechanism of crystallization is unclear although it is thought that negatively charged residues are necessary to improve crystallization (for further discussion see sections 3.3.1 and 3.3.2).⁷⁸ Nevertheless, the use of co-precipitation (or co-crystallization) agents could be crucial where the MOF

crystallization is not triggered by NPs or by enzymes. In addition to magnetic nanoparticles, several multicomponent composite systems based on both functional particles and enzymes have demonstrated to be relevant for application to catalysis,³²⁰⁻³²³ sensing,^{322, 324-327} biomedics,³²⁷⁻³³⁰ energy production,^{322, 331, 332} and nanomachines/micromotors.^{298, 333} In the field of heterogeneous catalysis, multicomponent composites are particularly appealing. One of the most recent trends in catalysis is to synthesize a single material that possesses different catalytic sites that can work synergistically to perform complex reaction schemes (e.g. cooperative¹, cascade³³⁴ and tandem³³⁵ reaction schemes). This kind of scheme has been proven to be successful in multi-enzymes@MOF composites, where up to three different enzymes (β -gal, GOx and HRP) were encapsulated in ZIF-8 particles and worked in concert to catalyze cascade reactions.³³ Examples of these materials were also highlighted in the section on infiltration, for example GOx/HRP@PCN-888 composite.¹⁸⁵ Similarly, metallic NPs embedded in MOFs have shown promising catalytic performances and tandem reaction schemes were investigated as well.³³⁶ Herein, we posit that the develop-

ment of multicomponent MOF composites based on enzymes and metallic NPs will pave the way to novel catalytic reaction schemes. Finally, infiltration has been used to form an electrocatalytic multicomponent biocomposite,¹⁹⁶ where an enzymatic reaction carried out by formate dehydrogenase (FDH) was coupled to the electrochemical regeneration of NADH cofactor. To form the catalytic system, FDH@NU-1006 biocomposites were deposited on a fluorine-doped tin oxide glass electrode modified with Cp*Rh (2,2'-bipyridyl-5,5'-dicarboxylic acid)Cl₂ complex). Upon exposure to CO₂ the FDH@NU-1006 biocomposite produces formic acid with electrons supplied by the NADH cofactor, which is itself electrochemically regenerated from NAD⁺. The bioelectrocatalytic system converts CO₂ into formic acid at a rate of $79 \pm 3 \text{ mM h}^{-1}$ (turnover number of 1.3×10^4). Part of the success of this system is that the FDH@NU-1006 composite exhibited significantly higher catalyst stability when subjected to non-native conditions compared to the free enzyme. Thus, it is envisaged that the judicious combination of the different biological, inorganic and MOF components will enable the preparation of composites with enhanced functional properties.

Table 5. Summary of the preparations and applications of multi-component MOF biocomposites, including information disclosing the preparation method (biomimetic/one-pot, infiltration, or surface adsorption).

MOF	Enzyme	Additional components	Immobilization method	Application	Ref.
ZIF-8	GOx	Polydopamine	biomimetic	biocatalysis	295
UiO-66	Candida Antarctica lipase B	Fe ₃ O ₄	inverse phase Pickering emulsion	biocatalysis	61
ZIF-8	β-galactosidase	agarose hydrogel			
ZIF-8	GOx	graphene oxide	co-precipitation in CaCO ₃	biosensor	63
		polydopamine	then, encapsulation in MOF shell		
		CaCO ₃			
MIL-88B-NH ₂	Lipase	Fe ₃ O ₄	bio-conjugation to MOF	biocatalysis	307
ZIF-90	trypsin	Fe ₃ O ₄	bio-conjugation to MOF	biocatalysis	316
		DOTA		analytic chemistry	
HKUST-1	HRP	Fe ₃ O ₄	surface adsorption followed by secondary growth	biocatalysis	311
	GOx				
ZIF-8	Laccase	carbon nanotubes	surface adsorption to ZIF-8 particles	biocatalysis	294
		bacterial cellulose		biosensor	
UiO-66-NH ₂	amidase	Fe ₃ O ₄	infiltration	biocatalysis	308
		Polydopamine			
NU-1006	formate dehydrogenase	F-doped SnO glass electrode modified with Cp*Rh (2,2'-bipyridyl-5,5'-dicarboxylic acid)Cl ₂	infiltration then attachment	biocatalyst	337
ZIF-8	HRP	Fe ₃ O ₄	Co-precipitation*	biocatalysis	291

* MNPs acts as co-crystallization seeds as a faster kinetic of crystallization of *sod* ZIF-8 is measured in presence of Fe₃O₄.

7. CHARACTERIZATION OF MOF IMMOBILIZED ENZYMES

7.1. Overview

The preceding sections have highlighted that MOFs are promising materials for enzyme immobilization technology.^{338, 142, 227, 339-342} The majority of studies (especially those describing encapsulation or pore infiltration of enzymes) have reported that MOF-based systems are exceptionally efficient at protecting enzymes against the denaturing effects of non-natural conditions during reaction or storage, and that they can enhance enzyme activity, significantly, with respect to the free enzyme in non-native conditions.^{33, 45, 343-346} These are important claims as they point towards advancing the use of enzymes in biotechnology. MOF-based enzyme immobilization is an area in which the chemical and material sciences have become strongly intertwined with protein (bio)chemistry and enzymology. Therefore, rigorous application of each field's standards is important in the assessment of these novel systems. A point of difference for some enzyme-MOF composites, discussed below in detail, is that some one-pot immobilization approaches can lead to encapsulation within the solid material.^{142, 227, 338, 341} Irrespective of the preparation method used (*vide infra*), enzyme-MOF composites can be classed as a heterogeneous enzyme catalyst. This is in contrast to canonical procedures of enzyme immobilization in which enzymes are adsorbed or grafted onto the surface of the solid support.^{142, 227, 338, 341} One-pot methods for the synthesis of enzyme@MOF biocomposites are highly variable (e.g., pH, type and concentration of organic linker) and typically employ different conditions from those applied in conventional immobilization. Careful evaluation of the key parameters of MOF-based enzyme immobilization is not only essential for comparison among studies, but it is also required to advance the mechanistic understanding and to identify both opportunities and limitations.³⁴¹

While processes for MOF-based enzyme immobilization can be categorized based on composition and enzyme location (sections 3-6), from an enzymology perspective, categorization according to whether the MOF formation precedes or occurs concomitantly with the immobilization process is useful.³⁴⁶ The former category is generally referred to as "post-synthetic" and involves methods such as infiltration and bioconjugation/grafting (adsorption and covalent attachment of the enzyme onto/into the solid material).^{142, 227, 340} The second category typically involves a one-pot encapsulation that yields the formation of the biocomposite. Examples of this approach include, among others, co-precipitation strategies and biomimetic mineralization.^{10, 346} We note that the one-pot encapsulation

does not necessarily lead to 100% incorporation of the enzyme into the bulk of the MOF material; indeed, a continuum of possibilities exist from full incorporation of the enzyme within the MOF crystal to complete enzyme adsorption to the surface of solid particles at the two extremes.

A fundamental difference between post-synthetic and one-pot procedures arises from the often strongly "non-native" conditions that the enzyme experiences during one-pot immobilization (see section 7.2).³⁴⁷ Therefore, enzyme robustness to conditions of the MOF formation is a highly crucial factor for the one-pot encapsulation. This is not the case for post-synthetic immobilization; however, in this case, it is important to consider the interactions between enzyme and the solid MOF (see section 7.3.2.2).³⁴¹ Additionally, characterization of the one-pot synthesis of enzyme-MOF composites is challenging due to the complex relationship between the enzyme, the MOF precursors, and the final structural properties of the MOF material.¹⁶ Thus, a systematic evaluation of the "biochemical" properties of enzyme-MOF preparations is crucial to the rational development and optimization of this rapidly growing class of biocomposites.

7.2. Key immobilization parameters

Error! Reference source not found. summarizes important performance parameters pertaining to enzyme immobilization.^{3, 348} The parameters give a balance (yield, Y) for activity (A) and protein (P) partitioning between the liquid and the solid phase.^{3, 349} They assess the specific activity of the immobilized enzyme (specific activity_{enzyme bound}) and compare it to the specific activity of the soluble enzyme reference (specific activity_{soluble enzyme}). Accordingly, an effectiveness factor of the immobilized enzyme (η) can be determined. The activity of the immobilized enzyme per unit mass of solid material (specific activity_{material}) is inversely correlated with the catalyst loading (P_{loading}), thus it is important to evaluate the immobilization efficiency. Experimentally, the initial total enzymatic activity is compared to the total immobilized activity, giving the activity yield (Y_A). By examining the residual activity of the unbound enzyme, one obtains the degree of enzyme deactivation during the immobilization (A_{lost}). Further quantification of the total amount of immobilized and unbound protein leads to the expression of the protein yield (Y_P). Using the Y_A and Y_P , it is possible to evaluate whether activity loss occurs on immobilized or unbound enzyme. We note that A_{lost} (activity lost during immobilization; Error! Reference source not found.) is a dominant factor of one-pot encapsulation methods. For example the immobilization (encapsulation and surface adsorption) of catalase in/on ZIF-8 leads to the complete loss of enzymatic activity.³⁹

Table 6. General evaluation parameters used to characterize immobilization performance, adapted from Illanes et al.³

Evaluation parameter	Equation	Unit
Activity balance	$Y_A = \frac{A_{immobilized}}{A_{contacted}}$ $= \frac{A_{immobilized}}{A_{immobilized} + A_{residual} + A_{lost}}$	- (1)
Protein balance	$Y_P = \frac{P_{immobilized}}{P_{contacted}} = \frac{P_{contacted} - P_{residual}}{P_{contacted}}$	- (2)
Protein loading	$P_{loading} = \frac{m_{protein\ immobilized}}{m_{carrier}}$	mg g _{carrier} ⁻¹ (3)
Specific activity (material)	$Specific\ activity_{material} = \frac{A_{immobilized}}{m_{material}}$	U g _{material} ⁻¹ (4)
Specific activity (enzyme bound)	$Specific\ activity_{enzyme\ bound} = \frac{A_{immobilized}}{P_{immobilized}}$	U g _{enzyme} ⁻¹ (5)
Effectiveness factor (η)	$\eta = \frac{Specific\ activity_{immobilized\ enzyme}}{Specific\ activity_{free\ enzyme}}$	- (6)

Y...yield

A...total activity (U)

P...total protein (mg)

m...mass (mg)

While Y_A (eq. 1) and Y_P (eq. 2) describe the overall immobilization performance of the composite, protein loading (eq. 3) and specific activity of solid catalyst (eq. 4) provide information regarding material-specific properties and are useful to compare different enzyme-MOF preparations. An increase in protein loading (eq. 3) is typically correlated with an enhancement of specific activity (material) (eq. 4), up to a certain point where the observable activity becomes limited by physical mass transfer, spatial confinement and crowding/aggregation of the enzymes, or a combination of these effects.^{3, 350}

Subsequent to immobilization, the effectiveness factor η (Error! Reference source not found., eq. 6) describes the change in specific activity: typically enzyme activity decreases ($\eta < 1$), but in very rare cases is enhanced. The specific activity, either referring to the material or to the protein immobilized, of an enzyme is obtained as U mg_{enzyme}⁻¹, where U is defined as $\mu\text{mol min}^{-1}$ substrate evaluated at the defined reaction conditions ($1\text{ U} = 1.67 \cdot 10^{-8}\text{ kat}$). The specific activity_{enzyme} is typically determined in a standard assay at optimal conditions, where the initial reaction rate is at its maximum. However, standard enzyme assays may

not always be compatible with MOF-based biocomposites (e.g., carry-over of metals from the sample into the assay).

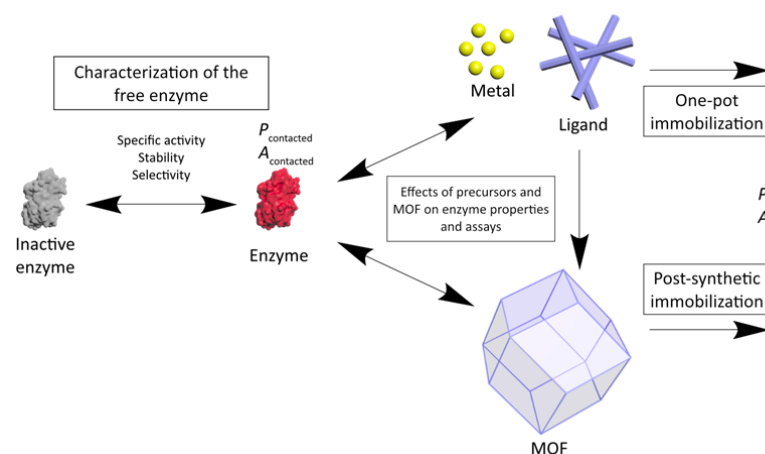


Figure 22 shows a general workflow for the characterization of MOF-based enzyme immobilization. As highlighted, an important aspect is to assess the influence of the precursors and the MOF on the free enzyme.

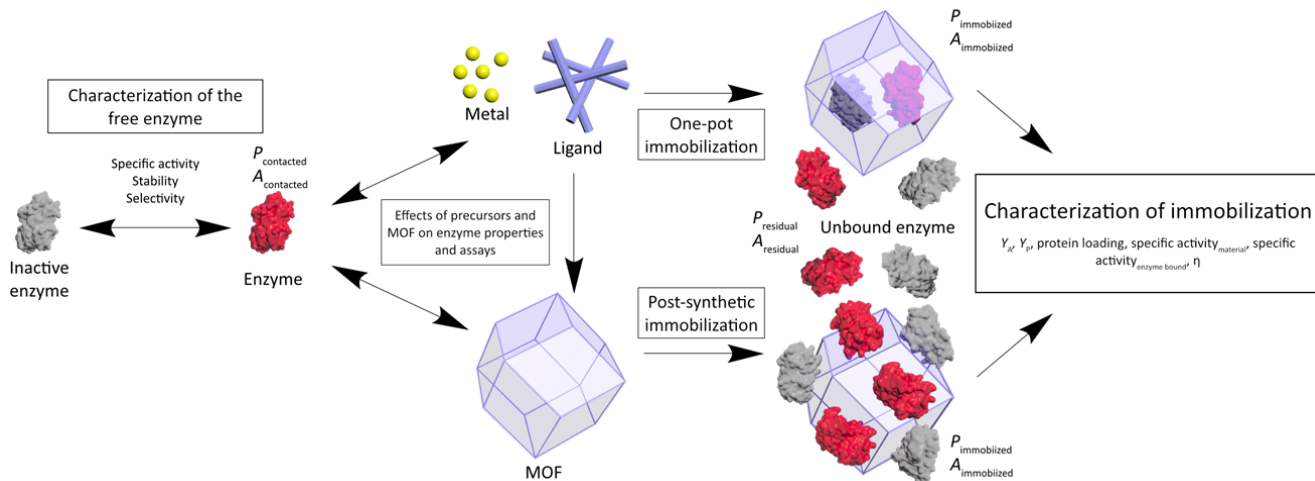


Figure 22. Characterization workflow of enzymes immobilized in/on MOFs using post-synthetic and one-pot approaches.

7.2. One-pot enzyme-MOF formation

The one-pot, *in situ*, approach to enzyme encapsulation within MOFs has been a field of growing interest in the past few years. This synthetic process engenders unique conditions for the enzyme and thus warrants a separate discussion from post-synthetic immobilization methods. The most widely studied MOF for enzyme immobilization via encapsulation is ZIF-8.³⁵¹ Most likely, this is because it can be synthesized using biocompatible conditions that appear to be well tolerated by several enzymes (**Table 7**). Furthermore, there are more reports describing one-pot encapsulation than post synthetic approaches despite the abundance of suitable mesoporous MOFs; this may be attributed to the novelty of the former strategy. The conditions used to synthesize ZIF-8 based biocomposites vary widely, e.g. type and concentration of MOF precursors, immobilization time, and temperature (typically in 20 °C – 30 °C range). The majority of studies utilize zinc nitrate as the

metal source, however, high protein loadings and good activity retention have also been reported for zinc acetate.^{33, 46, 352} Enzyme stability is affected by physical, biological and chemical factors,^{3, 4, 353} thus the immobilization conditions (pH, temperature, concentrations) require careful evaluation. For example, both metal ions and organic linkers can cause structural perturbation in enzymes that often results in loss of activity.³ Metal ions can promote structural changes by binding to thiol side chains of cysteine residues; in addition they can displace functionally important native metal sites in metalloproteins or catalyze amino acid side chain oxidation.³⁵⁴ With respect to the organic MOF components, 2-mIM can lead to an initial pH of 11 that drops to pH 9 after the addition of Zn^{2+} and formation of ZIF-8.³⁴⁷ Such pH values can lead to enzyme deactivation.^{353, 355} Mixing/agitation can also affect the enzyme stability, especially under heterogeneous conditions that involve formation of solid-liquid interfaces.³⁵⁶⁻³⁵⁸

Table 7. Comparison of encapsulation conditions and evaluation of biocatalyst@ZIF-8 and biocatalyst-on-ZIF-8, highlighting the variability of each procedure, sorted by effectiveness factor.

Enzyme	Method	Final Zn ²⁺ conc. [mM]	Final 2-ml M conc. [mM]	L/M ratio	Additives	Solvent	T (°C)	Time (h)	Mixing	Max. P _{loading} [mg _{enzyme} g _{material} ⁻¹]	Max. I] x 100 (%)	Enzymatic evaluation (activity, kinetics, stability)	Ref.
Cytochrome C Horseradish peroxidase Lipase	One-pot	13	13	1	Polyvinyl - pyrrolidone	MeOH	RT	24	Sonicate d, static	80* (Cyt C)	1130 (Cyt C)	Relative act., stability	17
Carbonic anhydrase	One-pot	53	not given	-	Polyvinyl - pyrrolidone	Zn(NO ₃) ₂ in 50% MeOH, rest in H ₂ O	RT	24	Agitated, static	240.2*	1030	Relative act., spec. act.-enzyme bound, stability	359
GOx+HRP, β-Gal + GOx + HRP, ADH + NAD ⁺ + LDH	One-pot	10	700	70	NAD ⁺ covalently bound to poly(allyl amine)	H ₂ O	RT	overnight	Agitated	30.5 (GOx)	750 (GOx + HRP)	Relative act., MM-kinetics, stability	33
Lipase B from <i>Candida antarctica</i> , Cytochrome C, Horseradish peroxidase	One-pot	1244	1040	0.8	-	H ₂ O	RT	12.5	Agitated, static	100* (HRP)	600 (Cyt C)	Relative act., stability	343
Lipase	One-pot	40	160	4	Sodium dodecyl sulfate	H ₂ O	RT	0.5	Agitated	100*	253	Relative act., MM-kinetics, Thermal deact. kinetics, stability	352
Glucose oxidase	One-pot	19	76	4	Fe ₃ O ₄ -cellulose particle	H ₂ O	20	2	Agitated	94.26	124.2	Relative act., spec. act.-enzyme bound	310
Lipase	Post-synthetic	50	3465	70	NH ₄ OH	H ₂ O	30	5	Sonicate d, agitated	8	97.9*	Spec. act.-enzyme bound, stability	360
Catalase	One-pot	4	833	199.8	NH ₃ , TMOS	H ₂ O	-	0.5	-	450*	81	Relative act., MM-kinetics, stability	361
Catalase, Cytochrome C, Glucose oxidase, Urate oxidase,	One-pot	35	2363	68	-	H ₂ O	RT	0.2	Agitated	184* (GOx)	78.9* (Cyt C after acetic	MM-kinetics, stability	46

Alcohol dehydrogenase												anhydri de)		
Carbonic anhydrase	Post-syntheti c	36	2514	70	-	H ₂ O	RT	10	Agitated	880	72		Spec. act. _{enzyme bound} , MM-kinetics, stability	43
Catalase	One- pot	417	667	1.6	-	H ₂ O	RT	0.5	-	200*	70*		Relative act.	362
Laccase	One- pot	45	3182	70.	-	H ₂ O	-	0.1	Agitated	21*	11		Relative act., spec. act. _{enzyme bound} , YA, stability	38
Glucose oxidase	One- pot	28	1086	38.5	Dopamine	H ₂ O	RT	0.5	Agitated	40*	0.7*		MM-kinetics, stability	295

NAD⁺...nicotinamide adenine dinucleotide hydrate

2-mIM...2-Methylimidazole

L/M...ligand / metal ratio

T...immobilization temperature

*...parameter calculated from extracted data

MM-kinetics...Michaelis-Menten kinetics

GOx+HRP...Glucose oxidase + Horseradish peroxidase

β-Gal + GOx + HRP ...β-Galactosidase + Glucose oxidase + Horseradish peroxidase

ADH + NAD⁺ + LDH...Alcohol dehydrogenase + NAD⁺ + Lactate dehydrogenase

Besides the MOF precursors, the reaction solution for one-pot enzyme immobilization often comprises other reagents that increase the complexity of system.^{17, 231, 276, 363} For example, PVP can be used to stabilize or enhance the activity of an enzyme during immobilization into MOFs.^{17, 359} Lyu et al. showed 11-fold increase in the peroxidase activity of CytC upon PVP modification prior to its encapsulation.¹⁷ Also Zhang et al. immobilized a mixture of PVP and carbonic anhydrase in ZIF-8 to create a biocatalytic membrane for CO₂/N₂ separation.³⁵⁹ The immobilized enzyme showed a 10-fold increase in activity compared to the soluble enzyme, which was attributed to the PVP. The example of CytC immobilization in ZIF-8 emphasizes the need for careful and standardized enzyme characterization. Using different procedures of immobilization and analysis (Error! Reference source not found.), effectiveness factors in the range 78% - 1130% have been obtained.^{17, 46, 343} In these cases, metal ion, ligand concentrations, solvents (methanol vs. H₂O), additives (PVP) and synthesis time were all varied. Unfortunately, the use of "relative activity" does not allow for a meaningful comparison of the results, since the initial activity of the enzyme may be largely different, depending on the enzyme preparation, handling and assay conditions.

One-pot immobilization approaches using ZIF-8 have typically obtained protein loadings of 100 mg_{enzyme} g_{material}⁻¹, although in many cases the maximum protein loading was not determined. More broadly in respect to protein loading using MOFs, post-synthetic immobilization has shown remarkably high values. For example, a loading, via physical adsorption, of 880 mg_{enzyme} g_{material}⁻¹ for carbonic anhydrase has been reported.⁴³ We note that protein loadings on conventional porous carriers (e.g. mesoporous silica) are typically lower by at least one order of magnitude.¹⁹³ One-pot immobilization approaches using ZIF-8 do show some variability. For GOx, different procedures showed loadings ranging from 30.5 to 184 mg_{enzyme} g_{material}⁻¹ when metal/ligand ratios of 4 to 70 were used.^{33, 46, 295, 310, 364} Furthermore, protein loading is not only affected by the immobilization conditions (Error! Reference source not found.). The surface chemistry of the enzyme can play a critical role in ZIF-8 formation. Proteins with negative surface charge are more likely to be encapsulated.⁹⁷

7.3. Highlights of MOF-immobilized enzyme performance

The structural and chemical diversity of MOFs along with the wide variety of conditions used for their preparation make comparisons between enzyme immobilization studies challenging. To this end rigorous characterization of

both the immobilization protocol and the immobilized enzyme (see Error! Reference source not found.) are crucial.¹² The wide range of parameters used for MOF-based enzyme immobilization is highlighted, via selected examples, in Error! Reference source not found.. Gascón et al. compared one-pot encapsulation to surface bound approaches of enzyme immobilization for a set of MOF materials (Fe-BTC MOF, MIL-53(Al), MIL-53-NH₂(Al), Mg-MOF-74).^{100, 266} Interestingly, encapsulation of a lipase and laccase in Fe-BTC was reported to show higher (80% and 10% increase in η) activity retention than grafting by physical adsorption.²⁶⁶ In addition, β -glucosidase immobilized using MIL-53-NH₂(Al) showed higher yield in both protein loading (99%) and specific activity_{material} (88%) when the one-pot encapsulation approach was used.¹⁰⁰ Presumably, the specific activity_{enzyme bound} was higher (87%) in the post-synthetic approach due to milder immobilization conditions used, thus, enzyme deactivation was reduced.

As a general note, enzyme immobilization usually involves a trade-off between protein loading and specific activity or effectiveness factor. This effect, is also observed for MOF-based enzyme immobilization,^{268, 282, 350, 363} and can be assessed by comparing the activity of the recovered enzyme and the protein loading achieved with respect to the total amount of protein used. For example, post-synthetic immobilization of a cellulase on magnetic, amino-functionalized UiO-66 (Zr, 2-aminoterephthalic acid) showed a decrease (~30%) in Y_A that was dependent on the protein loading.³⁶³ This is equivalent to stating that the effectiveness factor decreased with increased loading of protein. Despite these observations, the role of diffusion in limiting the effectiveness factor of enzyme-MOF materials is rarely assessed. An example is reported by Cao et al. who studied applied reaction engineering analysis, in terms of dimensionless parameters for diffusion into the pores (Thiele modulus³⁶⁵), to SEH immobilized on UiO-66-NH₂.²³¹ In this case the immobilized enzyme was used for synthesis of enantiopure (*R*)-1,2-octanediol in deep eutectic solvents and no evidence of performance limitation by internal mass transfer was found. Thus, the reported decrease in the effectiveness factor of the enzyme (5%) is likely due to an intrinsic loss of activity of the immobilized enzyme. However, this was assessed for enzyme aggregates cross-linked to the surface of UiO-66-NH₂, where internal mass transfer limitations are expected to play a minor role.³⁶⁶ As mass transfer could play a relevant role in enzymes@MOFs the related investigation of Thiele modulus would progress the understanding of these biocomposites.

Table 8. Highlights of performance evaluation of enzyme immobilization in MOFs.

Enzyme	MOF	Method	Metal source	Ligand	Additives	Characterization	Results	Ref.
Alcohol dehydrogenase, Lipase, Glucose oxidase	Fe-BTC	One-pot	FeCl ₃ •6H ₂ O	Benzene-1,3,5-tricarboxylic acid	-	P_{loading} , specific activity _{enzyme bound} compared to free (η) and determined specific activity _{material}	Alcohol dehydrogenase η : 0.58% Lipase η : 98%, Glucose oxidase η : 243%,	367
Cellulase	UiO-66-NH ₂	Post-synthetic (crosslinking)	ZrCl ₄	2-Aminoterephthalic acid	Poly(sodium 4-styrenesulfonate) modified Fe ₃ O ₄ nanoparticles	Y_A and P_{loading}	P_{loading} : 126.2 mg/g loading, Y_A : 78.4%, increased stability in the presence of vanillin and formic acid (16.8% and 21.5% vs. free enzyme)	363
Glucoamylase	ZIF-8	One-pot	Zn(CH ₃ COO) ₂ •2H ₂ O	2-Methylimidazole	-	Thermal deactivation kinetic parameters (rate constant k_d , half-life time $t_{1/2}$ of free vs. immobilized) Michaelis-Menten kinetic parameters	Reduced activity of immobilized glucoamylase but increased thermal stability and recyclability	344
Horseradish peroxidase, Cytochrome C, Microperoxidase-11	PCN-333(Al)	Post-synthetic (Infiltration)	AlCl ₃ •6H ₂ O	4,4',4''-(1,3,5-Triazine-2,4,6-triyl)tribenzotriazine	-	P_{loading}	P_{loading} : up to 1000 mg g ⁻¹ (horseradish peroxidase) 14 fold increased spec. act. of cytochrome C in water (vs. buffer)	193
Laccase	HKUST-1	Post-synthetic (adsorption)	Cu(NO ₃) ₂	Benzene-1,3,5-tricarboxylic acid	-	Activity recovery depending on amount adsorbed	P_{loading} : 502 mg/g, over 95% activity recovered	350
Laccase	Zr-MOF (MMU)	Post-synthetic (adsorption)	ZrCl ₄	Benzene-1,4-dicarboxylic acid	CTAB, DMF, trifluoroacetic acid, HCl	Y_A and P_{loading}	221.83 mg/g loading, 90% activity retained	268
Laccase, Lipase	Fe-BTC	One-pot & post-synthetic	FeCl ₃ •6H ₂ O	Benzene-1,3,5-tricarboxylic acid	NaOH	P_{loading} , specific activity _{enzyme bound} , specific activity _{material}	High encapsulation efficiency (\geq 98% for laccase and \geq 87% for lipase) and activity retention (97% lipase activity retained)	266
Lipase	ZnGlu-MNPs	Post-synthetic (crosslinking)	Zn(NO ₃) ₂ •6H ₂ O	Glutamic acid	N-hydroxysuccinimide and 1-ethyl-3-(3-	Y_A and P_{loading}	P_{loading} : 118.0 mg/g, Y_A : 82%, increased thermal, pH and solvent stability	282

Pectinase	UiO-66-NH ₂	Post-synthetic (adsorption)	ZrCl ₄	2-Aminoterephthalic acid	Polymethacrylic acid	<i>P</i> _{loading} , specific activity _{enzyme bound}	Increased temperature and pH range of immobilized pectinase vs. the free enzyme	276
Soybean epoxide hydrolase	UiO-66-NH ₂	Post-synthetic (adsorption)	ZrCl ₄	2-Aminoterephthalic acid	Enzyme immobilized through precipitation in (NH ₄) ₂ SO ₄ , followed by cross-linking with glutaraldehyde melamine sponge coated with sodium dodecyl benzene sulfonate	Specific activity _{enzyme bound} , internal mass transfer (η and Thiele modulus)	<i>P</i> _{loading} : 87.3 mg/g, <i>Y</i> _A : 88%, decreased <i>K</i> _m of immobilized SEH (6.5 mM vs. 19.2 mM), increased pH, temperature and organic solvent stability	231
α -Amylase	ZIF-67	One-pot	Co(NO ₃) ₂ •6H ₂ O	2-Methylimidazole		η	η : Up to 78%	368
β -Glucosidase, laccase	MIL-53(Al), MIL-53 - NH ₂ (Al), Mg-MOF-74	One-pot & post-synthetic	Al(NO ₃) ₃ •9H ₂ O, Mg(CH ₃ COO) ₂ •4H ₂ O	Benzene-1,4-dicarboxylic acid, 2-aminoterephthalic acid, 2,5-dihydroxyterephthalic acid,	TEA, NH ₄ OH, NaOH	<i>P</i> _{loading} , specific activity _{enzyme bound} , specific activity _{material}	Post-synthetic immobilization lead to increased activity retention, at lower loading vs. one-pot encapsulation	100

η ...Effectiveness factor

*P*_{loading}...Protein loading (mg_{protein}/g_{material})

*Y*_A...Activity yield

7.3.1. Experimental determination of key immobilization parameters

As shown in **Table 6**, determining immobilization parameters requires that both protein concentrations and activity are measured. Proper controls are necessary to ensure that the assays are compatible with the MOF materials and the precursors; for example, the MOF should not decompose under the assay conditions, and the assay should not be affected by the reagents used for the synthesis of the MOF biocomposite.^{40,291, 369}

7.3.1.1. Determination of protein concentrations^{44, 278}

Immobilization parameters, such as Y_p , P_{loading} and the specific activity, are all derived from the protein concentration. Thus, the selection of an appropriate protein assay is crucial.³⁷⁰ Of the broad variety of protein assays that are available³⁷⁰ colorimetric assays such as the Biuret, Lowry and Bradford protocols are commonly used.^{223, 224, 371} The Bradford assay is employed in commercialized reagents for protein determination and has been widely applied to MOF-based biocomposites.^{100, 344, 363, 372} The Bradford method utilizes the binding of Coomassie Blue G250 to positively charged amino acid residues and performs quantification at a wavelength of ca. 600 nm. However, the Bradford assay is not compatible with detergents and surfactants.³⁷⁰ The Biuret and Lowry methods^{223, 371} also present experimental limitations. For example, the Biuret method requires protein concentrations $\geq 0.3 \text{ mg mL}^{-1}$ and is influenced by amide group containing reagents while the Lowry method is affected by numerous reagents, including ions, detergents, disulfides, EDTA or phenols, only to name a few. Alternatively, the absorbance and fluorescence properties of a protein can be used for quantification. In such examples, enzyme-bound cofactors (e.g., heme iron, flavin, NAD and nicotinamide adenine dinucleotide phosphate (NADP)) can be used to determine protein concentration. Furthermore, inductively coupled plasma-mass spectrometry (ICP-MS) can be applied to accurately quantify the amount of sulfur within a sample, corresponding to the protein.^{76, 373, 374} Whichever method is used, it is important to consider interference from the medium (e.g. MOF material and its precursors) in a case-specific fashion. Moreover, suitable controls should always be performed.

P_{loading} (Error! Reference source not found.) is typically measured indirectly by determining the protein concentration in the supernatant (P_{residual}) after immobilization and weighing the solid material. Thermogravimetric analysis (TGA) enables a direct measurement of P_{loading} . For example, Chen et al. determined the weight loss of ZIF-8 into which

GOx and CytC had been immobilized during TGA between 200-450°C. From the data, P_{loading} of $154 \text{ mg}_{\text{enzyme}} \text{ g}_{\text{material}}^{-1}$ and $23 \text{ mg}_{\text{enzyme}} \text{ g}_{\text{material}}^{-1}$ were obtained for GOx and CytC, respectively.⁴⁶

7.3.1.2. Activity determination

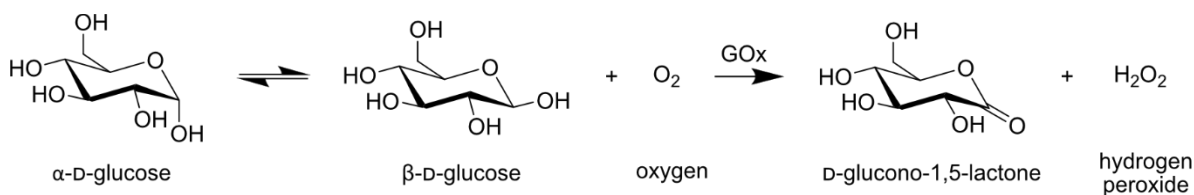
Activity assays are typically more sensitive to interference from solutes than protein assays. Accordingly, caution must be exercised when they are applied to enzyme-MOF composites and supernatants from MOF preparation. In general, assays for free enzyme activity may be inappropriate for immobilized enzyme activity. Nevertheless, when they are employed controls must be used, such as the enzyme free MOF or biocomposites containing inactive enzyme, to excluded background reactivity. The stability of MOF biocomposite during the assay should also be considered. Enzymes adsorbed to the MOF surface may be released into solution and could thus become active; furthermore, MOFs may decompose in buffers used in assays, enabling encapsulated enzymes to be released.^{40, 99} Another aspect that needs to be considered when performing assays is that encapsulation of an enzyme within a MOF shell can modify its kinetic behavior (further discussed in section 7.4.1).^{193, 231, 268, 276, 282, 344, 350, 363, 368}

Enzymatic activity is typically performed under constant bulk conditions, i.e. temperature, pH, ionic strength, solute concentration, and is recorded as the initial rate of substrate consumption or product formation during reaction at steady state.^{3, 356, 370}

$$v = -\frac{\Delta S}{\Delta t} = +f \frac{\Delta P}{\Delta t} \quad (7)$$

where v is the reaction rate, $-\Delta S/\Delta t$ is substrate consumption/time and $\Delta P/\Delta t$ is product formed/time. f is the stoichiometric factor for substrate consumed/product formed, depending on the reaction. Generally, it is useful to distinguish the initial rate v from the degree of conversion observed at later time points during the reaction. We note that the relationship between v and (soluble) enzyme concentration is linear but is more complex with respect to conversion.

Glucose oxidase is well established as a model enzyme for enzyme-MOF composites and provides a good case to discuss the requirements and issues encountered for activity assays (**Table**). GOx catalyzes the conversion of β -D-glucose and molecular oxygen to D-glucono-1,5-lactone and hydrogen peroxide (**Scheme 1**).^{375, 376} Subsequently, the D-glucono-1,5-lactone product hydrolyzes spontaneously to gluconic acid.



Scheme 1. Details of the reaction catalyzed by GOx.

GOx activity is determined from substrate consumption (glucose, O_2) or, more commonly, product formation (gluconic acid, H_2O_2). **Table** highlights the variation in assay conditions used to assess the activity of GOx@MOFs and GOx-on-MOFs. Assays can be performed in a continuous or discontinuous fashion. Continuous assays allow for monitoring of the reaction throughout its course, whereas discontinuous assays require stopping the reaction at given intervals. For example, the activity of GOx immobilized

@ZIF-8@cellulose@ Fe_3O_4 was detected using a discontinuous assay with measurement at a single time.³¹⁰ H_2O_2 was detected after 10 min, whereby the reaction was stopped and acidified to pH 3.5 (from pH 7). The sample was then heated to 100 °C in the presence of a redox indicator (indigo carmine) that was used to quantify the formed H_2O_2 .³¹⁰ Endpoint/single-point assays can be problematic as initial rates are not measured,³⁷⁰ thus continuous assays are preferred. Coupled assays are useful but often show complex dependence on/interference from the conditions used.

Table 9. Assay conditions used to determine GOx@MOF activity.

MOF	Assay type	Conditions	Target/Analyte	Glucose conc. (mM)	Comments	Application	Ref.
Fe-BTC	Continuous, coupled	Acetate buffer, pH 5.6, 25°C, 10 min	ABTS	500	-	Immobilization and characterization	367
HKUST-1/ Fe ₃ O ₄	Continuous, coupled	Phosphate buffer, pH 7.4,	<i>o</i> -methoxyphenol	0.3	-	Co-immobilization of GOx & HRP	311
MAF-2	Continuous	Acetate buffer, pH 5.5, 25°C	O ₂	30	O ₂ consumption measured by luminescence increase of MAF-2	Immobilization in luminescent MOF	377
MIL53(Al) MIL101(Cr)	Continuous, coupled	Acetate buffer, pH 5.10	<i>o</i> -dianisidine	92.5	-	Covalent immobilization on amino MOFs	281
PCN-888	Continuous, coupled	Tris buffer, pH 7.4	ABTS	9	Temperature not stated	Co-immobilization of GOx & HRP	185
ZIF-8	Discontinuous, endpoint	Phosphate buffer, pH 7, 37°C, 10 min	Indigo carmine	160	-	Immobilization on cellulose coated magnetic nanoparticles	310
ZIF-8	Continuous, coupled	Tris buffer, pH 7.5	TMB	0.8	Temperature not stated	Surface modification of enzymes alter immobilization	46
ZIF-8	Continuous, coupled	Phosphate buffer, pH 7.4, 10 mM NaCl	Amplex Red	5	Temperature not stated	Co-immobilization of GOx & HRP	33
ZIF-8	Discontinuous, coupled	Phosphate buffer, pH 7.4, 37°C	ABTS	16.67	-	Co-immobilization of GOx & HRP for glucose and phenol sensing	378
ZIF-8	Discontinuous, endpoint, coupled	Phosphate buffer, pH 7.4, 37°C, 5 min	ABTS	100	-	Co-immobilization of GOx & HRP using a DNA scaffold	45
ZIF-8	Discontinuous, endpoint	Phosphate buffer, pH 7.4, RT, 10 min	ABTS	0.1	-	Co-immobilization of GOx & HRP	364
ZIF-8	Continuous, coupled	Phosphate-buffered saline, pH 7.4	ABTS	400	-	Polydopamine cross-linking of GOx@ZIF-8 immobilization	295

ABTS...2,2'-Azino-bis(3-ethylbenzothiazoline-6-sulfonic acid

TMB...3,3',5,5'-tetramethylbenzidine

GOx...Glucose oxidase

HRP...Horseradish peroxidase

The different assay methods emphasize the need for a structural integrity assessment of the MOF material after the measurement. For example, GOx assay employed at the optimal pH (5.6) of GOx from *Aspergillus niger* would engender ZIF-8 decomposition.³⁷⁹ Chen et al. reported that the formation of gluconic acid by GOx encapsulated in ZIF-8 leads to a triggered release of co-immobilized drugs due to dissolution of the framework.³⁸⁰ Accordingly, the observed activity of the biocomposite may arise from GOx released into solution and therefore a definitive statement about the catalytic performance of the GOx@ZIF-8 biocomposite cannot be made under these conditions. Such release of enzymes into the medium is often termed “leaching” and can be observed for all types of carriers. Typically, leaching is detected by measuring enzyme concentration and/or activity in the supernatant.^{45, 381}

A common approach of determining GOx activity is to use a coupled enzymatic assay, where HRP and a redox dye are used to measure the H₂O₂ formed by the GOx.³⁸²⁻³⁸⁵ For example, in the widely employed ABTS assay, HRP catalyzes the conversion of H₂O₂ to water using ABTS as an electron donor. The oxidation of ABTS results in a blue/green color formation, which can be measured continuously, by monitoring a change in absorbance.^{364, 367} Thus, the initial reaction rate can be conveniently evaluated. Several redox dyes have been applied to GOx reactions, e.g., *o*-dianisidine, *o*-methoxyphenol, 3,3',5,5'-tetramethylbenzidine (TMB). As an alternative to absorbance-based detection methods, *N*-acetyl-3,7-dihydroxyphenoxazine (Amplex™ red) can be converted to highly fluorescent resorufin by HRP in the presence of H₂O₂ and thus is a sensitive probe of H₂O₂.³³ An important consideration of coupled assays is the need for an excess of coupled enzyme (HRP) throughout the reaction. This is required to rule out rate limitations imposed by the coupled enzyme, and not by GOx. Thus, a control reaction should not show an increase in rate associated with an increase HRP. A further consideration when working with heterogeneous biocatalysts and coupled assays is phase boundaries at liquid-solid and liquid-gas interfaces, as they can lead to enzyme inactivation.³⁵⁶⁻³⁵⁸ In contrast to coupled enzymatic assays, direct measurement of O₂ consumed during the oxidation of glucose does not require a secondary enzyme. This can be easily performed by following the reaction with an O₂ probe. An interesting approach for detection of the consumed O₂ was developed by Xu et al., who used the luminescent properties of MAF-2 (Cu⁺ and 3,5-diethyl-1,2,4-triazole) to create a glucose sensor by encapsulating GOx.³⁷⁷ The fluorescence of MAF-2 is quenched in the presence of O₂. Hence, the activity of GOx can be monitored by detecting an increase in fluorescence with decreasing O₂.

A feature of enzyme@MOF composites is that they can show a significant change in substrate selectivity.³⁸⁶ This is highlighted in the encapsulation of laccase within ZIF-8. Laccases belong to the class of oxidases and have a large substrate scope, catalyzing the oxidation of various phenolic compounds. An example is Laccase from *Corynebacterium glutamicum* that can oxidize 2,6-dimethoxyphenol (2,6-DMP), ABTS and syringaldazine (SGZ). When encapsulated in ZIF-8, Knedel et al. observed a change in the substrate selectivity of the enzyme.³⁸ The free enzyme readily converted 2,6-DMP, ABTS and SGZ, showing the highest activity for

ABTS whereas the laccase@ZIF-8 was inactive toward ABTS and retained some activity for 2,6-DMP (5 %) and SGZ (10 %). A possible explanation is that the pore window size of ZIF-8 (3.4 Å) restricts the diffusion of ABTS, which is the largest of the three substrates used.³⁸⁷

Finally, we note that the experimental conditions need to be reported in detail as they can influence activity measurements. The Standards for Reporting Enzymology Data commission (STRENDa) gives useful guidelines for the reporting of data from studies of enzymatic reactions.³⁸⁸ The application of these guidelines largely increases the quality of the reported data. For example, since the surface properties of an enzyme play a role in MOF formation, different isoforms of an enzyme may engender subtle differences in the structure/composition of the biocomposite.⁹⁷ Thus, reproduction of results will be difficult if the enzyme parameters, e.g. source and the purity, are not clearly reported. Furthermore, recombinantly produced enzymes often contain artificial modifications, such as fusion peptides (e.g., the His-tag) appended to the N- or C-terminus to facilitate purification. Any such modification may be critical for the enzyme behavior and needs to be stated in reports.

7.3.2. Advanced characterization of immobilized enzymes

7.3.2.1. Apparent enzyme kinetics

A common strategy of comparing free and immobilized enzymes is on the basis of steady-state kinetic parameters.⁹ In most cases, the initial reaction rate v depends on the substrate concentration $[S]$ in a hyperbolic fashion and is described by the well-known Michaelis-Menten rate law (equation 8).³⁸⁹ There are two parameters, V_{max} (the maximum reaction rate) and K_M (the Michaelis constant), and both can be influenced by the immobilization as discussed below. We note that activity determination (i.e., measurement of v) applies analogously to evaluation of kinetic parameters. To determine initial rates, the substrate depletion should usually be in the range 3 – 5%.³⁷⁰ Enzymatic reactions involving two or more substrates (i.e. GOx reactions) can be analyzed under conditions in which the concentration of one substrate (e.g. glucose) is varied while the concentration of the other substrate (e.g. O₂) is kept constant, ideally at a level that saturates the enzyme. We note that change in the concentration of the constant substrate can affect the observable K_M of the varied substrate.

$$v_0 = \frac{V_{max}[S]}{K_M + [S]} \quad (8)$$

The physical dimension of K_M can be either a mole or mass-based concentration. V_{max} is obtained at enzyme saturation with substrate ($[S] \gg K_M$) and is usually expressed as a molar rate (e.g., $\mu\text{mol mL}^{-1} \text{min}^{-1}$) but there exists broad variation in the use of unit definitions. V_{max} is related to the enzyme concentration by the relationship, $V_{max} = k_{cat}[E]_0$ where k_{cat} is a first-order catalytic constant (min^{-1}) that is sometimes also referred to as enzyme turnover number or turnover frequency and $[E]_0$ is the total concentration of enzyme catalytic centers able to undergo turnover. Exceptions notwithstanding (e.g. heme-iron sites that are conveniently titrated), the true active site concentration is rarely known. $[E]_0$ is therefore approximated from the measured protein concentration and the enzyme molecular mass.

When comparing immobilized vs soluble enzyme; K_M typically increases, the parameter for the maximum rate decreases, or alternatively both occur concomitantly. The increase in K_M may be a result of restricted substrate diffusion through the biocomposite. Experiments to distinguish the effects of diffusion from direct effects on the enzyme are summarized in specialized reviews.^{349, 390-392} Diffusional restrictions are dependent on the particle size (substrate concentration gradient)³⁴⁸ and pore size. Thus, small, μm -sized, MOF particles are unlikely to develop severe diffusional limitations due to the small diffusional distance, compared to large canonical carriers (e.g. agarose gel particles).^{40, 392} However, canonical carriers used in enzyme immobilization are meso- and macro-porous, with pore sizes of several tens of nanometers, which are larger than the majority of MOFs; thus diffusion may be hindered into the MOF pore network due to this small pore size. By introducing defects within the MOF matrix diffusional restrictions can be decreased, resulting in increased enzymatic activity.⁷⁹

A decrease in k_{cat} is usually a good indication for the loss of enzyme functionality due to immobilization. There are a variety of reasons that can explain a diminished k_{cat} value and these have been reviewed elsewhere.^{14, 349, 393, 394} Briefly, the enzyme may have become denatured during MOF formation or the substrate may not have access to the enzyme due to improper orientation (i.e. the active site of the enzyme is not accessible) or pore confinement (i.e. enzyme crowding³⁹⁵). The k_{cat} ratio between immobilized and soluble enzyme is a useful, alternative expression of enzyme effectiveness (cf. **Table 6**). Section 7.3.2.2 summarizes methods used to characterize MOF-immobilized enzymes with respect to parameters describing the protein conformation and spatial localization in the solid material.

Kinetic parameters have been determined for various MOF-based enzyme preparations.^{193, 231, 268, 276, 282, 344, 350, 363, 368} For example, the kinetic parameters of glucoamylase ($V_{max} = 4.5 \mu\text{mol min}^{-1}$, $K_M = 0.56 \mu\text{M}$), for the hydrolysis of maltodextrin, only marginally change when the enzyme was encapsulated in ZIF-8 ($V_{max}=4.1 \mu\text{mol min}^{-1}$, $K_M = 0.59 \mu\text{M}$).³⁴⁴ For α -amylase immobilized on a melamine sponge using ZIF-67 (Co^{2+} , 2-methylimidazole), the V_{max} decreased (5.72 to $4.06 \mu\text{mol min}^{-1}$) and K_M increased (0.63 to 0.77 mg mL^{-1}).³⁶⁸ The kinetic parameters for glucoamylase and α -amylase were determined by non-linear regression, where the Michaelis-Menten equation is fitted to the obtained initial reaction rates at varying substrate concentrations. We also note that several studies report heavily extrapolated kinetic parameters.^{19, 46, 124, 307, 362} Kinetic parameters for GOx, HRP and CytC encapsulated in ZIF-8 were only determined at substrate concentrations within the 1st order regime for reaction rate (linear dependence of v on $[S]$).⁴⁶ GOx@ZIF-8 showed a calculated K_M of 2.1 mM and was determined between 0.5 - 0.8 mM glucose concentrations. Similarly, for catalase embedded in ZIF-90 (Zn^{2+} , ICA), kinetic parameters were determined at H_2O_2 concentrations well below (0 - 0.75 mM) the calculated K_M (2.87 mM).¹²⁴ In general, v_0 should be obtained evenly distributed around K_M (+/- 4 points) and at least two measurements should be obtained at substrate concentrations yielding V_{max} .³⁷⁰ However, V_{max} may not always be attainable, due to substrate solubility or inhibition effects.

7.3.2.2. Structural analysis and localization of enzymes immobilized into MOFs

A detailed knowledge of enzyme localization is important for both extremes of enzyme immobilization into MOFs, namely binding on the solid surface or encapsulation into the solid material. Several methods can be employed to visualize the distribution of enzymes on solid supports.³⁹⁰ Microscopy data has been proved a valuable method for determining the distribution of the enzymes in/on the solid material and has thus facilitated interpreting the characteristics of the immobilized enzymes.³⁹⁴ These methods include, light microscopy, confocal laser scanning microscopy (CLSM), cryo-temperature field-emission scanning electron microscopy (Cryo-FESEM), and TEM, spherical aberration (Cs)-corrected scanning TEM.^{390, 396} Spectroscopy and scattering experiments have also been employed, including SAXS and Raman spectroscopy. CLSM in combination with fluorescent protein labelling has been widely applied to MOF biocomposites. For example, Chen et al. showed co-immobilized GOx and HRP in ZIF-8 using labelling with fluorescein isothiocyanate (GOx) and Rhodamine B (HRP).^{33, 45, 46} A potential issue with such experiments is that the dye modifies the surface chemistry of the protein. This can be avoided in proteins that possess fluorescently active cofactors (e.g. flavins) that can enable imaging without additional labeling.³⁹⁷ Given the typical the size of MOF particles, the spatial resolution of CLSM can be a limiting factor. Higher resolution TEM experiments, although time expensive, have also been used to detect cavities in ZIF-8, suggesting the presence of lipase from *Candida rugosa* was immobilized in the particle.³⁹⁸ SAXS has also employed to detect mesopores within ZIF-8, 10 - 30% larger than the gyration radius of bovine serum albumin, capable of harboring the protein.¹⁶ Furthermore, energy dispersive X-ray spectroscopy (EDX) mapping in combination with scanning electron microscopy (SEM) can be applied to investigate the distribution HRP in ZIF-8 by detecting Fe from the heme group of HRP.⁴⁵ Equally, HRP (Fe) distribution was detected in PCN-333(Al) using TEM coupled with EDX.¹⁹³

Protein orientation on the surface is an important parameter of immobilized enzyme effectiveness and has been investigated in a ZIF-8-based biocomposite using EPR spectroscopy.^{27, 399} Site-directed modification of cysteine residues with nitroxyl groups was used to introduce the spin labels for measurement. The results could be interpreted in terms of spin label being solvent exposed or buried in material. This enabled some inference as to the orientation of the enzyme and might help in the interpretation of activity loss occurring during the immobilization.

Protein secondary structure, as inferred from analysis with circular dichroism (CD), infrared (IR) or Raman spectroscopy, is often used to confirm proper folding of the enzyme immobilized in solid materials.³⁹⁰ Using Fourier-transform IR, Cao et al. demonstrated that the secondary structure of soybean epoxide hydrolase significantly changed after immobilization.²³¹ By analyzing free and immobilized enzyme, they estimated an increased α -helix content after immobilization. From this change they inferred an increase in stability of the immobilized enzyme, which is reflected by activity retention at elevated temperatures. Similarly, Liang et al. used FTIR to investigate the deactivation of catalase@ZIF-

8/MAF-7 and catalase-on-ZIF-8/MAF-7.³⁹ Using the second derivative of the spectra, the aggregation of catalase@ ZIF-8 and catalase-on-ZIF-8 could be detected, whereas for catalase@MAF-7 and catalase-on-MAF-7 the structure and activity was maintained. CD has also been applied to investigate the conformation of carbonic anhydrase immobilized in MIL-160 and ZIF-8.⁴³ Far UV CD spectra showed that carbonic anhydrase maintained its structure in hydrophilic MIL-160, whereas immobilization in hydrophobic ZIF-8 resulted in an increase in random coils and these data were complemented by FTIR analysis. Although CD is a commonly used technique to assess protein structure, light scattering from crystalline MOF-based biocomposites can hinder data acquisition. In another study, Raman spectroscopy was used to characterize the interaction between MP-11 and Tb-mesoMOF.¹⁹² Raman spectroscopy revealed increased π - π interactions between the heme cofactor of MP-11 and triazine / benzene rings of the linker molecule (4,4',4''-s-triazine-2,4,6-triyltribenzoate). From this, Chen et al. infer a decreased amount of enzyme leaching.¹⁹²

7.3.2.3. Enzyme-MOF materials in bio-catalysis: usage range, stability and catalyst recycling

Enzymes operate at an optimum pH, and minor increase/decrease of pH can result in reversible loss of activity.^{3, 400} Immobilization can alter the dependence of enzyme activity and stability on the reaction parameters such as temperature and pH.^{231, 268, 345, 350, 367} Indeed, several studies of enzyme/MOF biocomposites have determined the relevant pH and temperature profiles.^{45, 231, 345, 350, 367, 401} For example, HRP maintains activity (> 70%) over a broad pH range (pH 4.5 - 8), where free HRP loses activity with increasing pH (up to 80% at pH 8).³⁴⁵ Additionally, the active pH range (pH 6 - 8) of alcohol dehydrogenase from *Saccharomyces cerevisiae* increased after immobilization with Fe-BTC (pH 4 - 9.5).³⁶⁷ The reaction rate usually increases with increasing temperature until it reaches a maximum at the "optimum temperature". After this point the rate decreases with a further increase in temperature as a result of enzyme deactivation.^{3, 400} This loss of activity at elevated temperature is typically not reversible upon cooling. It has been reported that MOF-based immobilization can alter the temperature dependence of enzyme activity.³⁴⁵ For example, HRP immobilized in ZIF-8 shows an activity maximum at 70 °C (100 % relative activity), whereas the free enzyme loses activity above 40 °C (60% relative activity at 70 °C).³⁴⁵ The optimum temperature inferred from the temperature profile of v is usually higher (≥ 10 °C) than the temperature for usage of the enzyme (e.g., in a biocatalytic application). Selection of the operational temperature range is facilitated by enzyme stability studies and kinetic analysis of enzyme inactivation at different temperatures. Enzyme inactivation is often found to follow first-order kinetics, resulting in a de-

activation rate constant (k_d , h⁻¹) that is independent of enzyme concentration. An enzyme half-life time can be calculated (equation 9). The k_d often shows dependence on temperature according to Arrhenius' law (equation 10).^{3, 400}

$$t_h = \frac{\ln 2}{k_d} \quad (9)$$

$$k_d = A e^{-E_d/RT} \quad (10)$$

In equation 10, A is the Arrhenius constant, E_d the deactivation energy, R the ideal gas constant and T the temperature. k_d can be determined by evaluation of residual activity over time (semi-log plot) and E_d using an Arrhenius plot ($\ln k_d$ vs. $1/T$). The thermal deactivation kinetics have been determined for glucoamylase@ZIF-8 at 60, 70 and 80 °C.³⁴⁴ From this data the half-life of glucoamylase embedded in ZIF-8 increased from 9.1 min to 69.3 min (at 60 °C) and the corresponding deactivation energy from 42 to 66 kJ mol⁻¹.³⁴⁴

It has been reported that MOFs can enhance the tolerance of enzymes towards biological and chemical denaturants (proteases, proteolytic agents, organic solvents).^{41, 343} HRP immobilized in ZIF-8 retained 80% (free HRP: 20%) of its initial activity after treatment with urea and trypsin.⁴¹ Furthermore, ZIF-8 protected CalB and HRP from inactivation after treatment with anhydrous denaturing organic solvents (DMF, methanol, ethanol, dimethyl sulfoxide).³⁴³ Immobilized CalB and HRP retained >90% activity after incubation at 80°C in all solvents.³⁴³ This protection is most likely the result of restricted diffusion of the denaturant and tight encapsulation of the enzyme within the MOF matrix.^{11, 16}

MOFs can facilitate the recycling of biocatalysts.^{44, 307, 401} For sensor applications, initial rate measurements can be sufficient for the characterization of reusability as the stability is maintained over the measurement duration.³⁴⁵ Enzymes immobilized in MOFs for biocatalysis are commonly reported in terms of their relative activity at each cycle by repeated initial rate measurements.^{44, 402, 403} In batch processes, the reaction time typically is adjusted to reach a defined product concentration (e.g. maximum conversion). The biocatalyst is recovered after each cycle (by centrifugation or filtration). To give a more meaningful representation, performance should be reported based on product yield (per cycle) and initial activity after recycling. Alternatively, recycling can be achieved by retaining the enzyme in a continuous process.⁴⁰⁴ For instance, Zhu et al. immobilized formate dehydrogenase, formaldehyde dehydrogenase and alcohol dehydrogenase, in that order, in ZIF-8, and used the co-immobilized enzymes for the continuous formation of methanol in a flow reactor.⁴⁰⁵ Overall, the in-operando characterization of many enzyme-MOF materials in applied processes still needs to be assessed. Thus, the potential application of MOFs in biocatalysis still requires further examination.

Table 10. Recommended good practice guidelines.

Characteristic	Comments
Reporting of data	State enzyme, reaction and experiment details according to STRENDA* guidelines (Notably EC number, organism / species, strain of the enzyme origin and assay conditions)
Immobilization (see also Table 1)	Values in Table 1 should be calculated and reported

Protein concentration and activity require careful comparison to the free enzyme

Defining protein loading vs activity would help defining optimal composition

Both enzyme and support material should be characterized before and after immobilization to investigate potential structural changes.

Assays Influence of the MOF (and precursors) on the used assays (protein concentration / activity) should to be assessed

The structural integrity of the MOF material during assay conditions (pH, T, substrate, product) should be examined

To verify the procedure used, the specific activity of the free enzyme should be compared to available literature.

If possible, use continuous direct activity assays (vs. discontinuous coupled).

Standard enzyme assays typically measure the activity at optimal conditions, ensuring a maximum initial reaction rate

Enzyme kinetics Apparent enzyme kinetics should never be extrapolated from experimental data

The maximum reaction rate requires substrate saturated conditions

K_M and V_{max} can be subject to large change after immobilization, thus requiring adjustment of the experimental setup

Enzyme concentration needs to be stated when reporting V_{max}

Usage range, stability and recycling Stability and recycling experiments should be complemented by material characterization

...

* STRENDA stands for "Standards for Reporting Enzymology Data".⁸⁴

8. OUTLOOK

The structural and chemical mutability of MOFs provides a diverse platform for exploring the synthesis of enzyme-based biocomposites. In this review we have shown how researchers have used mesoporous MOF pore networks to house enzymes and facilitate biocatalytic reactions, modified the framework surface chemistry to covalently attach protein residues and devised synthesis conditions that allow for the in situ encapsulation of enzymes within a microporous MOF matrix. Some systems have shown excellent potential for practical applications; however, we note that it is important to benchmark these initial, promising, results to get a true understanding of how the MOF environment (e.g. surface or pore chemistry) affects the structure and activity of the enzyme (as highlighted in section 7). Furthermore, we have assembled some good practice guidelines that we believe will help those new to the research area that are summarized in Table 10.

The characterisation of MOF/enzyme biocomposites is not trivial and we believe that further effort in this area will lead to better design of bespoke composites and, as a result, engender significant advances in the field (See section 7.4.2.2). For example, research in the area of enzyme/polymer composites has shown that protein structure and activity can be stabilised by the polar and non-polar groups of random heteropolymers.⁴⁰⁶ Similar control of MOF functionality is conceivable via mixed-link synthesis strategies; however, detailed characterisation of the resulting composite would be crucial to interpreting and understanding the observed activity. Another fundamental question that needs to be fully determined with respect to MOF/enzyme biocomposites is the effect of sample heterogeneity. The size, morphology and structural irregularity (i.e. number of defects) of MOF crystals will influence the properties of the biocomposites and thus systematic studies are required to ascertain how these can be controlled and employed to improve specific applications such as controlled release profiles⁸¹. Although further fundamental studies are necessary given the state-of-the-art in the area it is not unrealistic to anticipate that MOF/enzyme composites will find applications in areas of commercial interest.

ASSOCIATED CONTENT

Supporting Information.

Animations showing: enzyme infiltration in small pores (01a_small_pore.mp4) and large pores (01b_large_pore.mp4); protective properties of enzyme encapsulated in MOFs (02_overview_enzyme_mof.mp4); soft templating approach (03_soft_templating.mp4); interfacial synthesis of MOFs (04_interfacial_growth.mp4); enzyme encapsulation using templating (05_encapsulation_by_templating.mp4); hydrophobic effects of MOFs on enzymes (10_hydrophobic_effects_of_mofs.mp4)

This material is available free of charge via the Internet at <http://pubs.acs.org>.

AUTHOR INFORMATION

Corresponding Author

*paolo.falcaro@tugraz.at

*christian.doonan@adelaide.edu.au

Present Addresses

† Present address: Weibin Liang, School of Chemical and Biomolecular Engineering, The University of Sydney, Sydney, NSW, 2006, Australia.

Author Contributions

The manuscript was written through contributions of all authors. ‡These authors contributed equally.

Funding Sources

Australian Research Council Discovery Project (DP170103531 and DP200102411)
(FP/2014-2020)/ERC Grant Agreement no. 771834
POPCRYSTAL)
TU Graz for the Lead Project (LP-03).

ACKNOWLEDGMENT

CJD, CJS and PF acknowledge the Australian Research Council for funding under the Discovery Projects scheme (DP170103531 and DP200102411), the European Union's Horizon 2020 Programme (FP/2014-2020)/ERC Grant Agreement no. 771834 - POPCRYSTAL) and TU Graz for the Lead Project (LP-03).

ABBREVIATIONS

AAOPE	acid-boosted one pot embedding
4-AAP	4-aminoantipyrine
ABTS	2,2'-azinobis(3-ethylbenzthiazoline)-6-sulfonate
AchE	acetylcholinesterase enzyme
Alb	albumin
Amplex™ red	N-acetyl-3,7-dihydroxyphenoxazine
ANL	Aspergillus niger lipase
APBQ	N-antipyryl-p-benzoquinoneimine
Arg	arginine
ArPPK2	polyphosphate kinase 2
Asp	aspartic acid
ATR-FTIR	Attenuated total reflection-Fourier transform infrared spectroscopy
AZDC	azobenzene dicarboxylate
bdc	1,4-benzenedicarboxylate
bim	benzimidazole
bpdc	4,4'-biphenyldicarboxylic acid and
bpy	4,4'-dipyridyl
bpydc	2,2'-bipyridine-5,5'-dicarboxylate
BSA	bovine serum albumin
BSL2	<i>Bacillus subtilis</i> lipase
BTC	1,3,5-benzenetricarboxylic acid
CalB	Candida Antarctica lipase B
CAPB	cocamidopropyl betaine
CA	Carbonic anhydrase
CalB	<i>Candida Antarctica</i> lipase B
CAT	catalase
CBAB	4-carboxybenzylidene-4-aminobenzoate
CD	circular dichroism
ChT	α -chymotrypsin
CLSM	confocal laser scanning microscopy
c-MWCNTs	carboxylated multiwalled carbon nanotubes
COF	covalent organic framework
CpG	cytosine-phosphate-guanine

Cp*Rh complex	2'-bipyridyl-5,5'-dicarboxylic acid)Cl ₂ complex	MIP of Paris	Materials from Institute of porous materials
Cryo-FESEM electron microscopy	cryo-temperature field-emission scanning electron microscopy	2-mIM	2-methylimidazole
CVD	chemical vapor deposition	MOF	metal-organic framework
CYCU	Chung Yuan Christian University	MP-8	microperoxidase-8
Cys	cysteine	MP-11	microperoxidase-11
CytC	cytochrome C	MTs	metallothioneins
C-ZIF-8	crystalline ZIF-8	mtz	3-methy-1,2,4-triazolate
DABCO	1,4-diazabicyclo[2.2.2]octane	M-ZIF-8	macroporous ZIF-8
DBCO-NHS ester imidyl ester	Dibenzocyclooctyne-N-hydroxysuccinimide ester	NAD	nicotinamide adenine dinucleotide
DCC	Dicyclohexyl carbodiimide	NADP	Nicotinamide adenine dinucleotide phosphate
DFP	diisopropyl fluorophosphate	NBD	4-chloro-7-nitrobenzofurazan
dia	diamondoid	NHS	N-hydroxysuccinimide
DIC	diisopropylcarbodiimide	NPs	nanoparticles
DMF	N,N-dimethylformamide	NU	Northwestern University
2,6-DMP	2,6-dimethoxyphenol	OAPB	oleyl amidopropyl betaine
DNA	deoxyribonucleic acid	oeg	triethylene glycol mono-methyl ether
DQ-OVA	DQ-ovalbumin	OPAA	organophosphorus acid anhydrolase
EDC	1-ethyl-3-(3-dimethylaminopropyl)carbodiimide	OVA	ovalbumin
EDTA	ethylenediaminetetraacetic acid	PCN	porous coordination network
EDX	energy dispersive X-ray spectroscopy	PDA	polydopamine
EGFP	enhanced green fluorescent protein	pda	1,4-phenylenediacetate
EPR	electron paramagnetic resonance spectroscopy	PDMS	polydimethylsiloxane
FCCS	fluorescence cross-correlation spectroscopy	PEI	polyethylenimine
FCS	fluorescence correlation spectroscopy	PEG	poly(ethylene glycol)
FDA	The Food and Drug Administration	PGA	penicillin G acylase
FDH	formate dehydrogenase	PH-ZIF-8	polycrystal hollow ZIF-8
FITC	fluorescein isothiocyanate	pI	isoelectric point
FTIR	Fourier transform infrared spectroscopy	PMOs	periodic mesoporous organosilicas
fum	fumarate	POST	Pohang University of Science and Technol-
GDH	glycerol dehydrogenase	ogy	
GFP	green fluorescent protein	PPL	porcine pancreatic lipase
Glu	glutamic acid	PSs	polystyrene spheres
GOx	glucose oxidase	PVP	polyvinylpyrrolidone
GSH	glutathione	UiO	<i>Universitetet i Oslo</i>
HA	hyaluronic acid	<i>RbITC</i>	Rhodamine B isothiocyanate
Hb	methemoglobin	<i>ROSs</i>	reactive oxygen species
HEP	heparin	SAMs	self-assembled monolayers
HEPES	N-(2-Hydroxyethyl)piperazine-N'-(2-ethanesulfonic acid)	SAXS	small-angle X-ray scattering
His	histidine	SBA-15	Santa Barbara Amorphous-15
HKUST	The Hong Kong University of Science and Technology	SDSL	site-directed spin labeling
HRP	horseradish peroxidase	SEE	single-enzyme encapsulation
ICA	2-imidazolecarboxaldehyde	SEH	soybean epoxide hydrolase
ICP-MS	inductively coupled plasma - mass spectrometry	SEM	scanning electron microscopy
IgG	immunoglobulin	SFG	sum frequency generation
IR	infrared	<i>SGZ</i>	syringaldazine
IRMOF	isoreticular metal-organic framework	<i>SNPs</i>	silica nanoparticles
kat	katsenite	<i>sod</i>	<i>sodalite</i>
LAC	laccase	<i>SODx</i>	superoxide dismutase
LDH	lactate dehydrogenase	<i>SOM-ZIF-8</i>	single-crystal ordered macropore zeolitic
Lys	lysine	imidazolate framework-8	
MAF	metal azolate framework	SPDP	N-succinimidyl 3-(2-pyridyldithio)propionate
Mb	myoglobin	STRENDA	The Standards for Reporting Enzymology
MCM-41	Mobil Composition of Matter No.41	Data commission	
MEE	multiple-enzyme encapsulation	sulfo-NHS	N-Hydroxysulfosuccinimide sodium salt
MFCs	Magnetic Framework Composites	<i>TATB</i>	4,4',4"-s-triazine-2,4,6-triyl-tribenzoic acid
MIL	Materials Institute Lavoisier	TEPA	tetraethylenepentamine
		TEM	transmission electron microscopy
		TGA	Thermogravimetric analysis
		THB	1,2,3-trihydroxybenzene (pyrogallol)
		TMB	3,3',5,5'-tetramethylbenzidine
		TRY	trypsin
		TYR	Tyrosinase

UV-vis	Ultraviolet-visible spectroscopy
ZIF	zeolitic imidazolate framework
ZPF	zeolitic pyrimidine framework
β -gal	β -galactosidase

REFERENCES

- Inamdar, S. M.; Shinde, V. S.; Patil, N. T., Enantioselective cooperative catalysis. *Org. Biomol. Chem.* 2015, 13, 8116-8162.
- Bornscheuer, U. T.; Huisman, G. W.; Kazlauskas, R. J.; Lutz, S.; Moore, J. C.; Robins, K., Engineering the third wave of biocatalysis. *Nature* 2012, 485, 185-194.
- Illanes, A., *Enzyme Biocatalysis: Principles and Applications*. Springer: 2008.
- Iyer, P. V.; Ananthanarayan, L., Enzyme stability and stabilization—Aqueous and non-aqueous environment. *Process Biochem.* 2008, 43, 1019-1032.
- Brena, B. M.; Batista-Viera, F., Immobilization of Enzymes. In *Immobilization of Enzymes and Cells*, Guisan, J. M., Ed. Humana Press: Totowa, NJ, 2006; pp 15-30.
- Sharma, A.; Gupta, G.; Ahmad, T.; Mansoor, S.; Kaur, B., *Enzyme Engineering: Current Trends and Future Perspectives*. *Food Rev. Int.* 2019, 1-34.
- Hofrichter, M.; Ullrich, R., Oxidations catalyzed by fungal peroxigenases. *Curr. Opin. Chem. Biol.* 2014, 19, 116-125.
- Quin, M. B.; Schmidt-Dannert, C., Engineering of Biocatalysts: from Evolution to Creation. *ACS Catal.* 2011, 1, 1017-1021.
- Guisan, J. M.; Bolivar, J. M.; López-Gallego, F.; Rocha-Martín, J., *Immobilization of Enzymes and Cells: Methods and Protocols*, 4th ed. Springer US: 2020.
- Doonan, C.; Ricco, R.; Liang, K.; Bradshaw, D.; Falcaro, P., Metal-Organic Frameworks at the Biointerface: Synthetic Strategies and Applications. *Acc. Chem. Res.* 2017, 50, 1423-1432.
- Hartmann, M.; Kostrov, X., Immobilization of enzymes on porous silicas – benefits and challenges. *Chem. Soc. Rev.* 2013, 42, 6277-6289.
- Furukawa, H.; Cordova, K. E.; O’Keeffe, M.; Yaghi, O. M., *The Chemistry and Applications of Metal-Organic Frameworks*. *Science* 2013, 341, 1230444.
- Jesionowski, T.; Zdarta, J.; Krajewska, B., Enzyme immobilization by adsorption: a review. *Adsorption* 2014, 20, 801-821.
- Rodrigues, R. C.; Ortiz, C.; Berenguer-Murcia, Á.; Torres, R.; Fernández-Lafuente, R., Modifying enzyme activity and selectivity by immobilization. *Chem. Soc. Rev.* 2013, 42, 6290-6307.
- Freedman, R. B., *Proteins: Structures and molecular properties*. by Thomas E. Creighton, W. H. Freeman & Co., 1983. £28.95 (xi + 515 pages) ISBN 0 7167 1566. *Trends Biochem. Sci.* 1985, 10, 82.
- Liang, K.; Ricco, R.; Doherty, C. M.; Styles, M. J.; Bell, S.; Kirby, N.; Mudie, S.; Haylock, D.; Hill, A. J.; Doonan, C. J.; Falcaro, P., Biomimetic mineralization of metal-organic frameworks as protective coatings for biomacromolecules. *Nat. Commun.* 2015, 6, 7240.
- Lyu, F.; Zhang, Y.; Zare, R. N.; Ge, J.; Liu, Z., One-Pot Synthesis of Protein-Embedded Metal-Organic Frameworks with Enhanced Biological Activities. *Nano Lett.* 2014, 14, 5761-5765.
- Jeong, G.-Y.; Ricco, R.; Liang, K.; Ludwig, J.; Kim, J.-O.; Falcaro, P.; Kim, D.-P., Bioactive MIL-88A Framework Hollow Spheres via Interfacial Reaction In-Droplet Microfluidics for Enzyme and Nanoparticle Encapsulation. *Chem. Mater.* 2015, 27, 7903-7909.
- Shieh, F.-K.; Wang, S.-C.; Yen, C.-I.; Wu, C.-C.; Dutta, S.; Chou, L.-Y.; Morabito, J. V.; Hu, P.; Hsu, M.-H.; Wu, K. C. W.; Tsung, C.-K., Imparting Functionality to Biocatalysts via Embedding Enzymes into Nanoporous Materials by a de Novo Approach: Size-Selective Sheltering of Catalase in Metal-Organic Framework Microcrystals. *J. Am. Chem. Soc.* 2015, 137, 4276-4279.
- Wilkins, D. K.; Grimshaw, S. B.; Receveur, V.; Dobson, C. M.; Jones, J. A.; Smith, L. J., Hydrodynamic Radii of Native and Denatured Proteins Measured by Pulse Field Gradient NMR Techniques. *Biochemistry* 1999, 38, 16424-16431.
- Liang, K.; Ricco, R.; Doherty, C. M.; Styles, M. J.; Bell, S.; Kirby, N.; Mudie, S.; Haylock, D.; Hill, A. J.; Doonan, C. J.; Falcaro, P., Biomimetic mineralization of metal-organic frameworks as protective coatings for biomacromolecules. *Nat. Commun.* 2015, 6, 7240.
- Yiu, H. H. P.; Wright, P. A., Enzymes supported on ordered mesoporous solids: a special case of an inorganic-organic hybrid. *J. Mater. Chem.* 2005, 15, 3690-3700.
- Navarro-Sánchez, J.; Almora-Barrios, N.; Lerma-Berlanga, B.; Ruiz-Pernía, J. J.; Lorenz-Fonfria, V. A.; Tuñón, I.; Martí-Gastaldo, C., Translocation of enzymes into a mesoporous MOF for enhanced catalytic activity under extreme conditions. *Chem. Sci.* 2019, 10, 4082-4088.
- Chen, Y.; Lykourinou, V.; Vetromile, C.; Hoang, T.; Ming, L.-J.; Larsen, R. W.; Ma, S., How Can Proteins Enter the Interior of a MOF? Investigation of Cytochrome c Translocation into a MOF Consisting of Mesoporous Cages with Microporous Windows. *J. Am. Chem. Soc.* 2012, 134, 13188-13191.
- Magner, E., Immobilisation of enzymes on mesoporous silicate materials. *Chem. Soc. Rev.* 2013, 42, 6213-6222.
- Yiu, H. H. P.; Wright, P. A., Enzymes supported on ordered mesoporous solids: a special case of an inorganic-organic hybrid. *J. Mater. Chem.* 2005, 15, 3690-3700.
- Pan, Y.; Li, H.; Farmakes, J.; Xiao, F.; Chen, B.; Ma, S.; Yang, Z., How Do Enzymes Orient When Trapped on Metal-Organic Framework (MOF) Surfaces? *J. Am. Chem. Soc.* 2018, 140, 16032-16036.
- Marreiros, J.; Caratelli, C.; Hajek, J.; Krajnc, A.; Fleury, G.; Bueken, B.; De Vos, D. E.; Mali, G.; Roefsaers, M. B. J.; Van Speybroeck, V.; Ameloot, R., Active Role of Methanol in Post-Synthetic Linker Exchange in the Metal-Organic Framework UiO-66. *Chem. Mater.* 2019, 31, 1359-1369.
- Fluch, U.; Paneta, V.; Primetzhofer, D.; Ott, S., Uniform distribution of post-synthetic linker exchange in metal-organic frameworks revealed by Rutherford backscattering spectrometry. *Chem. Commun.* 2017, 53, 6516-6519.
- Okada, K.; Ricco, R.; Tokudome, Y.; Styles, M. J.; Hill, A. J.; Takahashi, M.; Falcaro, P., Copper Conversion into Cu(OH)₂ Nanotubes for Positioning Cu₃(BTC)₂ MOF Crystals: Controlling the Growth on Flat Plates, 3D Architectures, and as Patterns. *Adv. Funct. Mater.* 2014, 24, 1969-1977.
- Cravillon, J.; Schröder, C. A.; Nayuk, R.; Gummel, J.; Huber, K.; Wiebecke, M., Fast Nucleation and Growth of ZIF-8 Nanocrystals Monitored by Time-Resolved In Situ Small-Angle and Wide-Angle X-Ray Scattering. *Angew. Chem., Int. Ed.* 2011, 50, 8067-8071.
- Gopinath, S.; Sugunan, S., Leaching studies over immobilized α -amylase. importance of the nature of enzyme attachment. *React. Kinet. Catal. Lett.* 2004, 83, 79-83.
- Chen, W.-H.; Vázquez-González, M.; Zoabi, A.; Abu-Reziq, R.; Willner, I., Biocatalytic cascades driven by enzymes encapsulated in metal-organic framework nanoparticles. *Nat. Catal.* 2018, 1, 689-695.
- Lian, X.; Chen, Y.-P.; Liu, T.-F.; Zhou, H.-C., Coupling two enzymes into a tandem nanoreactor utilizing a hierarchically structured MOF. *Chem. Sci.* 2016, 7, 6969-6973.
- Stock, N.; Biswas, S., Synthesis of Metal-Organic Frameworks (MOFs): Routes to Various MOF Topologies, Morphologies, and Composites. *Chem. Rev.* 2012, 112, 933-969.
- Chen, B.; Yang, Z.; Zhu, Y.; Xia, Y., Zeolitic imidazolate framework materials: recent progress in synthesis and applications. *J. Mater. Chem. A* 2014, 2, 16811-16831.
- Wu, X.; Yue, H.; Zhang, Y.; Gao, X.; Li, X.; Wang, L.; Cao, Y.; Hou, M.; An, H.; Zhang, L.; Li, S.; Ma, J.; Lin, H.; Fu, Y.; Gu, H.; Lou, W.; Wei, W.; Zare, R. N.; Ge, J., Packaging and delivering enzymes by amorphous metal-organic frameworks. *Nat. Commun.* 2019, 10, 5165.
- Knedel, T.-O.; Ricklefs, E.; Schlüsener, C.; Urlacher, V. B.; Janiak, C., Laccase Encapsulation in ZIF-8 Metal-Organic Framework Shows Stability Enhancement and Substrate Selectivity. *ChemistryOpen* 2019, 8, 1337-1344.
- Liang, W.; Xu, H.; Carraro, F.; Maddigan, N. K.; Li, Q.; Bell, S. G.; Huang, D. M.; Tarzia, A.; Solomon, M. B.; Amenitsch, H.;

- Vaccari, L.; Sumbly, C. J.; Falcaro, P.; Doonan, C. J., Enhanced Activity of Enzymes Encapsulated in Hydrophilic Metal–Organic Frameworks. *J. Am. Chem. Soc.* 2019, 141, 2348-2355.
40. Velásquez-Hernández, M. d. J.; Ricco, R.; Carraro, F.; Limpoco, F. T.; Linares-Moreau, M.; Leitner, E.; Wiltse, H.; Rattenberger, J.; Schröttner, H.; Frühwirth, P.; Stadler, E. M.; Gescheidt, G.; Amenitsch, H.; Doonan, C. J.; Falcaro, P., Degradation of ZIF-8 in phosphate buffered saline media. *CrystEngComm* 2019, 21, 4538-4544.
41. Chen, G.; Huang, S.; Kou, X.; Wei, S.; Huang, S.; Jiang, S.; Shen, J.; Zhu, F.; Ouyang, G., A Convenient and Versatile Amino-Acid-Boosted Biomimetic Strategy for the Nondestructive Encapsulation of Biomacromolecules within Metal–Organic Frameworks. *Angew. Chem., Int. Ed.* 2019, 58, 1463-1467.
42. Liang, K.; Coghlán, C. J.; Bell, S. G.; Doonan, C.; Falcaro, P., Enzyme encapsulation in zeolitic imidazolate frameworks: a comparison between controlled co-precipitation and biomimetic mineralization. *Chem. Commun.* 2016, 52, 473-476.
43. Liu, Q.; Chapman, J.; Huang, A.; Williams, K. C.; Wagner, A.; Garapati, N.; Sierros, K. A.; Dinu, C. Z., User-Tailored Metal–Organic Frameworks as Supports for Carbonic Anhydrase. *ACS Appl. Mater. Interfaces* 2018, 10, 41326-41337.
44. Pitzalis, F.; Carucci, C.; Naseri, M.; Fotouhi, L.; Magner, E.; Salis, A., Lipase Encapsulation onto ZIF-8: A Comparison between Biocatalysts Obtained at Low and High Zinc/2-Methylimidazole Molar Ratio in Aqueous Medium. *ChemCatChem* 2018, 10, 1578-1585.
45. Song, J.; He, W.; Shen, H.; Zhou, Z.; Li, M.; Su, P.; Yang, Y., Construction of multiple enzyme metal–organic frameworks biocatalyst via DNA scaffold: A promising strategy for enzyme encapsulation. *Chem. Eng. J.* 2019, 363, 174-182.
46. Chen, G.; Kou, X.; Huang, S.; Tong, L.; Shen, Y.; Zhu, W.; Zhu, F.; Ouyang, G., Modulating the Biofunctionality of Metal–Organic-Framework-Encapsulated Enzymes through Controllable Embedding Patterns. *Angew. Chem., Int. Ed.* 2020, 59, 2867-2874.
47. Carraro, F.; Velásquez-Hernández, M. d. J.; Astria, E.; Liang, W.; Twilight, L.; Parise, C.; Ge, M.; Huang, Z.; Ricco, R.; Zou, X.; Villanova, L.; Kappe, C. O.; Doonan, C.; Falcaro, P., Phase dependent encapsulation and release profile of ZIF-based biocomposites. *Chem. Sci.* 2020, 11, 3397-3404.
48. Sun, C.-Y.; Qin, C.; Wang, X.-L.; Yang, G.-S.; Shao, K.-Z.; Lan, Y.-Q.; Su, Z.-M.; Huang, P.; Wang, C.-G.; Wang, E.-B., Zeolitic imidazolate framework-8 as efficient pH-sensitive drug delivery vehicle. *Dalton Trans.* 2012, 41, 6906-6909.
49. Luzuriaga, M. A.; Benjamin, C. E.; Gaertner, M. W.; Lee, H.; Herbert, F. C.; Mallick, S.; Gassensmith, J. J., ZIF-8 degrades in cell media, serum, and some—but not all—common laboratory buffers. *Supramol. Chem.* 2019, 31, 485-490.
50. Allegretto, J. A.; Dostalek, J.; Rafti, M.; Menges, B.; Azzaroni, O.; Knoll, W., Shedding Light on the Dark Corners of Metal–Organic Framework Thin Films: Growth and Structural Stability of ZIF-8 Layers Probed by Optical Waveguide Spectroscopy. *J. Phys. Chem. A* 2019, 123, 1100-1109.
51. Krokidas, P.; Moncho, S.; Brothers, E. N.; Castier, M.; Economou, I. G., Tailoring the gas separation efficiency of metal organic framework ZIF-8 through metal substitution: a computational study. *Phys. Chem. Chem. Phys.* 2018, 20, 4879-4892.
52. Chen, S.-Y.; Lo, W.-S.; Huang, Y.-D.; Si, X.; Liao, F.-S.; Lin, S.-W.; Williams, B. P.; Sun, T.-Q.; Lin, H.-W.; An, Y.; Sun, T.; Ma, Y.; Yang, H.-C.; Chou, L.-Y.; Shieh, F.-K.; Tsung, C.-K., Probing Interactions between Metal–Organic Frameworks and Freestanding Enzymes in a Hollow Structure. *Nano Lett.* 2020, 20, 6630-6635.
53. Huang, S.; Kou, X.; Shen, J.; Chen, G.; Ouyang, G., “Armor-Plating” Enzymes with Metal–Organic Frameworks (MOFs). *Angew. Chem., Int. Ed.* n/a.
54. Chulkaivalsucharit, P.; Wu, X.; Ge, J., Synthesis of enzyme-embedded metal–organic framework nanocrystals in reverse micelles. *RSC Adv.* 2015, 5, 101293-101296.
55. Wang, S.; Chen, Y.; Wang, S.; Li, P.; Mirkin, C. A.; Farha, O. K., DNA-Functionalized Metal–Organic Framework Nanoparticles for Intracellular Delivery of Proteins. *J. Am. Chem. Soc.* 2019, 141, 2215-2219.
56. Li, Y.; Zhang, K.; Liu, P.; Chen, M.; Zhong, Y.; Ye, Q.; Wei, M. Q.; Zhao, H.; Tang, Z., Encapsulation of Plasmid DNA by Nanoscale Metal–Organic Frameworks for Efficient Gene Transportation and Expression. *Adv. Mater.* 2019, 31, 1901570.
57. Feng, Y.; Wang, H.; Zhang, S.; Zhao, Y.; Gao, J.; Zheng, Y.; Zhao, P.; Zhang, Z.; Zaworotko, M. J.; Cheng, P.; Ma, S.; Chen, Y., Antibodies@MOFs: An In Vitro Protective Coating for Preparation and Storage of Biopharmaceuticals. *Adv. Mater.* 2019, 31, 1805148.
58. Velasquez, M.; Astria, E.; Winkler, S.; Liang, W.; Amenitsch, H.; Poddar, A.; Shukla, R.; Prestwich, G.; Paderi, J.; Doonan, C.; Falcaro, P., Modulation of Metal-Azolate Frameworks for the Tunable Release of Encapsulated Glycosaminoglycans. *Chem. Sci.* 2020.
59. Kim, H.; Lah, M. S., Templated and template-free fabrication strategies for zero-dimensional hollow MOF superstructures. *Dalton Trans.* 2017, 46, 6146-6158.
60. Doherty, C. M.; Buso, D.; Hill, A. J.; Furukawa, S.; Kitagawa, S.; Falcaro, P., Using Functional Nano- and Microparticles for the Preparation of Metal–Organic Framework Composites with Novel Properties. *Acc. Chem. Res.* 2014, 47, 396-405.
61. Huo, J.; Aguilera-Sigalat, J.; El-Hankari, S.; Bradshaw, D., Magnetic MOF microreactors for recyclable size-selective biocatalysis. *Chem. Sci.* 2015, 6, 1938-1943.
62. Ameloot, R.; Vermoortele, F.; Vanhove, W.; Roeffaers, M. B. J.; Sels, B. F.; De Vos, D. E., Interfacial synthesis of hollow metal–organic framework capsules demonstrating selective permeability. *Nat. Chem.* 2011, 3, 382-387.
63. Wang, Y.; Hou, C.; Zhang, Y.; He, F.; Liu, M.; Li, X., Preparation of graphene nano-sheet bonded PDA/MOF microcapsules with immobilized glucose oxidase as a mimetic multi-enzyme system for electrochemical sensing of glucose. *J. Mater. Chem. B* 2016, 4, 3695-3702.
64. Ameloot, R.; Vermoortele, F.; Vanhove, W.; Roeffaers, M. B. J.; Sels, B. F.; De Vos, D. E., Interfacial synthesis of hollow metal–organic framework capsules demonstrating selective permeability. *Nat. Chem.* 2011, 3, 382-387.
65. Wang, X.; Shi, J.; Zhang, S.; Wu, H.; Jiang, Z.; Yang, C.; Wang, Y.; Tang, L.; Yan, A., MOF-templated rough, ultrathin inorganic microcapsules for enzyme immobilization. *J. Mater. Chem. B* 2015, 3, 6587-6598.
66. Li, M.; Qiao, S.; Zheng, Y.; Andaloussi, Y. H.; Li, X.; Zhang, Z.; Li, A.; Cheng, P.; Ma, S.; Chen, Y., Fabricating Covalent Organic Framework Capsules with Commodious Microenvironment for Enzymes. *J. Am. Chem. Soc.* 2020, 142, 6675-6681.
67. Jeong, G.-Y.; Ricco, R.; Liang, K.; Ludwig, J.; Kim, J.-O.; Falcaro, P.; Kim, D.-P., Bioactive MIL-88A Framework Hollow Spheres via Interfacial Reaction In-Droplet Microfluidics for Enzyme and Nanoparticle Encapsulation. *Chem. Mater.* 2015, 27, 7903-7909.
68. Li, M.; Qiao, S.; Zheng, Y.; Andaloussi, Y. H.; Li, X.; Zhang, Z.; Li, A.; Cheng, P.; Ma, S.; Chen, Y., Fabricating Covalent Organic Framework Capsules with Commodious Microenvironment for Enzymes. *J. Am. Chem. Soc.* 2020, 142, 6675-6681.
69. Wu, X.; Yang, C.; Ge, J., Green synthesis of enzyme/metal-organic framework composites with high stability in protein denaturing solvents. *Bioresour. Bioprocess.* 2017, 4, 24.
70. Herskovits, T. T.; Gadegbeku, B.; Jalliet, H., On the Structural Stability and Solvent Denaturation of Proteins: I. DENATURATION BY THE ALCOHOLS AND GLYCOLS. *J. Biol. Chem.* 1970, 245, 2588-2598.
71. LIANG, K.; RICCO, R.; DOHERTY, C. M.; FALCARO, P. HOST-GUEST METAL ORGANIC FRAMEWORK SYSTEMS. 2016, patent WO2016/000032, earliest priority date 2014.
72. Chen, T.-T.; Yi, J.-T.; Zhao, Y.-Y.; Chu, X., Biomimetic Metal–Organic Framework Nanoparticles Enable Intracellular Delivery and Endo-Lysosomal Release of Native Active Proteins. *J. Am. Chem. Soc.* 2018, 140, 9912-9920.
73. Pei, X.; Wu, Y.; Wang, J.; Chen, Z.; Liu, W.; Su, W.; Liu, F., Biomimetic mineralization of nitrile hydratase into a mesoporous cobalt-based metal–organic framework for efficient biocatalysis. *Nanoscale* 2020, 12, 967-972.

74. Lyu, F.; Zhang, Y.; Zare, R. N.; Ge, J.; Liu, Z., One-Pot Synthesis of Protein-Embedded Metal–Organic Frameworks with Enhanced Biological Activities. *Nano Lett.* 2014, 14, 5761–5765.
75. Liang, K.; Coghlan, C. J.; Bell, S. G.; Doonan, C.; Falcaro, P., Enzyme encapsulation in zeolitic imidazolate frameworks: a comparison between controlled co-precipitation and biomimetic mineralization. *Chem. Commun.* 2016, 52, 473–476.
76. Carraro, F.; Williams, J. D.; Linares-Moreau, M.; Parise, C.; Liang, W.; Amenitsch, H.; Doonan, C.; Kappe, C. O.; Falcaro, P., Continuous-Flow Synthesis of ZIF-8 Biocomposites with Tunable Particle Size. *Angew. Chem., Int. Ed.* 2020, 59, 8123–8127.
77. Ogata, A. F.; Rakowski, A. M.; Carpenter, B. P.; Fishman, D. A.; Merham, J. G.; Hurst, P. J.; Patterson, J. P., Direct Observation of Amorphous Precursor Phases in the Nucleation of Protein–Metal–Organic Frameworks. *J. Am. Chem. Soc.* 2020, 142, 1433–1442.
78. Astria, E.; Thonhofer, M.; Ricco, R.; Liang, W.; Chemelli, A.; Tarzia, A.; Alt, K.; Hagemeyer, C. E.; Rattenberger, J.; Schroettner, H.; Wrodnigg, T.; Amenitsch, H.; Huang, D. M.; Doonan, C. J.; Falcaro, P., Carbohydrates@MOFs. *Mater. Horiz.* 2019, 6, 969–977.
79. Hu, C.; Bai, Y.; Hou, M.; Wang, Y.; Wang, L.; Cao, X.; Chan, C.-W.; Sun, H.; Li, W.; Ge, J.; Ren, K., Defect-induced activity enhancement of enzyme-encapsulated metal-organic frameworks revealed in microfluidic gradient mixing synthesis. *Sci. Adv.* 2020, 6, eaax5785.
80. Liang, W.; Xu, H.; Carraro, F.; Maddigan, N. K.; Li, Q.; Bell, S. G.; Huang, D. M.; Tarzia, A.; Solomon, M. B.; Amenitsch, H.; Vaccari, L.; Sumbly, C. J.; Falcaro, P.; Doonan, C. J., Enhanced Activity of Enzymes Encapsulated in Hydrophilic Metal–Organic Frameworks. *J. Am. Chem. Soc.* 2019, 141, 2348–2355.
81. Carraro, F.; Velásquez-Hernández, M. d. J.; Astria, E.; Liang, W.; Twilight, L.; Parise, C.; Ge, M.; Huang, Z.; Ricco, R.; Zou, X.; Villanova, L.; Kappe, C. O.; Doonan, C.; Falcaro, P., Phase dependent encapsulation and release profile of ZIF-based biocomposites. *Chem. Sci.* 2020, 11, 3397–3404.
82. Liang, W.; Ricco, R.; Maddigan, N. K.; Dickinson, R. P.; Xu, H.; Li, Q.; Sumbly, C. J.; Bell, S. G.; Falcaro, P.; Doonan, C. J., Control of Structure Topology and Spatial Distribution of Biomacromolecules in Protein@ZIF-8 Biocomposites. *Chem. Mater.* 2018, 30, 1069–1077.
83. Hu, C.; Bai, Y.; Hou, M.; Wang, Y.; Wang, L.; Cao, X.; Chan, C.-W.; Sun, H.; Li, W.; Ge, J.; Ren, K., Defect-induced activity enhancement of enzyme-encapsulated metal-organic frameworks revealed in microfluidic gradient mixing synthesis. *Sci. Adv.* 2020, 6, eaax5785.
84. Teodorescu, M.; Bercea, M.; Morariu, S., Biomaterials of PVA and PVP in medical and pharmaceutical applications: Perspectives and challenges. *Biotechnol. Adv.* 2019, 37, 109–131.
85. Zhang, S.; Deng, Q.; Li, Y.; Zheng, M.; Wan, C.; Zheng, C.; Tang, H.; Huang, F.; Shi, J., Novel amphiphilic polyvinylpyrrolidone functionalized silicone particles as carrier for low-cost lipase immobilization. *R. Soc. Open Sci.* 2018, 5, 172368.
86. Jones, J. D.; Hulme, A. C.; Woollerton, L. S. C., The use of polyvinylpyrrolidone in the isolation of enzymes from apple fruits. *Phytochemistry* 1965, 4, 659–676.
87. Lisý, V.; Kovářů, H.; Lodin, Z., In vitro effects of polyvinylpyrrolidone and sucrose on the acetylcholinesterase, succinate dehydrogenase and lactate dehydrogenase activities in the brain. *Histochemie* 1971, 26, 205–211.
88. Schwarz, W., *Pvp: A Critical Review of the Kinetics and Toxicology of Polyvinylpyrrolidone (Povidone)*. Routledge & CRC Press: 1990.
89. Koczur, K. M.; Mourdikoudis, S.; Polavarapu, L.; Skrabalak, S. E., Polyvinylpyrrolidone (PVP) in nanoparticle synthesis. *Dalton Trans.* 2015, 44, 17883–17905.
90. Abedini, A. S., E.; Larki, F.; Zakaria, A.; Noroozi, M.; Soltani, N., Room Temperature Radiolytic Synthesized Cu@CuAlO₂-Al₂O₃ Nanoparticles. *Int. J. Mol. Sci.* 2012, 11, 11941–11953.
91. Lee, Y.-R.; Jang, M.-S.; Cho, H.-Y.; Kwon, H.-J.; Kim, S.; Ahn, W.-S., ZIF-8: A comparison of synthesis methods. *Chem. Eng. J.* 2015, 271, 276–280.
92. Lu, G.; Li, S.; Guo, Z.; Farha, O. K.; Hauser, B. G.; Qi, X.; Wang, Y.; Wang, X.; Han, S.; Liu, X.; DuChene, J. S.; Zhang, H.; Zhang, Q.; Chen, X.; Ma, J.; Loo, S. C. J.; Wei, W. D.; Yang, Y.; Hupp, J. T.; Huo, F., Imparting functionality to a metal–organic framework material by controlled nanoparticle encapsulation. *Nat. Chem.* 2012, 4, 310–316.
93. Jiang, H.; Yan, Q.; Chen, R.; Xing, W., Synthesis of Pd@ZIF-8 via an assembly method: Influence of the molar ratios of Pd/Zn²⁺ and 2-methylimidazole/Zn²⁺. *Microporous Mesoporous Mater.* 2016, 225, 33–40.
94. Liang, Z.; Zhang, C.; Yuan, H.; Zhang, W.; Zheng, H.; Cao, R., PVP-assisted transformation of a metal–organic framework into Co-embedded N-enriched meso/microporous carbon materials as bifunctional electrocatalysts. *Chem. Commun.* 2018, 54, 7519–7522.
95. Zhang, Z.; Chen, Y.; Xu, X.; Zhang, J.; Xiang, G.; He, W.; Wang, X., Well-Defined Metal–Organic Framework Hollow Nanocages. *Angew. Chem., Int. Ed.* 2014, 53, 429–433.
96. Li, H.; Meng, F.; Zhang, S.; Wang, L.; Li, M.; Ma, L.; Zhang, W.; Zhang, W.; Yang, Z.; Wu, T.; Lee, S.; Huo, F.; Lu, J., Crystal-Growth-Dominated Fabrication of Metal–Organic Frameworks with Orderly Distributed Hierarchical Porosity. *Angew. Chem., Int. Ed.* 2020, 59, 2457–2464.
97. Maddigan, N. K.; Tarzia, A.; Huang, D. M.; Sumbly, C. J.; Bell, S. G.; Falcaro, P.; Doonan, C. J., Protein surface functionalisation as a general strategy for facilitating biomimetic mineralisation of ZIF-8. *Chem. Sci.* 2018, 9, 4217–4223.
98. Zhao, Z.; Pang, J.; Liu, W.; Lin, T.; Ye, F.; Zhao, S., A bifunctional metal organic framework of type Fe(III)-BTC for cascade (enzymatic and enzyme-mimicking) colorimetric determination of glucose. *Microchim. Acta* 2019, 186, 295.
99. Yuan, S.; Feng, L.; Wang, K.; Pang, J.; Bosch, M.; Lollar, C.; Sun, Y.; Qin, J.; Yang, X.; Zhang, P.; Wang, Q.; Zou, L.; Zhang, Y.; Zhang, L.; Fang, Y.; Li, J.; Zhou, H.-C., Stable Metal–Organic Frameworks: Design, Synthesis, and Applications. *Adv. Mater.* 2018, 30, 1704303.
100. Gascón, V.; Castro-Miguel, E.; Díaz-García, M.; Blanco, R. M.; Sanchez-Sanchez, M., In situ and post-synthesis immobilization of enzymes on nanocrystalline MOF platforms to yield active biocatalysts. *J. Chem. Technol. Biotechnol.* 2017, 92, 2583–2593.
101. Zoungrana, T.; Findenegg, G. H.; Norde, W., Structure, Stability, and Activity of Adsorbed Enzymes. *J. Colloid Interface Sci.* 1997, 190, 437–448.
102. Cereghino, J. L.; Cregg, J. M., Heterologous protein expression in the methylotrophic yeast *Pichia pastoris*. *FEMS Microbiol. Rev.* 2000, 24, 45–66.
103. Cain, J. A.; Solis, N.; Cordwell, S. J., Beyond gene expression: The impact of protein post-translational modifications in bacteria. *J. Proteomics* 2014, 97, 265–286.
104. Jenkins, N.; Parekh, R. B.; James, D. C., Getting the glycosylation right: Implications for the biotechnology industry. *Nat. Biotechnol.* 1996, 14, 975–981.
105. Baumann, C.; Beil, A.; Jurt, S.; Niederwanger, M.; Palacios, O.; Capdevila, M.; Atrian, S.; Dallinger, R.; Zerbe, O., Structural Adaptation of a Protein to Increased Metal Stress: NMR Structure of a Marine Snail Metallothionein with an Additional Domain. *Angew. Chem., Int. Ed.* 2017, 56, 4617–4622.
106. Belmonte, L.; Rossetto, D.; Forlin, M.; Scintilla, S.; Bonfio, C.; Mansy, S. S., Cysteine containing dipeptides show a metal specificity that matches the composition of seawater. *Phys. Chem. Chem. Phys.* 2016, 18, 20104–20108.
107. Pace, N. J. W., E., Zinc-Binding Cysteines: Diverse Functions and Structural Motifs. *Biomolecules* 2014, 419–434.
108. Wang, H.; Han, L.; Zheng, D.; Yang, M.; Andaloussi, Y. H.; Cheng, P.; Zhang, Z.; Ma, S.; Zawortko, M. J.; Feng, Y.; Chen, Y., Protein-Structure-Directed Metal–Organic Zeolite-like Networks as Biomacromolecule Carriers. *Angew. Chem., Int. Ed.* 2020, 59, 6263–6267.
109. Maddigan, N. K.; Tarzia, A.; Huang, D. M.; Sumbly, C. J.; Bell, S. G.; Falcaro, P.; Doonan, C. J., Protein surface functionalisation as a general strategy for facilitating biomimetic mineralisation of ZIF-8. *Chem. Sci.* 2018, 9, 4217–4223.

110. Baumann, C.; Beil, A.; Jurt, S.; Niederwanger, M.; Palacios, O.; Capdevila, M.; Atrian, S.; Dallinger, R.; Zerbe, O., Structural Adaptation of a Protein to Increased Metal Stress: NMR Structure of a Marine Snail Metallothionein with an Additional Domain. *Angew. Chem. Int. Ed.* 2017, 56, 4617-4622.
111. Chen, G.; Huang, S.; Kou, X.; Wei, S.; Huang, S.; Jiang, S.; Shen, J.; Zhu, F.; Ouyang, G., A Convenient and Versatile Amino-Acid-Boosted Biomimetic Strategy for the Nondestructive Encapsulation of Biomacromolecules within Metal–Organic Frameworks. *Angew. Chem. Int. Ed.* 2019, 58, 1463-1467.
112. Liang, W.; Ricco, R.; Maddigan, N. K.; Dickinson, R. P.; Xu, H.; Li, Q.; Sumbly, C. J.; Bell, S. G.; Falcaro, P.; Doonan, C. J., Control of Structure Topology and Spatial Distribution of Biomacromolecules in Protein@ZIF-8 Biocomposites. *Chem. Mater.* 2018, 30, 1069-1077.
113. Zhang, S.; Du, M.; Shao, P.; Wang, L.; Ye, J.; Chen, J.; Chen, J., Carbonic Anhydrase Enzyme-MOFs Composite with a Superior Catalytic Performance to Promote CO₂ Absorption into Tertiary Amine Solution. *Environ. Sci. Technol.* 2018, 52, 12708-12716.
114. Rabe, M.; Verdes, D.; Seeger, S., Understanding protein adsorption phenomena at solid surfaces. *Adv. Colloid Interface Sci.* 2011, 162, 87-106.
115. Zhang, J.-P.; Zhu, A.-X.; Lin, R.-B.; Qi, X.-L.; Chen, X.-M., Pore Surface Tailored SOD-Type Metal–Organic Zeolites. *Adv. Mater.* 2011, 23, 1268-1271.
116. Zhang, K.; Lively, R. P.; Dose, M. E.; Brown, A. J.; Zhang, C.; Chung, J.; Nair, S.; Koros, W. J.; Chance, R. R., Alcohol and water adsorption in zeolitic imidazolate frameworks. *Chem. Commun.* 2013, 49, 3245-3247.
117. Katz, M. J.; Brown, Z. J.; Colón, Y. J.; Siu, P. W.; Scheidt, K. A.; Snurr, R. Q.; Hupp, J. T.; Farha, O. K., A facile synthesis of UiO-66, UiO-67 and their derivatives. *Chem. Commun.* 2013, 49, 9449-9451.
118. Wei, T.-H.; Wu, S.-H.; Huang, Y.-D.; Lo, W.-S.; Williams, B. P.; Chen, S.-Y.; Yang, H.-C.; Hsu, Y.-S.; Lin, Z.-Y.; Chen, X.-H.; Kuo, P.-E.; Chou, L.-Y.; Tsung, C.-K.; Shieh, F.-K., Rapid mechanochemical encapsulation of biocatalysts into robust metal–organic frameworks. *Nat. Commun.* 2019, 10, 5002.
119. Huang, Y.-H.; Lo, W.-S.; Kuo, Y.-W.; Chen, W.-J.; Lin, C.-H.; Shieh, F.-K., Green and rapid synthesis of zirconium metal–organic frameworks via mechanochemistry: UiO-66 analog nanocrystals obtained in one hundred seconds. *Chem. Commun.* 2017, 53, 5818-5821.
120. Klimakow, M.; Klobes, P.; Thünemann, A. F.; Rademann, K.; Emmerling, F., Mechanochemical Synthesis of Metal–Organic Frameworks: A Fast and Facile Approach toward Quantitative Yields and High Specific Surface Areas. *Chem. Mater.* 2010, 22, 5216-5221.
121. Li, X.; Zhang, Z.; Xiao, W.; Deng, S.; Chen, C.; Zhang, N., Mechanochemistry-assisted encapsulation of metal nanoparticles in MOF matrices via a sacrificial strategy. *J. Mater. Chem. A* 2019, 7, 14504-14509.
122. Noorian, S. A.; Hemmatinejad, N.; Navarro, J. A. R., Bioactive molecule encapsulation on metal–organic framework via simple mechanochemical method for controlled topical drug delivery systems. *Microporous Mesoporous Mater.* 2020, 302, 110199.
123. Liang, K.; Richardson, J. J.; Doonan, C. J.; Mulet, X.; Ju, Y.; Cui, J.; Caruso, F.; Falcaro, P., An Enzyme-Coated Metal–Organic Framework Shell for Synthetically Adaptive Cell Survival. *Angew. Chem., Int. Ed.* 2017, 56, 8510-8515.
124. Liao, F.-S.; Lo, W.-S.; Hsu, Y.-S.; Wu, C.-C.; Wang, S.-C.; Shieh, F.-K.; Morabito, J. V.; Chou, L.-Y.; Wu, K. C. W.; Tsung, C.-K., Shielding against Unfolding by Embedding Enzymes in Metal–Organic Frameworks via a de Novo Approach. *J. Am. Chem. Soc.* 2017, 139, 6530-6533.
125. Yang, X.; Tang, Q.; Jiang, Y.; Zhang, M.; Wang, M.; Mao, L., Nanoscale ATP-Responsive Zeolitic Imidazole Framework-90 as a General Platform for Cytosolic Protein Delivery and Genome Editing. *J. Am. Chem. Soc.* 2019, 141, 3782-3786.
126. Hartmann, M., Ordered Mesoporous Materials for Bioadsorption and Biocatalysis. *Chem. Mater.* 2005, 17, 4577-4593.
127. Hudson, S.; Cooney, J.; Magner, E., Proteins in Mesoporous Silicates. *Angew. Chem., Int. Ed.* 2008, 47, 8582-8594.
128. Lykourinou, V.; Chen, Y.; Wang, X.-S.; Meng, L.; Hoang, T.; Ming, L.-J.; Musselman, R. L.; Ma, S., Immobilization of MP-11 into a Mesoporous Metal–Organic Framework, MP-11@mesoMOF: A New Platform for Enzymatic Catalysis. *J. Am. Chem. Soc.* 2011, 133, 10382-10385.
129. Carlsson, N.; Gustafsson, H.; Thörn, C.; Olsson, L.; Holmberg, K.; Åkerman, B., Enzymes immobilized in mesoporous silica: A physical–chemical perspective. *Adv. Colloid Interface Sci.* 2014, 205, 339-360.
130. Bayne, L.; Ulijn, R. V.; Halling, P. J., Effect of pore size on the performance of immobilised enzymes. *Chem. Soc. Rev.* 2013, 42, 9000-9010.
131. Papat, A.; Hartono, S. B.; Stahr, F.; Liu, J.; Qiao, S. Z.; Qing Lu, G., Mesoporous silica nanoparticles for bioadsorption, enzyme immobilisation, and delivery carriers. *Nanoscale* 2011, 3, 2801-2818.
132. Balkus, K. J.; Gabrielov, A. G., Zeolite Encapsulated Metal Complexes. In *Inclusion Chemistry with Zeolites: Nanoscale Materials by Design*, Herron, N.; Corbin, D. R., Eds. Springer Netherlands: Dordrecht, 1995; pp 159-184.
133. Taulelle, F., Crystallogenesi of microporous metallophosphates. *Curr. Opin. Solid State Mater. Sci.* 2001, 5, 397-405.
134. Iler, R. K., *The Chemistry of Silica* Wiley, New York: 1979.
135. Pinnavaia, T. J., Intercalated Clay Catalysts. *Science* 1983, 220, 365-371.
136. Landis, M. E.; Aufdembrink, B. A.; Chu, P.; Johnson, I. D.; Kirker, G. W.; Rubin, M. K., Preparation of molecular sieves from dense layered metal oxides. *J. Am. Chem. Soc.* 1991, 113, 3189-3190.
137. Kresge, C. T.; Leonowicz, M. E.; Roth, W. J.; Vartuli, J. C.; Beck, J. S., Ordered mesoporous molecular sieves synthesized by a liquid-crystal template mechanism. *Nature* 1992, 359, 710-712.
138. Hatton, B.; Landskron, K.; Whitnall, W.; Perovic, D.; Ozin, G. A., Past, Present, and Future of Periodic Mesoporous Organosilicas The PMOs. *Acc. Chem. Res.* 2005, 38, 305-312.
139. Chen, Y.; Shi, J., Chemistry of Mesoporous Organosilica in Nanotechnology: Molecularly Organic–Inorganic Hybridization into Frameworks. *Adv. Mater.* 2016, 28, 3235-3272.
140. Zhou, Z.; Taylor, R. N. K.; Kullmann, S.; Bao, H.; Hartmann, M., Mesoporous Organosilicas With Large Cage-Like Pores for High Efficiency Immobilization of Enzymes. *Adv. Mater.* 2011, 23, 2627-2632.
141. Li, P.; Chen, Q.; Wang, T. C.; Vermeulen, N. A.; Mehdi, B. L.; Dohnalkova, A.; Browning, N. D.; Shen, D.; Anderson, R.; Gómez-Gualdrón, D. A.; Cetin, F. M.; Jagiello, J.; Asiri, A. M.; Stoddart, J. F.; Farha, O. K., Hierarchically Engineered Mesoporous Metal–Organic Frameworks toward Cell-free Immobilized Enzyme Systems. *Chem* 2018, 4, 1022-1034.
142. Drout, R. J.; Robison, L.; Farha, O. K., Catalytic applications of enzymes encapsulated in metal–organic frameworks. *Coord. Chem. Rev.* 2019, 381, 151-160.
143. Pisklak, T. J.; Macías, M.; Coutinho, D. H.; Huang, R. S.; Balkus, K. J., Hybrid materials for immobilization of MP-11 catalyst. *Top Catal.* 2006, 38, 269-278.
144. Chen, Y.; Hong, S.; Fu, C.-W.; Hoang, T.; Li, X.; Valencia, V.; Zhang, Z.; Perman, J. A.; Ma, S., Investigation of the Mesoporous Metal–Organic Framework as a New Platform To Study the Transport Phenomena of Biomolecules. *ACS Appl. Mater. Interfaces* 2017, 9, 10874-10881.
145. Chen, Y.; Lykourinou, V.; Hoang, T.; Ming, L.-J.; Ma, S., Size-Selective Biocatalysis of Myoglobin Immobilized into a Mesoporous Metal–Organic Framework with Hierarchical Pore Sizes. *Inorg. Chem.* 2012, 51, 9156-9158.
146. Park, Y. K.; Choi, S. B.; Kim, H.; Kim, K.; Won, B.-H.; Choi, K.; Choi, J.-S.; Ahn, W.-S.; Won, N.; Kim, S.; Jung, D. H.; Choi, S.-H.; Kim, G.-H.; Cha, S.-S.; Jhon, Y. H.; Yang, J. K.; Kim, J., Crystal Structure and Guest Uptake of a Mesoporous Metal–Organic Framework Containing Cages of 3.9 and 4.7 nm in Diameter. *Angew. Chem. Int. Ed.* 2007, 46, 8230-8233.
147. Chen, Y.; Han, S.; Li, X.; Zhang, Z.; Ma, S., Why Does Enzyme Not Leach from Metal–Organic Frameworks (MOFs)? Unveiling the Interactions between an Enzyme Molecule and a MOF. *Inorg. Chem.* 2014, 53, 10006-10008.

148. Deng, H.; Grunder, S.; Cordova, K. E.; Valente, C.; Furukawa, H.; Hmadeh, M.; Gándara, F.; Whalley, A. C.; Liu, Z.; Asahina, S.; Kazumori, H.; O’Keeffe, M.; Terasaki, O.; Stoddart, J. F.; Yaghi, O. M., Large-Pore Apertures in a Series of Metal-Organic Frameworks. *Science* 2012, 336, 1018-1023.
149. Song, L.; Zhang, J.; Sun, L.; Xu, F.; Li, F.; Zhang, H.; Si, X.; Jiao, C.; Li, Z.; Liu, S.; Liu, Y.; Zhou, H.; Sun, D.; Du, Y.; Cao, Z.; Gabelica, Z., Mesoporous metal-organic frameworks: design and applications. *Energy Environ Sci.* 2012, 5, 7508-7520.
150. Sumida, K.; Liang, K.; Reboul, J.; Ibarra, I. A.; Furukawa, S.; Falcaro, P., Sol-Gel Processing of Metal-Organic Frameworks. *Chem. Mater.* 2017, 29, 2626-2645.
151. Li, P.; Modica, Justin A.; Howarth, Ashlee J.; Vargas L, E.; Moghadam, Peyman Z.; Snurr, Randall Q.; Mrksich, M.; Hupp, Joseph T.; Farha, Omar K., Toward Design Rules for Enzyme Immobilization in Hierarchical Mesoporous Metal-Organic Frameworks. *Chem* 2016, 1, 154-169.
152. Sun, Q.; Aguila, B.; Lan, P. C.; Ma, S., Tuning Pore Heterogeneity in Covalent Organic Frameworks for Enhanced Enzyme Accessibility and Resistance against Denaturants. *Adv. Mater.* 2019, 31, 1900008.
153. Sun, Q.; Fu, C.-W.; Aguila, B.; Perman, J.; Wang, S.; Huang, H.-Y.; Xiao, F.-S.; Ma, S., Pore Environment Control and Enhanced Performance of Enzymes Infiltrated in Covalent Organic Frameworks. *J. Am. Chem. Soc.* 2018, 140, 984-992.
154. Geng, K.; He, T.; Liu, R.; Dalapati, S.; Tan, K. T.; Li, Z.; Tao, S.; Gong, Y.; Jiang, Q.; Jiang, D., Covalent Organic Frameworks: Design, Synthesis, and Functions. *Chem. Rev.* 2020, 120, 8814-8933.
155. Diercks, C. S.; Yaghi, O. M., The atom, the molecule, and the covalent organic framework. *Science* 2017, 355, eaal1585.
156. Huang, N.; Wang, P.; Jiang, D., Covalent organic frameworks: a materials platform for structural and functional designs. *Nat. Rev. Mater.* 2016, 1, 16068.
157. Kim, Y.; Yang, T.; Yun, G.; Ghasemian, M. B.; Koo, J.; Lee, E.; Cho, S. J.; Kim, K., Hydrolytic Transformation of Microporous Metal-Organic Frameworks to Hierarchical Micro- and Mesoporous MOFs. *Angew. Chem., Int. Ed.* 2015, 54, 13273-13278.
158. Yuan, S.; Zou, L.; Qin, J.-S.; Li, J.; Huang, L.; Feng, L.; Wang, X.; Bosch, M.; Alsalmeh, A.; Cagin, T.; Zhou, H.-C., Construction of hierarchically porous metal-organic frameworks through linker labilization. *Nat. Commun.* 2017, 8, 15356.
159. Li, K.; Lin, S.; Li, Y.; Zhuang, Q.; Gu, J., Aqueous-Phase Synthesis of Mesoporous Zr-Based MOFs Templated by Amphoteric Surfactants. *Angew. Chem., Int. Ed.* 2018, 57, 3439-3443.
160. Shen, K.; Zhang, L.; Chen, X.; Liu, L.; Zhang, D.; Han, Y.; Chen, J.; Long, J.; Luque, R.; Li, Y.; Chen, B., Ordered macro-microporous metal-organic framework single crystals. *Science* 2018, 359, 206-210.
161. Cao, Y.; Ma, Y.; Wang, T.; Wang, X.; Huo, Q.; Liu, Y., Facile Fabricating Hierarchically Porous Metal-Organic Frameworks via a Template-Free Strategy. *Cryst. Growth Des.* 2016, 16, 504-510.
162. Cao, Y.; Wu, Z.; Wang, T.; Xiao, Y.; Huo, Q.; Liu, Y., Immobilization of *Bacillus subtilis* lipase on a Cu-BTC based hierarchically porous metal-organic framework material: a biocatalyst for esterification. *Dalton Trans.* 2016, 45, 6998-7003.
163. Furukawa, S.; Reboul, J.; Diring, S.; Sumida, K.; Kitagawa, S., Structuring of metal-organic frameworks at the mesoscopic/macrosopic scale. *Chem. Soc. Rev.* 2014, 43, 5700-5734.
164. Feng, L.; Wang, K.-Y.; Willman, J.; Zhou, H.-C., Hierarchy in Metal-Organic Frameworks. *ACS Central Science* 2020, 6, 359-367.
165. Sumida, K.; Liang, K.; Reboul, J.; Ibarra, I. A.; Furukawa, S.; Falcaro, P., Sol-Gel Processing of Metal-Organic Frameworks. *Chem. Mater.* 2017, 29, 2626-2645.
166. Dusastre, V., MOF patterns. *Nat. Mater.* 2013, 12, 778-778.
167. Falcaro, P.; Buso, D.; Hill, A. J.; Doherty, C. M., Patterning Techniques for Metal Organic Frameworks. *Adv. Mater.* 2012, 24, 3153-3168.
168. Zanchetta, E.; Malfatti, L.; Ricco, R.; Styles, M. J.; Lisi, F.; Coghlan, C. J.; Doonan, C. J.; Hill, A. J.; Brusatin, G.; Falcaro, P., ZnO as an Efficient Nucleating Agent for Rapid, Room Temperature Synthesis and Patterning of Zn-Based Metal-Organic Frameworks. *Chem. Mater.* 2015, 27, 690-699.
169. Koh, K.; Wong-Foy, A. G.; Matzger, A. J., MOF@MOF: microporous core-shell architectures. *Chem. Commun.* 2009, 6162-6164.
170. Feng, L.; Wang, K.-Y.; Day, G. S.; Zhou, H.-C., The chemistry of multi-component and hierarchical framework compounds. *Chem. Soc. Rev.* 2019, 48, 4823-4853.
171. Yuan, S.; Zou, L.; Qin, J.-S.; Li, J.; Huang, L.; Feng, L.; Wang, X.; Bosch, M.; Alsalmeh, A.; Cagin, T.; Zhou, H.-C., Construction of hierarchically porous metal-organic frameworks through linker labilization. *Nat. Commun.* 2017, 8, 15356.
172. Cao, Y.; Wu, Z.; Wang, T.; Xiao, Y.; Huo, Q.; Liu, Y., Immobilization of *Bacillus subtilis* lipase on a Cu-BTC based hierarchically porous metal-organic framework material: a biocatalyst for esterification. *Dalton Trans.* 2016, 45, 6998-7003.
173. Cao, Y.; Ma, Y.; Wang, T.; Wang, X.; Huo, Q.; Liu, Y., Facile Fabricating Hierarchically Porous Metal-Organic Frameworks via a Template-Free Strategy. *Cryst. Growth Des.* 2016, 16, 504-510.
174. Li, P.; Moon, S.-Y.; Guelta, M. A.; Harvey, S. P.; Hupp, J. T.; Farha, O. K., Encapsulation of a Nerve Agent Detoxifying Enzyme by a Mesoporous Zirconium Metal-Organic Framework Engenders Thermal and Long-Term Stability. *J. Am. Chem. Soc.* 2016, 138, 8052-8055.
175. Linder-Patton, O. M.; Bloch, W. M.; Coghlan, C. J.; Sumida, K.; Kitagawa, S.; Furukawa, S.; Doonan, C. J.; Sumbly, C. J., Particle size effects in the kinetic trapping of a structurally-locked form of a flexible MOF. *CrystEngComm* 2016, 18, 4172-4179.
176. Shivanna, M.; Yang, Q.-Y.; Bajpai, A.; Sen, S.; Hosono, N.; Kusaka, S.; Pham, T.; Forrest, K. A.; Space, B.; Kitagawa, S.; Zatorotko, M. J., Readily accessible shape-memory effect in a porous interpenetrated coordination network. *Sci. Adv.* 2018, 4, eaq1636.
177. Hermansdörfer, J.; Friedrich, M.; Kempe, R., Colloidal Size Effect and Metal-Particle Migration in M@MOF/PCP Catalysis. *Chem. Eur. J.* 2013, 19, 13652-13657.
178. Li, P.; Moon, S.-Y.; Guelta, M. A.; Lin, L.; Gómez-Gualdrón, D. A.; Snurr, R. Q.; Harvey, S. P.; Hupp, J. T.; Farha, O. K., Nanosizing a Metal-Organic Framework Enzyme Carrier for Accelerating Nerve Agent Hydrolysis. *ACS Nano* 2016, 10, 9174-9182.
179. Li, P.; Klet, R. C.; Moon, S.-Y.; Wang, T. C.; Deria, P.; Peters, A. W.; Klahr, B. M.; Park, H.-J.; Al-Juaid, S. S.; Hupp, J. T.; Farha, O. K., Synthesis of nanocrystals of Zr-based metal-organic frameworks with csq-net: significant enhancement in the degradation of a nerve agent simulant. *Chem. Commun.* 2015, 51, 10925-10928.
180. Liu, Y.; Moon, S.-Y.; Hupp, J. T.; Farha, O. K., Dual-Function Metal-Organic Framework as a Versatile Catalyst for Detoxifying Chemical Warfare Agent Simulants. *ACS Nano* 2015, 9, 12358-12364.
181. Yang, J.; Yang, Y.-W., Metal-Organic Frameworks for Biomedical Applications. *Small* 2020, 16, 1906846.
182. Horcajada, P.; Gref, R.; Baati, T.; Allan, P. K.; Maurin, G.; Couvreur, P.; Férey, G.; Morris, R. E.; Serre, C., Metal-Organic Frameworks in Biomedicine. *Chem. Rev.* 2012, 112, 1232-1268.
183. Simon-Yarza, T.; Mielcarek, A.; Couvreur, P.; Serre, C., Nanoparticles of Metal-Organic Frameworks: On the Road to In Vivo Efficacy in Biomedicine. *Advanced Materials* 2018, 30, 1707365.
184. Marshall, C. R.; Staudhammer, S. A.; Brozek, C. K., Size control over metal-organic framework porous nanocrystals. *Chem. Sci.* 2019, 10, 9396-9408.
185. Lian, X.; Chen, Y.-P.; Liu, T.-F.; Zhou, H.-C., Coupling two enzymes into a tandem nanoreactor utilizing a hierarchically structured MOF. *Chem. Sci.* 2016, 7, 6969-6973.
186. Lian, X.; Erazo-Oliveras, A.; Pellois, J.-P.; Zhou, H.-C., High efficiency and long-term intracellular activity of an enzymatic nanofactory based on metal-organic frameworks. *Nat. Commun.* 2017, 8, 2075.
187. Lian, X.; Huang, Y.; Zhu, Y.; Fang, Y.; Zhao, R.; Joseph, E.; Li, J.; Pellois, J.-P.; Zhou, H.-C., Enzyme-MOF Nanoreactor Activates Nontoxic Paracetamol for Cancer Therapy. *Angew. Chem., Int. Ed.* 2018, 57, 5725-5730.

188. Lian, X.; Huang, Y.; Zhu, Y.; Fang, Y.; Zhao, R.; Joseph, E.; Li, J.; Pellois, J.-P.; Zhou, H.-C., Enzyme-MOF Nanoreactor Activates Nontoxic Paracetamol for Cancer Therapy. *Angew. Chem. Int. Ed.* 2018, 57, 5725-5730.
189. Gkaniatsou, E.; Sicard, C.; Ricoux, R.; Benahmed, L.; Bourdreux, F.; Zhang, Q.; Serre, C.; Mahy, J.-P.; Steunou, N., Enzyme Encapsulation in Mesoporous Metal–Organic Frameworks for Selective Biodegradation of Harmful Dye Molecules. *Angew. Chem., Int. Ed.* 2018, 57, 16141-16146.
190. McGuire, C. V.; Forgan, R. S., The surface chemistry of metal–organic frameworks. *Chem. Commun.* 2015, 51, 5199-5217.
191. Yin, Z.; Wan, S.; Yang, J.; Kurmoo, M.; Zeng, M.-H., Recent advances in post-synthetic modification of metal–organic frameworks: New types and tandem reactions. *Coord. Chem. Rev.* 2019, 378, 500-512.
192. Chen, Y.; Han, S.; Li, X.; Zhang, Z.; Ma, S., Why Does Enzyme Not Leach from Metal–Organic Frameworks (MOFs)? Unveiling the Interactions between an Enzyme Molecule and a MOF. *Inorg. Chem.* 2014, 53, 10006-10008.
193. Feng, D.; Liu, T.-F.; Su, J.; Bosch, M.; Wei, Z.; Wan, W.; Yuan, D.; Chen, Y.-P.; Wang, X.; Wang, K.; Lian, X.; Gu, Z.-Y.; Park, J.; Zou, X.; Zhou, H.-C., Stable metal-organic frameworks containing single-molecule traps for enzyme encapsulation. *Nat. Commun.* 2015, 6, 5979.
194. Gong, C.; Shen, Y.; Chen, J.; Song, Y.; Chen, S.; Song, Y.; Wang, L., Microperoxidase-11@PCN-333 (Al)/three-dimensional macroporous carbon electrode for sensing hydrogen peroxide. *Sens. Actuators B Chem.* 2017, 239, 890-897.
195. Chen, Y.; Li, P.; Modica, J. A.; Drout, R. J.; Farha, O. K., Acid-Resistant Mesoporous Metal–Organic Framework toward Oral Insulin Delivery: Protein Encapsulation, Protection, and Release. *J. Am. Chem. Soc.* 2018, 140, 5678-5681.
196. Chen, Y.; Li, P.; Noh, H.; Kung, C.-W.; Buru, C. T.; Wang, X.; Zhang, X.; Farha, O. K., Stabilization of Formate Dehydrogenase in a Metal–Organic Framework for Bioelectrocatalytic Reduction of CO₂. *Angew. Chem., Int. Ed.* 2019, 58, 7682-7686.
197. Lian, X.; Fang, Y.; Joseph, E.; Wang, Q.; Li, J.; Banerjee, S.; Lollar, C.; Wang, X.; Zhou, H.-C., Enzyme–MOF (metal–organic framework) composites. *Chem. Soc. Rev.* 2017, 46, 3386-3401.
198. Thörn, C.; Udatha, D. B. R. K. G.; Zhou, H.; Christakopoulos, P.; Topakas, E.; Olsson, L., Understanding the pH-dependent immobilization efficacy of feruloyl esterase-C on mesoporous silica and its structure–activity changes. *J. Mol. Catal. B Enzym.* 2013, 93, 65-72.
199. Secundo, F., Conformational changes of enzymes upon immobilisation. *Chem. Soc. Rev.* 2013, 42, 6250-6261.
200. Campbell, E. C.; Grant, J.; Wang, Y.; Sandhu, M.; Williams, R. J.; Nisbet, D. R.; Perriman, A. W.; Lupton, D. W.; Jackson, C. J., Hydrogel-Immobilized Supercharged Proteins. *Adv. Biosyst.* 2018, 2, 1700240.
201. Futami, J.; Kitazoe, M.; Murata, H.; Yamada, H., Exploiting protein cationization techniques in future drug development. *Expert Opin. Drug Discov.* 2007, 2, 261-269.
202. Chowdhury, R.; Stromer, B.; Pokharel, B.; Kumar, C. V., Control of Enzyme–Solid Interactions via Chemical Modification. *Langmuir* 2012, 28, 11881-11889.
203. Liu, W.-L.; Lo, S.-H.; Singco, B.; Yang, C.-C.; Huang, H.-Y.; Lin, C.-H., Novel trypsin–FITC@MOF bioreactor efficiently catalyzes protein digestion. *J. Mater. Chem. B* 2013, 1, 928-932.
204. Liu, W.-L.; Wu, C.-Y.; Chen, C.-Y.; Singco, B.; Lin, C.-H.; Huang, H.-Y., Fast Multipoint Immobilized MOF Bioreactor. *Chem. Eur. J.* 2014, 20, 8923-8928.
205. Liu, W.-L.; Yang, N.-S.; Chen, Y.-T.; Lirio, S.; Wu, C.-Y.; Lin, C.-H.; Huang, H.-Y., Lipase-Supported Metal–Organic Framework Bioreactor Catalyzes Warfarin Synthesis. *Chem. Eur. J.* 2015, 21, 115-119.
206. Zhang, D.; Zhu, Y.; Liu, L.; Ying, X.; Hsiung, C.-E.; Sougrat, R.; Li, K.; Han, Y., Atomic-resolution transmission electron microscopy of electron beam–sensitive crystalline materials. *Science* 2018, eaao0865.
207. Zhu, Y.; Ciston, J.; Zheng, B.; Miao, X.; Czarnik, C.; Pan, Y.; Sougrat, R.; Lai, Z.; Hsiung, C.-E.; Yao, K.; Pinnau, I.; Pan, M.; Han, Y., Unravelling surface and interfacial structures of a metal–organic framework by transmission electron microscopy. *Nat. Mater.* 2017, 16, 532-536.
208. Li, X.; Wang, J.; Liu, X.; Liu, L.; Cha, D.; Zheng, X.; Yousef, A. A.; Song, K.; Zhu, Y.; Zhang, D.; Han, Y., Direct Imaging of Tunable Crystal Surface Structures of MOF MIL-101 Using High-Resolution Electron Microscopy. *J. Am. Chem. Soc.* 2019, 141, 12021-12028.
209. Grall, R.; Hidalgo, T.; Delic, J.; Garcia-Marquez, A.; Chevillard, S.; Horcajada, P., In vitro biocompatibility of mesoporous metal (III; Fe, Al, Cr) trimesate MOF nanocarriers. *J. Mater. Chem. B* 2015, 3, 8279-8292.
210. Jian, M.; Liu, B.; Zhang, G.; Liu, R.; Zhang, X., Adsorptive removal of arsenic from aqueous solution by zeolitic imidazolate framework-8 (ZIF-8) nanoparticles. *Colloids Surf. A Physicochem. Eng. Asp.* 2015, 465, 67-76.
211. Islamoglu, T.; Goswami, S.; Li, Z.; Howarth, A. J.; Farha, O. K.; Hupp, J. T., Postsynthetic Tuning of Metal–Organic Frameworks for Targeted Applications. *Acc. Chem. Res.* 2017, 50, 805-813.
212. Tanabe, K. K.; Cohen, S. M., Postsynthetic modification of metal–organic frameworks—a progress report. *Chem. Soc. Rev.* 2011, 40, 498-519.
213. Hoarau, M.; Badieyan, S.; Marsh, E. N. G., Immobilized enzymes: understanding enzyme – surface interactions at the molecular level. *Org. Biomol. Chem.* 2017, 15, 9539-9551.
214. Hanefeld, U.; Gardossi, L.; Magner, E., Understanding enzyme immobilisation. *Chem. Soc. Rev.* 2009, 38, 453-468.
215. Chen, P.-C.; Huang, X.-J.; Xu, Z.-K., Activation and deformation of immobilized lipase on self-assembled monolayers with tailored wettability. *Phys. Chem. Chem. Phys.* 2015, 17, 13457-13465.
216. Hu, Y.; Dai, L.; Liu, D.; Du, W., Rationally designing hydrophobic UiO-66 support for the enhanced enzymatic performance of immobilized lipase. *Green Chem.* 2018, 20, 4500-4506.
217. Marshall, R. J.; Hobday, C. L.; Murphie, C. F.; Griffin, S. L.; Morrison, C. A.; Moggach, S. A.; Forgan, R. S., Amino acids as highly efficient modulators for single crystals of zirconium and hafnium metal–organic frameworks. *J. Mater. Chem. A* 2016, 4, 6955-6963.
218. Gutov, O. V.; Molina, S.; Escudero-Adán, E. C.; Shafir, A., Modulation by Amino Acids: Toward Superior Control in the Synthesis of Zirconium Metal–Organic Frameworks. *Chem. Eur. J.* 2016, 22, 13582-13587.
219. Mantion, A.; Massüger, L.; Rabu, P.; Palivan, C.; McCusker, L. B.; Taubert, A., Metal–Peptide Frameworks (MPFs): “Bioinspired” Metal Organic Frameworks. *J. Am. Chem. Soc.* 2008, 130, 2517-2526.
220. Long, P.; Zhao, Q.; Dong, J.; Li, J., Synthesis of metal-organic frameworks from the system metal/L-glutamic acid/TEA/H₂O. *J. Coord. Chem.* 2009, 62, 1959-1963.
221. Wang, S.; Wahiduzzaman, M.; Davis, L.; Tissot, A.; Shepard, W.; Marrot, J.; Martineau-Corcoss, C.; Hamdane, D.; Maurin, G.; Devautour-Vinot, S.; Serre, C., A robust zirconium amino acid metal-organic framework for proton conduction. *Nat. Commun.* 2018, 9, 4937.
222. Röder, R.; Preiß, T.; Hirschle, P.; Steinborn, B.; Zimpel, A.; Höhn, M.; Rädler, J. O.; Bein, T.; Wagner, E.; Wuttke, S.; Lächelt, U., Multifunctional Nanoparticles by Coordinative Self-Assembly of His-Tagged Units with Metal–Organic Frameworks. *J. Am. Chem. Soc.* 2017, 139, 2359-2368.
223. Gornall, A. G.; Bardawill, C. J.; David, M. M., DETERMINATION OF SERUM PROTEINS BY MEANS OF THE BIURET REACTION. *J. Biol. Chem.* 1949, 177, 751-766.
224. Bradford, M. M., A rapid and sensitive method for the quantitation of microgram quantities of protein utilizing the principle of protein-dye binding. *Anal. Chem.* 1976, 48, 248-254.
225. Jung, S.; Kim, Y.; Kim, S.-J.; Kwon, T.-H.; Huh, S.; Park, S., Bio-functionalization of metal–organic frameworks by covalent protein conjugation. *Chem. Commun.* 2011, 47, 2904-2906.

226. An, H.; Li, M.; Gao, J.; Zhang, Z.; Ma, S.; Chen, Y., Incorporation of biomolecules in Metal-Organic Frameworks for advanced applications. *Coord. Chem. Rev.* 2019, 384, 90-106.
227. Huang, S.; Kou, X.; Shen, J.; Chen, G.; Ouyang, G., "Armor-Plating" Enzymes with Metal-Organic Frameworks (MOFs). *Angew. Chem., Int. Ed.* 2020, Ahead of Print.
228. Hermanson, G. T., Chapter 3 - The Reactions of Bioconjugation. In *Bioconjugate Techniques (Third Edition)*, Hermanson, G. T., Ed. Academic Press: Boston, 2013; pp 229-258.
229. Avrameas, S., Coupling of enzymes to proteins with glutaraldehyde: Use of the conjugates for the detection of antigens and antibodies. *Immunochemistry* 1969, 6, 43-52.
230. Doherty, C. M.; Greci, G.; Riccò, R.; Mardel, J. I.; Reboul, J.; Furukawa, S.; Kitagawa, S.; Hill, A. J.; Falcaro, P., Combining UV Lithography and an Imprinting Technique for Patterning Metal-Organic Frameworks. *Adv. Mater.* 2013, 25, 4701-4705.
231. Cao, S.-L.; Yue, D.-M.; Li, X.-H.; Smith, T. J.; Li, N.; Zong, M.-H.; Wu, H.; Ma, Y.-Z.; Lou, W.-Y., Novel Nano/Micro-Biocatalyst: Soybean Epoxide Hydrolase Immobilized on UiO-66-NH₂ MOF for Efficient Biosynthesis of Enantiopure (R)-1, 2-Octanediol in Deep Eutectic Solvents. *ACS Sustain. Chem. Eng.* 2016, 4, 3586-3595.
232. Chen, W.-H.; Liao, W.-C.; Sohn, Y. S.; Fadeev, M.; Cecconello, A.; Nechushtai, R.; Willner, I., Stimuli-Responsive Nucleic Acid-Based Polyacrylamide Hydrogel-Coated Metal-Organic Framework Nanoparticles for Controlled Drug Release. *Adv. Funct. Mater.* 2018, 28, 1705137.
233. Morris, W.; Briley, W. E.; Auyeung, E.; Cabezas, M. D.; Mirkin, C. A., Nucleic Acid-Metal Organic Framework (MOF) Nanoparticle Conjugates. *J. Am. Chem. Soc.* 2014, 136, 7261-7264.
234. Abánades Lázaro, I.; Haddad, S.; Sacca, S.; Orellana-Tavra, C.; Fairen-Jimenez, D.; Forgan, R. S., Selective Surface PEGylation of UiO-66 Nanoparticles for Enhanced Stability, Cell Uptake, and pH-Responsive Drug Delivery. *Chem* 2017, 2, 561-578.
235. Chen, W.-H.; Yang Sung, S.; Fadeev, M.; Cecconello, A.; Nechushtai, R.; Willner, I., Targeted VEGF-triggered release of an anti-cancer drug from aptamer-functionalized metal-organic framework nanoparticles. *Nanoscale* 2018, 10, 4650-4657.
236. Cleland, W. W., Dithiothreitol, a New Protective Reagent for SH Groups*. *Biochemistry* 1964, 3, 480-482.
237. Koniev, O.; Wagner, A., Developments and recent advancements in the field of endogenous amino acid selective bond forming reactions for bioconjugation. *Chem. Soc. Rev.* 2015, 44, 5495-5551.
238. Yang, Y.; Chen, Q.; Wu, J.-P.; Kirk, T. B.; Xu, J.; Liu, Z.; Xue, W., Reduction-Responsive Codelivery System Based on a Metal-Organic Framework for Eliciting Potent Cellular Immune Response. *ACS Appl. Mater. Interfaces* 2018, 10, 12463-12473.
239. Koutsopoulos, S.; Patzsch, K.; Bosker, W. T. E.; Norde, W., Adsorption of Trypsin on Hydrophilic and Hydrophobic Surfaces. *Langmuir* 2007, 23, 2000-2006.
240. Koutsopoulos, S.; van der Oost, J.; Norde, W., Structural Features of a Hyperthermostable Endo- β -1,3-glucanase in Solution and Adsorbed on "Invisible" Particles. *Biophys. J.* 2005, 88, 467-474.
241. Sun, Q.; He, H.; Gao, W.-Y.; Aguila, B.; Wojtas, L.; Dai, Z.; Li, J.; Chen, Y.-S.; Xiao, F.-S.; Ma, S., Imparting amphiphobicity on single-crystalline porous materials. *Nat. Commun.* 2016, 7, 13300.
242. Liu, C.; Liu, Q.; Huang, A., A superhydrophobic zeolitic imidazolate framework (ZIF-90) with high steam stability for efficient recovery of bioalcohols. *Chem. Commun.* 2016, 52, 3400-3402.
243. Sun, Y.; Sun, Q.; Huang, H.; Aguila, B.; Niu, Z.; Perman, J. A.; Ma, S., A molecular-level superhydrophobic external surface to improve the stability of metal-organic frameworks. *J. Mater. Chem. A* 2017, 5, 18770-18776.
244. Rodríguez-Hermida, S.; Tsang, M. Y.; Vignatti, C.; Stylianou, K. C.; Guillerm, V.; Pérez-Carvajal, J.; Teixidor, F.; Viñas, C.; Choquesillo-Lazarte, D.; Verdugo-Escamilla, C.; Peral, I.; Juanhuix, J.; Verdager, A.; Imaz, I.; MasPOCH, D.; Giner Planas, J., Switchable Surface Hydrophobicity-Hydrophilicity of a Metal-Organic Framework. *Angew. Chem., Int. Ed.* 2016, 128, 16283-16287.
245. Gauthier, M. A.; Klok, H.-A., Polymer-protein conjugates: an enzymatic activity perspective. *Polym. Chem.* 2010, 1, 1352-1373.
246. Virgen-Ortíz, J. J.; dos Santos, J. C. S.; Berenguer-Murcia, Á.; Barbosa, O.; Rodrigues, R. C.; Fernandez-Lafuente, R., Polyethyleneimine: a very useful ionic polymer in the design of immobilized enzyme biocatalysts. *J. Mater. Chem. B* 2017, 5, 7461-7490.
247. Zimpel, A.; Al Danaf, N.; Steinborn, B.; Kuhn, J.; Höhn, M.; Bauer, T.; Hirschle, P.; Schrimpf, W.; Engelke, H.; Wagner, E.; Barz, M.; Lamb, D. C.; Lächelt, U.; Wuttke, S., Coordinative Binding of Polymers to Metal-Organic Framework Nanoparticles for Control of Interactions at the Biointerface. *ACS Nano* 2019, 13, 3884-3895.
248. Brzozowski, A. M.; Derewenda, U.; Derewenda, Z. S.; Dodson, G. G.; Lawson, D. M.; Turkenburg, J. P.; Bjorkling, F.; Huge-Jensen, B.; Patkar, S. A.; Thim, L., A model for interfacial activation in lipases from the structure of a fungal lipase-inhibitor complex. *Nature* 1991, 351, 491-494.
249. Verger, R., 'Interfacial activation' of lipases: facts and artifacts. *Trends Biotechnol.* 1997, 15, 32-38.
250. Schmid, R. D.; Verger, R., Lipases: Interfacial Enzymes with Attractive Applications. *Angew. Chem., Int. Ed.* 1998, 37, 1608-1633.
251. Che, C.-M.; Siu, F.-M., Metal complexes in medicine with a focus on enzyme inhibition. *Curr. Opin. Chem. Biol.* 2010, 14, 255-261.
252. Kilpin, K. J.; Dyson, P. J., Enzyme inhibition by metal complexes: concepts, strategies and applications. *Chem. Sci.* 2013, 4, 1410-1419.
253. Xu, M.; Yuan, S.; Chen, X.-Y.; Chang, Y.-J.; Day, G.; Gu, Z.-Y.; Zhou, H.-C., Two-Dimensional Metal-Organic Framework Nanosheets as an Enzyme Inhibitor: Modulation of the α -Chymotrypsin Activity. *J. Am. Chem. Soc.* 2017, 139, 8312-8319.
254. Xie, Y.; Zhou, J.; Jiang, S., Parallel tempering Monte Carlo simulations of lysozyme orientation on charged surfaces. *J. Chem. Phys.* 2010, 132, 065101.
255. Talasaz, A. H.; Nemat-Gorgani, M.; Liu, Y.; Stähl, P.; Dutton, R. W.; Ronaghi, M.; Davis, R. W., Prediction of protein orientation upon immobilization on biological and nonbiological surfaces. *Proc. Natl. Acad. Sci.* 2006, 103, 14773-14778.
256. Utesch, T.; Sezer, M.; Weidinger, I. M.; Mroginski, M. A., Adsorption of Sulfite Oxidase on Self-Assembled Monolayers from Molecular Dynamics Simulations. *Langmuir* 2012, 28, 5761-5769.
257. Vertegel, A. A.; Siegel, R. W.; Dordick, J. S., Silica Nanoparticle Size Influences the Structure and Enzymatic Activity of Adsorbed Lysozyme. *Langmuir* 2004, 20, 6800-6807.
258. Wang, S.; McGuirk, C. M.; d'Aquino, A.; Mason, J. A.; Mirkin, C. A., Metal-Organic Framework Nanoparticles. *Adv. Mater.* 2018, 30, 1800202.
259. Wang, X.-G.; Cheng, Q.; Yu, Y.; Zhang, X.-Z., Controlled Nucleation and Controlled Growth for Size Predictable Synthesis of Nanoscale Metal-Organic Frameworks (MOFs): A General and Scalable Approach. *Angew. Chem., Int. Ed.* 2018, 57, 7836-7840.
260. Zhao, Y.; Zhang, Q.; Li, Y.; Zhang, R.; Lu, G., Large-Scale Synthesis of Monodisperse UiO-66 Crystals with Tunable Sizes and Missing Linker Defects via Acid/Base Co-Modulation. *ACS Appl. Mater. Interfaces* 2017, 9, 15079-15085.
261. Zhao, M.; Zhang, X.; Deng, C., Rational synthesis of novel recyclable Fe₃O₄@MOF nanocomposites for enzymatic digestion. *Chem. Commun.* 2015, 51, 8116-8119.
262. Ma, W.; Jiang, Q.; Yu, P.; Yang, L.; Mao, L., Zeolitic Imidazolate Framework-Based Electrochemical Biosensor for in Vivo Electrochemical Measurements. *Anal. Chem.* 2013, 85, 7550-7557.
263. Qin, F.-X.; Jia, S.-Y.; Wang, F.-F.; Wu, S.-H.; Song, J.; Liu, Y., Hemin@metal-organic framework with peroxidase-like activity and its application to glucose detection. *Catal. Sci.* 2013, 3, 2761-2768.
264. Ling, P.; Qian, C.; Gao, F.; Lei, J., Enzyme-immobilized metal-organic framework nanosheets as tandem catalysts for the generation of nitric oxide. *Chem. Commun.* 2018, 54, 11176-11179.
265. Ren, S.; Feng, Y.; Wen, H.; Li, C.; Sun, B.; Cui, J.; Jia, S., Immobilized carbonic anhydrase on mesoporous cruciate flower-like metal organic framework for promoting CO₂ sequestration. *Int. J. Biol. Macromol.* 2018, 117, 189-198.

266. Gascón, V.; Jiménez, M. B.; Blanco, R. M.; Sanchez-Sanchez, M., Semi-crystalline Fe-BTC MOF material as an efficient support for enzyme immobilization. *Catal. Today* 2018, 304, 119-126.
267. Patra, S.; Hidalgo Crespo, T.; Permyakova, A.; Sicard, C.; Serre, C.; Chaussé, A.; Steunou, N.; Legrand, L., Design of metal-organic framework-enzyme based bioelectrodes as a novel and highly sensitive biosensing platform. *J. Mater. Chem. B* 2015, 3, 8983-8992.
268. Pang, S.; Wu, Y.; Zhang, X.; Li, B.; Ouyang, J.; Ding, M., Immobilization of laccase via adsorption onto bimodal mesoporous Zr-MOF. *Process Biochem.* 2016, 51, 229-239.
269. Wang, X.; Lu, X.; Wu, L.; Chen, J., 3D metal-organic framework as highly efficient biosensing platform for ultrasensitive and rapid detection of bisphenol A. *Biosens. Bioelectron.* 2015, 65, 295-301.
270. Lu, X.; Wang, X.; Wu, L.; Wu, L.; Dhanjai; Fu, L.; Gao, Y.; Chen, J., Response Characteristics of Bisphenols on a Metal-Organic Framework-Based Tyrosinase Nanosensor. *ACS Appl. Mater. Interfaces* 2016, 8, 16533-16539.
271. Patra, S.; Sene, S.; Mousty, C.; Serre, C.; Chaussé, A.; Legrand, L.; Steunou, N., Design of Laccase-Metal Organic Framework-Based Bioelectrodes for Biocatalytic Oxygen Reduction Reaction. *ACS Appl. Mater. Interfaces* 2016, 8, 20012-20022.
272. Niu, H.; Ding, M.; Sun, X.; Zhuang, W.; Liu, D.; Ying, H.; Zhu, C.; Chen, Y., Immobilization of a polyphosphate kinase 2 by coordinative self-assembly of his-tagged units with metal-organic frameworks and its application in ATP regeneration from AMP. *Colloids Surf. B Biointerfaces* 2019, 181, 261-269.
273. Tan, W.; Wei, T.; Huo, J.; Loubidi, M.; Liu, T.; Liang, Y.; Deng, L., Electrostatic Interaction-Induced Formation of Enzyme-on-MOF as Chemo-Biocatalyst for Cascade Reaction with Unexpectedly Acid-Stable Catalytic Performance. *ACS Appl. Mater. Interfaces* 2019, 11, 36782-36788.
274. Hassabo, A. A.; Mousa, A. M.; Abdel-Gawad, H.; Selim, M. H.; Abdelhameed, R. M., Immobilization of l-methioninase on a zirconium-based metal-organic framework as an anticancer agent. *J. Mater. Chem. B* 2019, 7, 3268-3278.
275. Zhou, M.; Ju, X.; Zhou, Z.; Yan, L.; Chen, J.; Yao, X.; Xu, X.; Li, L.-Z., Development of an Immobilized Cellulase System Based on Metal-Organic Frameworks for Improving Ionic Liquid Tolerance and In Situ Saccharification of Bagasse. *ACS Sustain. Chem. Eng.* 2019.
276. Li, Y.; Liu, J.; Zhang, K.; Lei, L.; Lei, Z., UiO-66-NH₂@PMAA: A Hybrid Polymer-MOFs Architecture for Pectinase Immobilization. *Ind. Eng. Chem. Res.* 2018, 57, 559-567.
277. Zhong, X.; Xia, H.; Huang, W.; Li, Z.; Jiang, Y., Biomimetic metal-organic frameworks mediated hybrid multi-enzyme mimic for tandem catalysis. *Chem. Eng. J.* 2020, 381, 122758.
278. Wang, Y.; Zhang, N.; Zhang, E.; Han, Y.; Qi, Z.; Ansorge-Schumacher, M. B.; Ge, Y.; Wu, C., Heterogeneous Metal-Organic-Framework-Based Biohybrid Catalysts for Cascade Reactions in Organic Solvent. *Chem. Eur. J.* 2019, 25, 1716-1721.
279. Wen, L.; Gao, A.; Cao, Y.; Svec, F.; Tan, T.; Lv, Y., Layer-by-Layer Assembly of Metal-Organic Frameworks in Macroporous Polymer Monolith and Their Use for Enzyme Immobilization. *Macromol. Rapid Commun.* 2016, 37, 551-557.
280. Wang, W.; Wang, L.; Huang, Y.; Xie, Z.; Jing, X., Nanoscale Metal-Organic Framework-Hemoglobin Conjugates. *Chem. Asian J.* 2016, 11, 750-756.
281. Tudisco, C.; Zolubas, G.; Seoane, B.; Zafarani, H. R.; Kazemzad, M.; Gascon, J.; Hagedoorn, P. L.; Rassaei, L., Covalent immobilization of glucose oxidase on amino MOFs via post-synthetic modification. *RSC Adv.* 2016, 6, 108051-108055.
282. Xia, G.-H.; Cao, S.-L.; Xu, P.; Li, X.-H.; Zhou, J.; Zong, M.-H.; Lou, W.-Y., Preparation of a Nanobiocatalyst by Efficiently Immobilizing *Aspergillus niger* Lipase onto Magnetic Metal-Biomolecule Frameworks (BioMOF). *ChemCatChem* 2017, 9, 1794-1800.
283. Jung, S.; Park, S., Dual-Surface Functionalization of Metal-Organic Frameworks for Enhancing the Catalytic Activity of *Candida antarctica* Lipase B in Polar Organic Media. *ACS Catal.* 2017, 7, 438-442.
284. Shih, Y.-H.; Lo, S.-H.; Yang, N.-S.; Singco, B.; Cheng, Y.-J.; Wu, C.-Y.; Chang, I.-H.; Huang, H.-Y.; Lin, C.-H., Trypsin-Immobilized Metal-Organic Framework as a Biocatalyst In Proteomics Analysis. *ChemPlusChem* 2012, 77, 982-986.
285. Wang, Q.; Astruc, D., State of the Art and Prospects in Metal-Organic Framework (MOF)-Based and MOF-Derived Nanocatalysis. *Chem. Rev.* 2020, 120, 1438-1511.
286. Bradshaw, D.; Garai, A.; Huo, J., Metal-organic framework growth at functional interfaces: thin films and composites for diverse applications. *Chem. Soc. Rev.* 2012, 41, 2344-2381.
287. Falcaro, P.; Ricco, R.; Yazdi, A.; Imaz, I.; Furukawa, S.; Maspoeh, D.; Ameloot, R.; Evans, J. D.; Doonan, C. J., Application of metal and metal oxide nanoparticles@MOFs. *Coord. Chem. Rev.* 2016, 307, 237-254.
288. Quax, W. J.; Mrabet, N. T.; Luiten, R. G. M.; Schuurhuizen, P. W.; Stanssens, P.; Lasters, I., Enhancing the Thermostability of Glucose Isomerase by Protein Engineering. 1991; Vol. 9, p 738-742.
289. Ricco, R.; Malfatti, L.; Takahashi, M.; Hill, A. J.; Falcaro, P., Applications of magnetic metal-organic framework composites. *J. Mater. Chem. A* 2013, 1, 13033-13045.
290. Wang, C.; Liu, X.; Keser Demir, N.; Chen, J. P.; Li, K., Applications of water stable metal-organic frameworks. *Chem. Soc. Rev.* 2016, 45, 5107-5134.
291. Ricco, R.; Wied, P.; Nidetzky, B.; Amenitsch, H.; Falcaro, P., Magnetically responsive horseradish peroxidase@ZIF-8 for biocatalysis. *Chem. Commun.* 2020.
292. Du, Y.; Gao, J.; Liu, H.; Zhou, L.; Ma, L.; He, Y.; Huang, Z.; Jiang, Y., Enzyme@silica nanoflower@metal-organic framework hybrids: A novel type of integrated nanobiocatalysts with improved stability. *Nano Res.* 2018, 11, 4380-4389.
293. Zhang, S.; Shi, J.; Zhang, Y.; Wu, Y.; Chen, Y.; Messersmith, P. B.; Jiang, Z., Polymer@MOFs capsules prepared through controlled interfacial mineralization for switching on/off enzymatic reactions. *Appl. Mater. Today* 2018, 13, 320-328.
294. Li, X.; Li, D.; Zhang, Y.; Lv, P.; Feng, Q.; Wei, Q., Encapsulation of enzyme by metal-organic framework for single-enzymatic biofuel cell-based self-powered biosensor. *Nano Energy* 2020, 68, 104308.
295. Wu, X.; Yang, C.; Ge, J.; Liu, Z., Polydopamine tethered enzyme/metal-organic framework composites with high stability and reusability. *Nanoscale* 2015, 7, 18883-18886.
296. Zhang, X.; Zeng, Y.; Zheng, A.; Cai, Z.; Huang, A.; Zeng, J.; Liu, X.; Liu, J., A fluorescence based immunoassay for galectin-4 using gold nanoclusters and a composite consisting of glucose oxidase and a metal-organic framework. *Microchim. Acta* 2017, 184, 1933-1940.
297. Wang, Q.; Zhang, X.; Huang, L.; Zhang, Z.; Dong, S., GOx@ZIF-8(NiPd) Nanoflower: An Artificial Enzyme System for Tandem Catalysis. *Angew. Chem., Int. Ed.* 2017, 56, 16082-16085.
298. Jimenez-Falcao, S.; de Luis, B.; García-Fernández, A.; Llopis-Lorente, A.; Diez, P.; Sánchez, A.; Sancenón, F.; Martínez-Ruiz, P.; Martínez-Mañez, R.; Villalonga, R., Glucose-Responsive Enzyme-Controlled Mesoporous Nanomachine with a Layer-by-Layer Supramolecular Architecture. *ACS Appl. Bio Mater.* 2019, 2, 3321-3328.
299. Ma, Y.; Liu, H.; Wu, J.; Yuan, L.; Wang, Y.; Du, X.; Wang, R.; Marwa, P. W.; Petlulu, P.; Chen, X.; Zhang, H., The adverse health effects of bisphenol A and related toxicity mechanisms. *Environ. Res.* 2019, 176, 108575.
300. Han, C.; Verploegh, R. J.; Sholl, D. S., Assessing the Impact of Point Defects on Molecular Diffusion in ZIF-8 Using Molecular Simulations. *J. Phys. Chem. Lett.* 2018, 9, 4037-4044.
301. Peng, F.; Yin, H.; Cao, S.-L.; Lou, W.-Y., Chapter 6 - Enzyme Nanocarriers. In *Advances in Enzyme Technology*, Singh, R. S.; Singhania, R. R.; Pandey, A.; Larroche, C., Eds. Elsevier: 2019; pp 153-168.
302. Falcaro, P.; Normandin, F.; Takahashi, M.; Scopece, P.; Amenitsch, H.; Costacurta, S.; Doherty, C. M.; Laird, J. S.; Lay, M. D. H.; Lisi, F.; Hill, A. J.; Buso, D., Dynamic Control of MOF-5 Crystal Positioning Using a Magnetic Field. *Adv. Mater.* 2011, 23, 3901-3906.
303. Schejñ, A.; Mazet, T.; Falk, V.; Balan, L.; Aranda, L.; Medjahdi, G.; Schneider, R., Fe₃O₄@ZIF-8: magnetically recoverable

- catalysts by loading Fe₃O₄ nanoparticles inside a zinc imidazolate framework. *Dalton Trans.* 2015, 44, 10136-10140.
304. Doherty, C. M.; Knystautas, E.; Buso, D.; Villanova, L.; Konstas, K.; Hill, A. J.; Takahashi, M.; Falcaro, P., Magnetic framework composites for polycyclic aromatic hydrocarbon sequestration. *J. Mater. Chem.* 2012, 22, 11470-11474.
305. Ke, F.; Yuan, Y.-P.; Qiu, L.-G.; Shen, Y.-H.; Xie, A.-J.; Zhu, J.-F.; Tian, X.-Y.; Zhang, L.-D., Facile fabrication of magnetic metal-organic framework nanocomposites for potential targeted drug delivery. *J. Mater. Chem.* 2011, 21, 3843-3848.
306. Zhuang, J.; Kuo, C.-H.; Chou, L.-Y.; Liu, D.-Y.; Weerapana, E.; Tsung, C.-K., Optimized Metal-Organic-Framework Nanospheres for Drug Delivery: Evaluation of Small-Molecule Encapsulation. *ACS Nano* 2014, 8, 2812-2819.
307. Samui, A.; Chowdhuri, A. R.; Mahto, T. K.; Sahu, S. K., Fabrication of a magnetic nanoparticle embedded NH₂-MIL-88B MOF hybrid for highly efficient covalent immobilization of lipase. *RSC Adv.* 2016, 6, 66385-66393.
308. Lin, C.; Xu, K.; Zheng, R.; Zheng, Y., Immobilization of amidase into a magnetic hierarchically porous metal-organic framework for efficient biocatalysis. *Chem. Commun.* 2019, 55, 5697-5700.
309. Hou, C.; Wang, Y.; Ding, Q.; Jiang, L.; Li, M.; Zhu, W.; Pan, D.; Zhu, H.; Liu, M., Facile synthesis of enzyme-embedded magnetic metal-organic frameworks as a reusable mimic multi-enzyme system: mimetic peroxidase properties and colorimetric sensor. *Nanoscale* 2015, 7, 18770-18779.
310. Cao, S.-L.; Xu, H.; Lai, L.-H.; Gu, W.-M.; Xu, P.; Xiong, J.; Yin, H.; Li, X.-H.; Ma, Y.-Z.; Zhou, J.; Zong, M.-H.; Lou, W.-Y., Magnetic ZIF-8/cellulose/Fe₃O₄ nanocomposite: preparation, characterization, and enzyme immobilization. *Bioresour. Bioprocess.* 2017, 4, 56.
311. Chen, S.; Wen, L.; Svec, F.; Tan, T.; Lv, Y., Magnetic metal-organic frameworks as scaffolds for spatial co-location and positional assembly of multi-enzyme systems enabling enhanced cascade biocatalysis. *RSC Adv.* 2017, 7, 21205-21213.
312. Jamshaid, T.; Neto, E. T. T.; Eissa, M. M.; Zine, N.; Kunita, M. H.; El-Salhi, A. E.; Elaissari, A., Magnetic particles: From preparation to lab-on-a-chip, biosensors, microsystems and microfluidics applications. *Trends Analyt. Chem.* 2016, 79, 344-362.
313. Hejazian, M.; Li, W.; Nguyen, N.-T., Lab on a chip for continuous-flow magnetic cell separation. *Lab Chip* 2015, 15, 959-970.
314. Sun, J.; Zhou, S.; Hou, P.; Yang, Y.; Weng, J.; Li, X.; Li, M., Synthesis and characterization of biocompatible Fe₃O₄ nanoparticles. *J. Biomed. Mater. Res. A* 2007, 80A, 333-341.
315. Mehta, J.; Bhardwaj, N.; Bhardwaj, S. K.; Kim, K.-H.; Deep, A., Recent advances in enzyme immobilization techniques: Metal-organic frameworks as novel substrates. *Coord. Chem. Rev.* 2016, 322, 30-40.
316. Zhai, R.; Yuan, Y.; Jiao, F.; Hao, F.; Fang, X.; Zhang, Y.; Qian, X., Facile synthesis of magnetic metal organic frameworks for highly efficient proteolytic digestion used in mass spectrometry-based proteomics. *Anal. Chim. Acta* 2017, 994, 19-28.
317. Zhai, R.; Yuan, Y.; Jiao, F.; Hao, F.; Fang, X.; Zhang, Y.; Qian, X., Facile synthesis of magnetic metal organic frameworks for highly efficient proteolytic digestion used in mass spectrometry-based proteomics. *Anal. Chim. Acta* 2017, 994, 19-28.
318. Ricco, R.; Wied, P.; Nidetzky, B.; Amenitsch, H.; Falcaro, P., Magnetically responsive horseradish peroxidase@ZIF-8 for biocatalysis. *Chem. Commun.* 2020, 56, 5775-5778.
319. Khan, N. A.; Hasan, Z.; Jhung, S. H., Beyond pristine metal-organic frameworks: Preparation and application of nanostructured, nanosized, and analogous MOFs. *Coord. Chem. Rev.* 2018, 376, 20-45.
320. Cai, L.; Chen, L.; Zhang, L.; Lu, G.; He, X.; Zhang, S.; Sun, H.; Liu, Z.; Zhao, B., Recyclable, Biocompatible, Magnetic Titanium Dioxide Nanoparticles with Immobilized Enzymes for Biocatalysis. *ChemPlusChem* 2013, 78, 1437-1439.
321. Huang, C.; Bai, H.; Li, C.; Shi, G., A graphene oxide/hemoglobin composite hydrogel for enzymatic catalysis in organic solvents. *Chem. Commun.* 2011, 47, 4962-4964.
322. Ivnitski, D.; Artyushkova, K.; Rincón, R. A.; Atanassov, P.; Luckarift, H. R.; Johnson, G. R., Entrapment of Enzymes and Carbon Nanotubes in Biologically Synthesized Silica: Glucose Oxidase-Catalyzed Direct Electron Transfer. *Small* 2008, 4, 357-364.
323. Betancor, L.; Luckarift, H. R., Bioinspired enzyme encapsulation for biocatalysis. *Trends Biotechnol.* 2008, 26, 566-572.
324. Qiu, Z.; Shu, J.; Tang, D., Bioresponsive Release System for Visual Fluorescence Detection of Carcinoembryonic Antigen from Mesoporous Silica Nanocontainers Mediated Optical Color on Quantum Dot-Enzyme-Impregnated Paper. *Anal. Chem.* 2017, 89, 5152-5160.
325. Bai, Y.; Yang, H.; Yang, W.; Li, Y.; Sun, C., Gold nanoparticles-mesoporous silica composite used as an enzyme immobilization matrix for amperometric glucose biosensor construction. *Sens. Actuators B Chem.* 2007, 124, 179-186.
326. Yu, J.; Yu, D.; Zhao, T.; Zeng, B., Development of amperometric glucose biosensor through immobilizing enzyme in a Pt nanoparticles/mesoporous carbon matrix. *Talanta* 2008, 74, 1586-1591.
327. Ispas, C. R.; Crivat, G.; Andrescu, S., Review: Recent Developments in Enzyme-Based Biosensors for Biomedical Analysis. *Anal. Lett.* 2012, 45, 168-186.
328. Croissant, J. G.; Fatieiev, Y.; Almalik, A.; Khashab, N. M., Mesoporous Silica and Organosilica Nanoparticles: Physical Chemistry, Biosafety, Delivery Strategies, and Biomedical Applications. *Adv. Funct. Mater.* 2018, 7, 1700831.
329. Maji, S. K.; Mandal, A. K.; Nguyen, K. T.; Borah, P.; Zhao, Y., Cancer Cell Detection and Therapeutics Using Peroxidase-Active Nanohybrid of Gold Nanoparticle-Loaded Mesoporous Silica-Coated Graphene. *ACS Appl. Mater. Interfaces* 2015, 7, 9807-9816.
330. Hu, Y.; Catchmark, J. M., In vitro biodegradability and mechanical properties of bioabsorbable bacterial cellulose incorporating cellulases. *Acta Biomater.* 2011, 7, 2835-2845.
331. Wang, F.-T.; Wang, Y.-H.; Xu, J.; Huang, K.-J.; Liu, Z.-h.; Lu, Y.-f.; Wang, S.-y.; Han, Z.-w., Boosting performance of self-powered biosensing device with high-energy enzyme biofuel cells and cruciform DNA. *Nano Energy* 2020, 68, 104310.
332. Moreira, A. B. R.; Perez, V. H.; Zanin, G. M.; de Castro, H. F., Biodiesel Synthesis by Enzymatic Transesterification of Palm Oil with Ethanol Using Lipases from Several Sources Immobilized on Silica-PVA Composite. *Energy Fuels* 2007, 21, 3689-3694.
333. Llopis-Lorente, A.; García-Fernández, A.; Lucena-Sánchez, E.; Díez, P.; Sancenón, F.; Villalonga, R.; Wilson, D. A.; Martínez-Mañez, R., Stimulus-responsive nanomotors based on gated enzyme-powered Janus Au-mesoporous silica nanoparticles for enhanced cargo delivery. *Chem. Commun.* 2019, 55, 13164-13167.
334. Muschiol, J.; Peters, C.; Oberleitner, N.; Mihovilovic, M. D.; Bornscheuer, U. T.; Rudroff, F., Cascade catalysis – strategies and challenges en route to preparative synthetic biology. *Chem. Commun.* 2015, 51, 5798-5811.
335. Lohr, T. L.; Marks, T. J., Orthogonal tandem catalysis. *Nat. Chem.* 2015, 7, 477-482.
336. Huang, Y.-B.; Liang, J.; Wang, X.-S.; Cao, R., Multifunctional metal-organic framework catalysts: synergistic catalysis and tandem reactions. *Chem. Soc. Rev.* 2017, 46, 126-157.
337. Chen, Y.; Li, P.; Noh, H.; Kung, C.-W.; Buru, C. T.; Wang, X.; Zhang, X.; Farha, O. K., Stabilization of Formate Dehydrogenase in a Metal-Organic Framework for Bioelectrocatalytic Reduction of CO₂. *Angew. Chem. Int. Ed.* 2019, 58, 7682-7686.
338. Bilal, M.; Adeel, M.; Rasheed, T.; Iqbal, H. M. N., Multifunctional metal-organic frameworks-based biocatalytic platforms: recent developments and future prospects. *J. Mater. Res. Technol.* 2019, 8, 2359-2371.
339. Cui, J.; Ren, S.; Sun, B.; Jia, S., Optimization protocols and improved strategies for metal-organic frameworks for immobilizing enzymes: Current development and future challenges. *Coord. Chem. Rev.* 2018, 370, 22-41.
340. Nadar, S. S.; Rathod, V. K., Magnetic-metal organic framework (magnetic-MOF): A novel platform for enzyme immobilization and nanozyme applications. *Int. J. Biol. Macromol.* 2018, 120, 2293-2302.

341. Liang, S.; Wu, X.-L.; Xiong, J.; Zong, M.-H.; Lou, W.-Y., Metal-organic frameworks as novel matrices for efficient enzyme immobilization: An update review. *Coord. Chem. Rev.* 2020, 406, 213149.
342. Nadar, S. S.; Vaidya, L.; Rathod, V. K., Enzyme embedded metal organic framework (enzyme-MOF): De novo approaches for immobilization. *Int. J. Biol. Macromol.* 2020, 149, 861-876.
343. Wu, X.; Yang, C.; Ge, J., Green synthesis of enzyme/metal-organic framework composites with high stability in protein denaturing solvents. *Bioresour. Bioprocess.* 2017, 4, 24.
344. Nadar, S. S.; Rathod, V. K., Facile synthesis of glucoamylase embedded metal-organic frameworks (glucoamylase-MOF) with enhanced stability. *Int. J. Biol. Macromol.* 2017, 95, 511-519.
345. Wang, L.; Zhi, W.; Lian, D.; Wang, Y.; Han, J.; Wang, Y., HRP@ZIF-8/DNA Hybrids: Functionality Integration of ZIF-8 via Biomineralization and Surface Absorption. *ACS Sustain. Chem. Eng.* 2019, 7, 14611-14620.
346. Majewski, M. B.; Howarth, A. J.; Li, P.; Wasielewski, M. R.; Hupp, J. T.; Farha, O. K., Enzyme encapsulation in metal-organic frameworks for applications in catalysis. *CrystEngComm* 2017, 19, 4082-4091.
347. Kida, K.; Okita, M.; Fujita, K.; Tanaka, S.; Miyake, Y., Formation of high crystalline ZIF-8 in an aqueous solution. *CrystEngComm* 2013, 15, 1794-1801.
348. Doran, P. M., *Bioprocess Engineering Principles*. Elsevier Science: 2013.
349. Liese, A.; Hilterhaus, L., Evaluation of immobilized enzymes for industrial applications. *Chem. Soc. Rev.* 2013, 42, 6236-6249.
350. Zhong, Z.; Pang, S.; Wu, Y.; Jiang, S.; Ouyang, J., Synthesis and characterization of mesoporous Cu-MOF for laccase immobilization. *J. Chem. Technol. Biotechnol.* 2017, 92, 1841-1847.
351. Park, K. S.; Ni, Z.; Côté, A. P.; Choi, J. Y.; Huang, R.; Uribe-Romo, F. J.; Chae, H. K.; O'Keeffe, M.; Yaghi, O. M., Exceptional chemical and thermal stability of zeolitic imidazolate frameworks. *Proc. Natl. Acad. Sci.* 2006, 103, 10186-10191.
352. Vaidya, L. B.; Nadar, S. S.; Rathod, V. K., Entrapment of surfactant modified lipase within zeolitic imidazolate framework (ZIF)-8. *Int. J. Biol. Macromol.* 2020, 146, 678-686.
353. Tanford, C., Protein Denaturation. In *Advances in Protein Chemistry*, Anfinsen, C. B.; Anson, M. L.; Edsall, J. T.; Richards, F. M., Eds. Academic Press: 1968; Vol. 23, pp 121-282.
354. Tamás, M. J. S., S.K.; Ibstedt, S.; Jacobson, T.; Christen, P., Heavy Metals and Metalloids As a Cause for Protein Misfolding and Aggregation. *Biomolecules* 2014, 252-267.
355. Protein Unfolding and Denaturants. In *eLS*.
356. Doran, P. M., Chapter 12 - Homogeneous Reactions. In *Bioprocess Engineering Principles (Second Edition)*, Doran, P. M., Ed. Academic Press: London, 2013; pp 599-703.
357. Charm, S. E.; Wong, B. L., Shear effects on enzymes. *Enzyme Microb. Technol.* 1981, 3, 111-118.
358. Bekard, I. B.; Asimakis, P.; Bertolini, J.; Dunstan, D. E., The effects of shear flow on protein structure and function. *Biopolymers* 2011, 95, 733-745.
359. Zhang, Y.; Wang, H.; Liu, J.; Hou, J.; Zhang, Y., Enzyme-embedded metal-organic framework membranes on polymeric substrates for efficient CO₂ capture. *J. Mater. Chem. A* 2017, 5, 19954-19962.
360. Cheong, L.-Z.; Wei, Y.; Wang, H.; Wang, Z.; Su, X.; Shen, C., Facile fabrication of a stable and recyclable lipase@amine-functionalized ZIF-8 nanoparticles for esters hydrolysis and transesterification. *J Nanopart. Res.* 2017, 19, 280.
361. Cui, J.; Feng, Y.; Jia, S., Silica encapsulated catalase@metal-organic framework composite: A highly stable and recyclable biocatalyst. *Chem. Eng. J.* 2018, 351, 506-514.
362. Cui, J.; Feng, Y.; Lin, T.; Tan, Z.; Zhong, C.; Jia, S., Mesoporous Metal-Organic Framework with Well-Defined Cruciate Flower-Like Morphology for Enzyme Immobilization. *ACS Appl. Mater. Interfaces* 2017, 9, 10587-10594.
363. Qi, B.; Luo, J.; Wan, Y., Immobilization of cellulase on a core-shell structured metal-organic framework composites: Better inhibitors tolerance and easier recycling. *Bioresour. Technol.* 2018, 268, 577-582.
364. Wu, X.; Ge, J.; Yang, C.; Hou, M.; Liu, Z., Facile synthesis of multiple enzyme-containing metal-organic frameworks in a biomolecule-friendly environment. *Chem. Commun.* 2015, 51, 13408-13411.
365. Thiele, E. W., Relation between Catalytic Activity and Size of Particle. *Ind. Eng. Chem. Res.* 1939, 31, 916-920.
366. Illanes, A., *Enzyme Biocatalysis - Principles and Applications*. Springer: 2008.
367. Gascón, V.; Carucci, C.; Jiménez, M. B.; Blanco, R. M.; Sánchez-Sánchez, M.; Magner, E., Rapid In Situ Immobilization of Enzymes in Metal-Organic Framework Supports under Mild Conditions. *ChemCatChem* 2017, 9, 1182-1186.
368. Nadar, S. S.; Rathod, V. K., One pot synthesis of α -amylase metal organic framework (MOF)-sponge via dip-coating technique. *Int. J. Biol. Macromol.* 2019, 138, 1035-1043.
369. Ricco, R.; Wied, P.; Nidetzky, B.; Amenitsch, H.; Falcaro, P., Magnetically responsive horseradish peroxidase@ZIF-8 for biocatalysis. *Chem. Commun.* 2020, 56, 5775-5778.
370. Purich, D. L., *Enzyme Kinetics: Catalysis and Control: A Reference of Theory and Best-Practice Methods*. Elsevier Science: 2010.
371. Lowry, O. H.; Rosebrough, N. J.; Farr, A. L.; Randall, R. J., PROTEIN MEASUREMENT WITH THE FOLIN PHENOL REAGENT. *J. Biol. Chem.* 1951, 193, 265-275.
372. Zhou, M.; Ju, X.; Zhou, Z.; Yan, L.; Chen, J.; Yao, X.; Xu, X.; Li, L.-Z., Development of an Immobilized Cellulase System Based on Metal-Organic Frameworks for Improving Ionic Liquid Tolerance and In Situ Saccharification of Bagasse. *ACS Sustain. Chem. Eng.* 2019, 7, 19185-19193.
373. Pröfrock, D.; Prange, A., Inductively Coupled Plasma-Mass Spectrometry (ICP-MS) for Quantitative Analysis in Environmental and Life Sciences: A Review of Challenges, Solutions, and Trends. *Appl. Spectrosc.* 2012, 66, 843-868.
374. Liang, W.; Carraro, F.; Solomon, M. B.; Bell, S. G.; Amenitsch, H.; Sumbly, C. J.; White, N. G.; Falcaro, P.; Doonan, C. J., Enzyme Encapsulation in a Porous Hydrogen-Bonded Organic Framework. *J. Am. Chem. Soc.* 2019, 141, 14298-14305.
375. Wong, C. M.; Wong, K. H.; Chen, X. D., Glucose oxidase: natural occurrence, function, properties and industrial applications. *Appl. Microbiol. Biotechnol.* 2008, 78, 927-938.
376. Wilson, R.; Turner, A. P. F., Glucose oxidase: an ideal enzyme. *Biosens. Bioelectron.* 1992, 7, 165-185.
377. Xu, Y.; Liu, S.-Y.; Liu, J.; Zhang, L.; Chen, D.; Chen, J.; Ma, Y.; Zhang, J.-P.; Dai, Z.; Zou, X., In Situ Enzyme Immobilization with Oxygen-Sensitive Luminescent Metal-Organic Frameworks to Realize "All-in-One" Multifunctions. *Chem. Eur. J.* 2019, 25, 5463-5471.
378. Liu, H.; Du, Y.; Gao, J.; Zhou, L.; He, Y.; Ma, L.; Liu, G.; Huang, Z.; Jiang, Y., Compartmentalization of Biocatalysts by Immobilizing Bienzyme in Hollow ZIF-8 for Colorimetric Detection of Glucose and Phenol. *Ind. Eng. Chem. Res.* 2020, 59, 42-51.
379. Bright, H. J.; Appleby, M., The pH Dependence of the Individual Steps in the Glucose Oxidase Reaction. *J. Biol. Chem.* 1969, 244, 3625-3634.
380. Chen, W.-H.; Luo, G.-F.; Vázquez-González, M.; Cazelles, R.; Sohn, Y. S.; Nechushtai, R.; Mandel, Y.; Willner, I., Glucose-Responsive Metal-Organic-Framework Nanoparticles Act as "Smart" Sense-and-Treat Carriers. *ACS Nano* 2018, 12, 7538-7545.
381. Hwang, E. T.; Gu, M. B., Enzyme stabilization by nano/microsized hybrid materials. *Eng. Life Sci.* 2013, 13, 49-61.
382. Bateman, R. C.; Evans, J. A., Using the Glucose Oxidase/Peroxidase System in Enzyme Kinetics. *J. Chem. Educ.* 1995, 72, A240.
383. Zhou, M.; Diwu, Z.; Panchuk-Voloshina, N.; Haugland, R. P., A Stable Nonfluorescent Derivative of Resorufin for the Fluorometric Determination of Trace Hydrogen Peroxide: Applications in Detecting the Activity of Phagocyte NADPH Oxidase and Other Oxidases. *Anal. Biochem.* 1997, 253, 162-168.

384. John Goka, A. K.; Farthing, M. J. G., The Use of 3, 3', 5, 5'-Tetramethylbenzidine as a Peroxidase Substrate in Microplate Enzyme-Linked Immunosorbent Assay. *J. Immunoassay* 1987, 8, 29-41.
385. Setti, L.; Scali, S.; Angeli, I. D.; Pifferi, P. G., Horseradish peroxidase-catalyzed oxidative coupling of 3-methyl 2-benzothiazolone hydrazone and methoxyphenols. *Enzyme Microb. Technol.* 1998, 22, 656-661.
386. Thurston, C. F., The structure and function of fungal lacases. *Microbiology* 1994, 140, 19-26.
387. Gao, W.-Y.; Cardenal, A. D.; Wang, C.-H.; Powers, D. C., In Operando Analysis of Diffusion in Porous Metal-Organic Framework Catalysts. *Chem. Eur. J.* 2019, 25, 3465-3476.
388. Swainston, N.; Baici, A.; Bakker, B. M.; Cornish-Bowden, A.; Fitzpatrick, P. F.; Halling, P.; Leyh, T. S.; O'Donovan, C.; Raushel, F. M.; Reschel, U.; Rohwer, J. M.; Schnell, S.; Schomburg, D.; Tipton, K. F.; Tsai, M.-D.; Westerhoff, H. V.; Wittig, U.; Wohlgemuth, R.; Kettner, C., STRENDA DB: enabling the validation and sharing of enzyme kinetics data. *FEBS J.* 2018, 285, 2193-2204.
389. Michaelis, L. M., M. L., Die Kinetik Der Invertiirwirkulig. *Biochem. Z.* 1913, 49.
390. Bolivar, J. M.; Eisl, I.; Nidetzky, B., Advanced characterization of immobilized enzymes as heterogeneous biocatalysts. *Catal. Today* 2016, 259, 66-80.
391. van Roon, J.; Beefink, R.; Schroën, K.; Tramper, H., Assessment of intraparticle biocatalytic distributions as a tool in rational formulation. *Curr. Opin. Biotechnol.* 2002, 13, 398-405.
392. van Roon, J. L.; Schroën, C. G. P. H.; Tramper, J.; Beefink, H. H., Biocatalysts: Measurement, modelling and design of heterogeneity. *Biotechnol. Adv.* 2007, 25, 137-147.
393. Guisan, J. M.; López-Gallego, F.; Bolivar, J. M.; Rocha-Martín, J.; Fernandez-Lorente, G., The Science of Enzyme Immobilization. In *Immobilization of Enzymes and Cells: Methods and Protocols*, Guisan, J. M.; Bolivar, J. M.; López-Gallego, F.; Rocha-Martín, J., Eds. Springer US: New York, NY, 2020; pp 1-26.
394. Bolivar, J. M.; Nidetzky, B., On the relationship between structure and catalytic effectiveness in solid surface-immobilized enzymes: Advances in methodology and the quest for a single-molecule perspective. *BBA-Proteins Proteom.* 2020, 1868, 140333.
395. Minton, A. P., The Influence of Macromolecular Crowding and Macromolecular Confinement on Biochemical Reactions in Physiological Media. *J. Biol. Chem.* 2001, 276, 10577-10580.
396. van Roon, J. L.; Boom, R. M.; Paasman, M. A.; Tramper, J.; Schroën, C. G. P. H.; Beefink, H. H., Enzyme distribution and matrix characteristics in biocatalytic particles. *J. Biotechnol.* 2005, 119, 400-415.
397. Esposito, R.; Delfino, I.; Lepore, M., Time-Resolved Flavin Adenine Dinucleotide Fluorescence Study of the Interaction Between Immobilized Glucose Oxidase and Glucose. *J. Fluoresc.* 2013, 23, 947-955.
398. Qi, L.; Luo, Z.; Lu, X., Biomimetic Mineralization Inducing Lipase-Metal-Organic Framework Nanocomposite for Pickering Interfacial Biocatalytic System. *ACS Sustain. Chem. Eng.* 2019, 7, 7127-7139.
399. Wang, X.; Lan, P. C.; Ma, S., Metal-Organic Frameworks for Enzyme Immobilization: Beyond Host Matrix Materials. *ACS Cent. Sci.* 2020.
400. Bisswanger, H., *Practical Enzymology*, Second Edition. Wiley - VCH: 2012.
401. He, H.; Han, H.; Shi, H.; Tian, Y.; Sun, F.; Song, Y.; Li, Q.; Zhu, G., Construction of Thermophilic Lipase-Embedded Metal-Organic Frameworks via Biomimetic Mineralization: A Biocatalyst for Ester Hydrolysis and Kinetic Resolution. *ACS Appl. Mater. Interfaces* 2016, 8, 24517-24524.
402. Samui, A.; Sahu, S. K., One-pot synthesis of microporous nanoscale metal organic frameworks conjugated with laccase as a promising biocatalyst. *New J. Chem.* 2018, 42, 4192-4200.
403. Gao, X.; Zhai, Q.; Hu, M.; Li, S.; Song, J.; Jiang, Y., Design and preparation of stable CPO/HRP@H-MOF(Zr) composites for efficient bio-catalytic degradation of organic toxicants in wastewater. *J. Chem. Technol. Biotechnol.* 2019, 94, 1249-1258.
404. Eckard, A. D.; Muthukumarappan, K.; Gibbons, W., Enzyme recycling in a simultaneous and separate saccharification and fermentation of corn stover: A comparison between the effect of polymeric micelles of surfactants and polypeptides. *Bioresour. Technol.* 2013, 132, 202-209.
405. Zhu, D.; Ao, S.; Deng, H.; Wang, M.; Qin, C.; Zhang, J.; Jia, Y.; Ye, P.; Ni, H., Ordered Coimmobilization of a Multienzyme Cascade System with a Metal Organic Framework in a Membrane: Reduction of CO₂ to Methanol. *ACS Appl. Mater. Interfaces* 2019, 11, 33581-33588.
406. Panganiban, B.; Qiao, B.; Jiang, T.; DelRe, C.; Obadia, M. M.; Nguyen, T. D.; Smith, A. A. A.; Hall, A.; Sit, I.; Crosby, M. G.; Dennis, P. B.; Drockenmuller, E.; Olvera de la Cruz, M.; Xu, T., Random heteropolymers preserve protein function in foreign environments. *Science* 2018, 359, 1239-1243.

Authors are required to submit a graphic entry for the Table of Contents (TOC) that, in conjunction with the manuscript title, should give the reader a representative idea of one of the following: A key structure, reaction, equation, concept, or theorem, etc., that is discussed in the manuscript. Consult the journal's Instructions for Authors for TOC graphic specifications.

